



UNIVERSIDAD
DE MÁLAGA

ESCUELA DE INGENIERÍAS INDUSTRIALES

DEPARTAMENTO DE MATEMÁTICA APLICADA

DOCTORADO EN SISTEMAS DE ENERGÍA ELÉCTRICA

DOCTORAL DISSERTATION

PRESCRIPTIVE ANALYTICS IN ELECTRICITY MARKETS

Author

M. Eng. *Miguel Angel Muñoz Díaz*

Supervisors

Prof. Dr. *Juan Miguel Morales González*


Prof. Dr. *Salvador Pineda Morente*

September 2022



UNIVERSIDAD
DE MÁLAGA

AUTOR: Miguel Ángel Muñoz Díaz

 <https://orcid.org/0000-0003-2115-5725>

EDITA: Publicaciones y Divulgación Científica. Universidad de Málaga



Esta obra está bajo una licencia de Creative Commons Reconocimiento-NoComercial-SinObraDerivada 4.0 Internacional:

<http://creativecommons.org/licenses/by-nc-nd/4.0/legalcode>

Cualquier parte de esta obra se puede reproducir sin autorización

pero con el reconocimiento y atribución de los autores.

No se puede hacer uso comercial de la obra y no se puede alterar, transformar o hacer obras derivadas.

Esta Tesis Doctoral está depositada en el Repositorio Institucional de la Universidad de Málaga (RIUMA): riuma.uma.es



DECLARACIÓN DE AUTORÍA Y ORIGINALIDAD DE LA TESIS PRESENTADA PARA OBTENER EL TÍTULO DE DOCTOR

D./Dña MIGUEL ANGEL MUÑOZ DIAZ

Estudiante del programa de doctorado SISTEMAS DE ENERGÍA ELÉCTRICA de la Universidad de Málaga, autor/a de la tesis, presentada para la obtención del título de doctor por la Universidad de Málaga, titulada: PRESCRIPTIVE ANALYTICS IN ELECTRICITY MARKETS.

Realizada bajo la tutorización de SALVADOR PINEDA MORENTE y dirección de JUAN MIGUEL MORALES GONZÁLEZ Y SALVADOR PINEDA MORENTE (si tuviera varios directores deberá hacer constar el nombre de todos)

DECLARO QUE:

La tesis presentada es una obra original que no infringe los derechos de propiedad intelectual ni los derechos de propiedad industrial u otros, conforme al ordenamiento jurídico vigente (Real Decreto Legislativo 1/1996, de 12 de abril, por el que se aprueba el texto refundido de la Ley de Propiedad Intelectual, regularizando, aclarando y armonizando las disposiciones legales vigentes sobre la materia), modificado por la Ley 2/2019, de 1 de marzo.

Igualmente asumo, ante a la Universidad de Málaga y ante cualquier otra instancia, la responsabilidad que pudiera derivarse en caso de plagio de contenidos en la tesis presentada, conforme al ordenamiento jurídico vigente.

En Málaga, a 05 de SEPTIEMBRE de 2022

Fdo.: MIGUEL ANGEL MUÑOZ DIAZ Doctorando/a	Fdo.: SALVADOR PINEDA MORENTE Tutor/a
Fdo.: JUAN MIGUEL MORALES GONZÁLEZ, SALVADOR PINEDA MORENTE Director/es de tesis	



UNIVERSIDAD
DE MÁLAGA

Dr. Juan Miguel Morales González, profesor titular del departamento de Matemática Aplicada de la Universidad de Málaga, en calidad de director y Dr. Salvador Pineda Morente, profesor titular del departamento de Ingeniería Eléctrica de la Universidad de Málaga, en calidad de director y tutor de la tesis de título “PRESCRIPTIVE ANALYTICS IN ELECTRICITY MARKETS” realizada por el doctorando Miguel Ángel Muñoz Díaz dentro del programa de doctorado de Sistemas de Energía Eléctrica, certifican que:

- Han procedido a la revisión de la presente memoria y reúne los requisitos necesarios para ser sometida al juicio de la Comisión correspondiente.
- Las publicaciones que avalan la mencionada tesis no han sido utilizadas en tesis doctorales anteriores.
- Los comentarios de los evaluadores externos han sido tenidos en consideración y se han realizado los cambios oportunos.

Y para que conste a efectos de lo establecido en el artículo octavo del Real Decreto 99/2011, autorizan la presentación y defensa de este trabajo para optar al Grado de Doctor por la Universidad de Málaga.

En Málaga, a 05 de Septiembre de 2022

Fdo. JUAN MIGUEL MORALES GONZÁLEZ
Director de la tesis

Fdo. SALVADOR PINEDA MORENTE
Director y tutor de la tesis

A mis padres.
A Lorena.

Acknowledgments

This thesis concludes a long journey that has made me grow as a researcher and person. I would not want to let this occasion pass without expressing my gratitude to the people who have made it possible.

My deepest thanks to my supervisors, Prof. Juan M. Morales and Prof. Salvador Pineda. I truly admire their dedication to science which really inspired me. I thank them for their outstanding supervision and for showing me the route in the vast ocean of knowledge. I would have never safely reached harbor without their guidance.

Also, all my gratitude goes to Prof. Pierre Pinson and Prof. Jalal Kazempour, who have been incredible hosts for me at the Technical University of Denmark (DTU). I very much appreciate their kindness and excellent supervision.

My experience in the Joint Research Centre (JRC) of the European Commission in The Netherlands was another beautiful chapter of this journey. I learned a lot from the colleagues I met there and had very enriching experiences. I want to thank my supervisor there, Ph.D. Catalin Felix Covrig, for the many things I learned from him and all the great moments we shared.

Thanks to the rest of the members of the OASYS research group, Adrián, Ricardo, Álvaro, Asun, Jesús, Lisa, Antonio, José, Conchi and Manolo, a piece of all of you is in this thesis. I will remember fondly the scientific discussions, the volleyball and padel games and the coffee breaks. I would like to dedicate a few more words to my table neighbor and also Ph.D. student Adrián for the many bibliography references and links he provided and to Lisa for being a critical part of the OASYS engine and for the help in making this thesis a proper English-written document.

Mention is also due to the ELMA group and the other people I met in DTU for making me feel like I was home and for the enriching conversations we shared.

Equally, thanks to the rest of my friends, who shared my successes, understood my absences and cheered me up when I needed it.

My wife, Lorena, deserves special mention. Thank you very much for all the love and support you have given me, for being there in the difficult moments and sharing the happy ones.

Last but not least, thanks to my family for their support and unconditional love,

specially to my mother. Just seeing you “tocar el cielo con los dedos” when I become a doctor has been worth the effort. I wish I can give you many more happy moments and thanks for all you have given me.

Institutional Acknowledgments

I thankfully acknowledge the funding provided by the Spanish Ministry of Science, Innovation and Universities through the State Training Subprogram 2018 of the State Program for the Promotion of Talent and its Employability in R&D&I, within the framework of the State Plan for Scientific and Technical Research and Innovation 2017-2020 and by the European Social Fund. I also acknowledge the Universidad de Málaga for the auxiliary resources and facilities provided to assist in this research.

Some of the works developed within this thesis were also supported in part by the European Research Council (ERC) under the EU Horizon 2020 research and innovation program (grant agreement No. 755705) and in part by the Spanish Ministry of Science and Innovation (AEI / 10.13039 / 501100011033) through project PID2020-115460GB-I00.

I express my gratitude to the coordinator of my Ph.D. program José Antonio Aguado for his fast and efficient assistance in solving all my queries.

Finally, I thankfully acknowledge the computer resources, technical expertise, and assistance provided by the SCBI (Supercomputing and Bioinformatics) center of the University of Málaga.

Scientific publications supporting this thesis

The following is a list of the papers published within this doctoral thesis:

1. **M. A. Muñoz**, J. M. Morales, and S. Pineda, “Feature-driven Improvement of Renewable Energy Forecasting and Trading,” *IEEE Transactions on Power Systems*, vol. 35, no. 5, pp. 3753 - 3763, February 2020. (Q1). DOI: <https://doi.org/10.1109/TPWRS.2020.2975246>
2. **M. A. Muñoz**, S. Pineda, and J. M. Morales, “A Bilevel Framework for Decision-making Under Uncertainty with Contextual Information,” *Omega*, vol.108, pp. 102575, November, 2021. (Q1). DOI: <https://doi.org/10.1016/j.omega.2021.102575>

In addition, the following working papers are also part of this thesis:

1. J. M. Morales, **M. A. Muñoz**, S. Pineda, “Prescribing Net Demand for Electricity Market Clearing”.
2. **M. A. Muñoz**, J. Kazempour, P. Pinson, “Online Decision Making for Trading Wind Energy”.

Abstract

Decision making is critical for any business to survive in a market environment. Examples of decision making tasks are inventory management, resource allocation or portfolio selection. Optimization, understood as the scientific discipline that studies how to solve mathematical programming problems, can help make more efficient decisions in many of these situations. Particularly relevant, because of their frequency and difficulty, are those decisions affected by *uncertainty*, i.e., in which some of the parameters that precisely determine the optimization problem are unknown when the decision must be made.

Fortunately, the development of information technologies has led to an explosion in the availability of *data* that can be used to assist decisions affected by uncertainty. However, most of the available historical data do not correspond to the unknown parameter of the problem but originate from other related sources. This subset of data, potentially valuable for obtaining better decisions, is called *contextual information*. This thesis is framed within a new scientific effort that seeks to exploit the potential of data and, in particular, of contextual information in decision making. To this end, in this thesis, we have developed mathematical frameworks and data-driven optimization models that exploit contextual information to make better decisions in problems characterized by the presence of uncertain parameters.

Electricity markets are a clear example of a sector in which decision making plays a crucial role in its daily activity. Moreover, uncertainty is intrinsic to electricity markets and affects most of the tasks that agents operating in them must carry out. Many of these tasks involve decisions characterized by low risk and being addressed periodically. In this thesis, we refer to these tasks as *iterative decisions*. This thesis applies the aforementioned innovative frameworks for decision making under uncertainty using contextual information to iterative decision making tasks faced in their daily operation by agents participating in electricity markets.

Resumen (extendido)

La toma de decisiones es un elemento clave en la operación diaria de cualquier negocio. Ejemplos de toma de decisiones son la gestión de inventarios, la asignación de recursos o la elección de los proyectos en los que invertir. La optimización, entendida como la disciplina científica que estudia cómo resolver problemas de programación matemática, puede ayudar a tomar decisiones más eficientes en muchas de estas situaciones. Particularmente relevantes, por su frecuencia y dificultad, son aquellas decisiones afectadas por la *incertidumbre*, objeto de estudio de esta tesis.

Los mercados eléctricos son un claro exponente de sector en el que la toma de decisiones, y en particular, la toma de decisiones bajo incertidumbre, juega un papel crucial en su actividad diaria. Esta tesis desarrolla y aplica marcos innovadores de toma de decisiones bajo incertidumbre a problemas operativos de los mercados eléctricos. Las próximas secciones están dedicadas a hacer una revisión sobre los paradigmas más destacados utilizados para la toma de decisiones bajo incertidumbre en el contexto de los mercados de electricidad, resaltando los elementos más relevantes sobre los que se asienta este trabajo. Seguidamente, resumimos el contenido de los capítulos que componen este documento y enumeramos las contribuciones de esta tesis.

Toma de decisiones bajo incertidumbre en los mercados de electricidad

Se avecinan tiempos emocionantes y a la vez desafiantes para el sector energético. La liberalización de los mercados eléctricos ha dado lugar a que muchos agentes de mercado individuales tengan que competir entre sí para mantenerse en el negocio. Para ello, las decisiones de los agentes deben alcanzar determinados objetivos, por ejemplo, producir beneficios, reducir la huella de carbono o gestionar el riesgo. Determinar el conjunto de acciones más adecuado para alcanzar los objetivos del agente es un problema de toma de decisiones. Ejemplos típicos de problemas de toma de decisiones a los que se enfrentan los agentes son la programación horaria de centrales [79], la gestión de los embalses y demás reservas de agua turbinables [127] o la determinación de la oferta que maximiza los beneficios de los participantes en los mercados mayoristas de electricidad [66]. Desgraciadamente, el funcionamiento cotidiano de estos agentes se enfrenta a un

reto fundamental: la incertidumbre está presente en la mayoría de las decisiones que tienen que tomar. En efecto, muchos de los parámetros que definen de forma inequívoca los problemas a los que los agentes deben enfrentarse a diario solo se revelan una vez tomada la decisión, por ejemplo, la demanda total de energía, las precipitaciones durante el año hidrológico o el precio del mercado diario de electricidad.

Las técnicas empleadas por los agentes para hacer frente a la incertidumbre han madurado en paralelo a la creciente aleatoriedad que han experimentado los mercados eléctricos en su historia. El grado de incertidumbre que impregnaba los mercados eléctricos en el siglo pasado era significativamente menor en comparación con la situación actual. Las centrales eléctricas despachables constituían en exclusiva el portfolio de unidades de generación que participaban en los mercados eléctricos en aquella época, es decir, la producción de energía era controlable y cierta salvo por interrupciones accidentales poco comunes. Así, la principal fuente de incertidumbre procedía de variables como la demanda de energía, que seguía patrones relativamente predecibles, y del precio de la electricidad, fuertemente dependiente del coste de los combustibles fósiles y, por lo tanto, también anticipable. En esta etapa, las técnicas utilizadas por los agentes para hacer frente a la incertidumbre en sus problemas de toma de decisiones se basaban sobre todo en herramientas predictivas utilizadas junto con programas matemáticos deterministas, suficientes para proporcionar un funcionamiento fiable de los mercados.

El panorama descrito en el párrafo anterior cambió radicalmente con la exitosa integración de la energía eólica en el mix de generación. Este cambio estuvo motivado por dos razones: la generación eólica depende de las condiciones meteorológicas, lo que dificulta la planificación de la generación, y, al mismo tiempo, elevados volúmenes de esta energía pueden influir en el precio de la electricidad en los mercados mayoristas. El efecto combinado de ambas características provocó un aumento sustancial de la incertidumbre en los mercados eléctricos y desencadenó la búsqueda de formulaciones alternativas de los problemas de toma de decisiones que abordaran dicho fenómeno. A pesar de los avances logrados, todavía es necesario un mayor esfuerzo para madurar nuevos marcos de decisión que puedan hacer frente a la mayor cuota de energía renovable necesaria para descarbonizar el sector energético y manejar la complejidad generada por nuevas tecnologías como los vehículos eléctricos, la demanda flexible y las instalaciones de almacenamiento.

Paralelamente a estas transformaciones, el desarrollo de las redes inteligentes y de las tecnologías de la información ha provocado una explosión en la cantidad de datos disponibles. No se trata de un cambio menor. Por el contrario, la disponibilidad masiva de datos ha provocado un cambio de paradigma en el que los datos se entienden ahora como el motor que debe impulsar las decisiones, creando un nuevo impulso en la investigación que aprovecha la programación matemática y las técnicas estadísticas y de aprendizaje automático para desarrollar nuevos marcos basados en datos para la toma

de decisiones. Para entender los puntos clave que sustentan el nuevo paradigma centrado en los datos, es necesario comprender antes las diferentes fuentes que los generan. Hay subconjuntos de datos que provienen directamente de los parámetros inciertos que afectan al problema de interés, cuyo uso para guiar la toma de decisiones es ya habitual en la literatura. Por el contrario, existe otro subconjunto de datos que no provienen directamente de los parámetros que afectan al problema de decisión, pero que tienen valor para explicar la aleatoriedad de dichos parámetros inciertos. Nos referimos a este último como *información contextual*. La información contextual también se conoce como información auxiliar y su uso en problemas de toma de decisiones es innovador y apenas estudiado.

Esta tesis se enmarca dentro de este nuevo paradigma centrado en datos en el que la información contextual ayuda en la toma de decisiones y estudia su aplicación en los mercados eléctricos. Para entender como la información contextual puede mejorar la toma de decisiones, es necesario entender primero las técnicas clásicas utilizadas con tal fin. La siguiente sección está dedicada a revisar los paradigmas clásicos de toma de decisiones comúnmente utilizados en los mercados eléctricos.

Paradigmas clásicos de toma de decisiones

Hay una serie de enfoques, muy bien establecidos en la literatura, que aprovechan la programación matemática, las técnicas estadísticas y los datos para la toma de decisiones bajo incertidumbre. El marco “predecir, luego optimizar” resuelve un problema de optimización sustituyendo el parámetro incierto por un valor “probable”. Para ello, es natural utilizar técnicas estadísticas y de aprendizaje automático para aproximar el valor esperado de la variable aleatoria con la que se modela el parámetro incierto. Un ejemplo clásico es, por ejemplo, la predicción de la demanda de energía eléctrica requerida para el día siguiente, cuyos modelos de predicción están ampliamente curados por la práctica y cuya estimación se utiliza, entre otros cometidos, para determinar las reservas de energía a desplegar a través de varios modelos de optimización.

Uno de los enfoques más populares dentro del marco predecir y optimizar consiste en minimizar una función de pérdida (por ejemplo, el clásico error cuadrático medio) sobre un conjunto de muestras históricas para obtener un modelo predictivo del valor esperado. Otro enfoque clásico consiste en suponer primero una familia de distribuciones paramétricas candidatas a modelar el parámetro incierto para luego obtener aquella que logra un mejor ajuste mediante el criterio de máxima verosimilitud. A continuación, se puede calcular analíticamente el valor esperado de la distribución ajustada para utilizarlo como estimación del valor real. En cualquiera de los casos, la estimación del valor esperado, a menudo denominada en la bibliografía como “previsión puntual”, se introduce en la tarea original de toma de decisiones, sustituyendo el parámetro incierto y dando lugar a un problema de optimización determinista. Estas técnicas producen

estimadores de propósito general que pueden utilizarse en otras aplicaciones y logran rendimientos razonables cuando la precisión de la predicción es relativamente alta. Sin embargo, esta metodología suele dar lugar a rendimientos subóptimos, por ejemplo, si la familia de distribuciones se selecciona erróneamente o cuando la sobreestimación o subestimación del parámetro incierto da lugar a pérdidas asimétricas.

En efecto, el marco predecir y optimizar solo aproxima al verdadero problema de la toma de decisiones porque no considera el impacto económico de la incertidumbre ni garantiza la viabilidad de la decisión prescrita. Estas deficiencias motivaron el desarrollo de otros paradigmas. La programación estocástica resuelve este problema considerando la distribución de los parámetros inciertos y cómo dicha distribución se traslada en posibles retornos económicos, determinando una decisión factible que maximiza los rendimientos esperados. La introducción de la programación estocástica en los mercados eléctricos dio lugar a un amplio corpus de investigación con muchas aplicaciones notables, como la programación horaria de centrales incluyendo centrales eólicas [10, 133], la gestión estocástica de los embalses de agua y de reservas turbinables [52], y métodos estocásticos para determinar la oferta óptima de compra o venta de electricidad en el mercado mayorista [14, 41].

A pesar del importante desarrollo que ha supuesto la programación estocástica, este marco no está exento de inconvenientes. En primer lugar, la verdadera distribución del parámetro incierto (y, por tanto, la distribución del resultado económico) es típicamente desconocida y debe inferirse a partir de muestras [3], lo que puede introducir un sesgo fundamental cuando la familia de distribuciones paramétricas se selecciona erróneamente. Como alternativa, la distribución de resultados puede aproximarse utilizando escenarios discretos [73, 25]. Sin embargo, el número de escenarios necesarios en las tareas de decisión a escala real da lugar a problemas intratables por sus grandes requisitos computacionales. Peor aún, aunque se conozca la verdadera distribución, la evaluación del coste medio incurrido por una decisión dada puede requerir el cálculo de la esperanza de una función de un vector aleatorio continuo (es decir, una integral multivariable), que es, en sí misma, una tarea difícil en general [68].

Los programas estocásticos que tienen en cuenta el valor esperado de los rendimientos producen soluciones con *buenos* resultados en promedio. La preocupación por otras propiedades, por ejemplo, el rendimiento económico obtenido en los escenarios menos favorables o la variabilidad de dichos rendimientos, motivó la investigación en medidas de riesgo alternativas para sustituir al valor esperado, como el valor condicional en riesgo o la varianza [151, 116, 28]. Las mismas razones dieron lugar a paradigmas de toma de decisiones completamente nuevos, con los notables ejemplos de la optimización robusta y la optimización distribucionalmente robusta. Como ventaja a destacar, estos paradigmas pueden producir problemas matemáticos más manejables que sus homólogos estocásticos, dando lugar a reformulaciones con complejidades computacionales más

favorables [16].

Estos no son los únicos paradigmas de toma de decisiones que se utilizan en los mercados eléctricos. Procedente de una comunidad científica diferente, el paradigma del aprendizaje en línea se centra en tareas de decisión de naturaleza repetitiva y caracterizadas por unos requisitos de inversión bajos o moderados. Este tipo de tareas, a las que en esta tesis nos referimos como *tareas de decisión iterativas*, también pueden ser abordadas por la programación estocástica, robusta y distribucionalmente robusta. Sin embargo, su tratamiento por parte del paradigma de aprendizaje en línea es específico y el marco conceptual sustancialmente diferente. La aplicación de este marco a los mercados eléctricos es más reciente pero igualmente exitosa, con aplicaciones al Flujo de Cargas Óptimo [61, 70], a los mercados en tiempo real [67] o a la respuesta a la demanda [85, 84].

Históricamente, ninguna de estas metodologías consideraba directamente la información contextual para la toma de decisiones, ignorando los beneficios que este recurso puede aportar para mejorar la toma de decisiones. La siguiente sección analiza la información contextual con más detalle, discutiendo su potencial para mejorar los paradigmas aquí presentados y revisando algunos trabajos representativos del estado del arte que proponen marcos innovadores para aprovechar este recurso.

Información Contextual

El *contexto* que rodea a la operación de los mercados eléctricos incluye una gran cantidad de fuentes de información potencialmente relevantes para la toma de decisiones, por ejemplo, datos de satélites, patrones de comportamiento o precios de futuros de materias primas. Antes de analizar cómo aprovechar la información contextual provenientes de estas fuentes, conviene describir con más detalle la naturaleza de la información contextual. Parte de la información contextual adopta la forma de realizaciones de una variable (o vector) aleatoria, discreta o continua y que está relacionada con los parámetros inciertos a través de una distribución de probabilidad conjunta usualmente desconocida. Por el contrario, muchos fragmentos de información contextual no tienen un carácter aleatorio, como el día de la semana o la hora del día en la que se revela el evento incierto. Independientemente de su naturaleza, cualquier pieza de información que se utilice como información contextual debe estar disponible antes de tomar la decisión.

A continuación, presentamos un pequeño ejemplo para ilustrar mejor el papel de la información contextual en un problema de toma de decisiones. En este ejemplo una empresa comercializadora tiene que determinar la energía que debe comprar en un mercado mayorista de electricidad para satisfacer la demanda total de energía de sus clientes durante el día siguiente. El precio de la electricidad en cada hora y la demanda total de energía son los principales parámetros que afectan a su decisión, que solo se

revelan *a posteriori* una vez se ha realizado la oferta en el mercado. Es de esperar que el comercializador disponga de un conjunto de datos con los precios y la demanda histórica de electricidad que puede utilizar junto con información contextual, como las previsiones meteorológicas, el calendario de festivos y el precio de los derivados financieros, para tomar mejores decisiones.

Con una visión limitada de su potencial, la información contextual se ha utilizado en el aprendizaje automático para pronosticar una cantidad incierta, generalmente unidimensional, en el marco predecir y optimizar. En la mayoría de los algoritmos de aprendizaje automático, el objetivo es estimar el parámetro incierto con la mayor precisión posible, es decir, minimizar el error cuadrático medio, sin tener en cuenta el efecto que la sobreestimación o subestimación de la variable objetivo puede tener en los resultados de la decisión. Siguiendo un camino independiente, los otros enfoques clásicos de toma de decisiones descritos en la sección anterior, a saber, la programación estocástica, robusta y distribucionalmente robusta, ha ignorado sistemáticamente la información contextual en problemas de optimización hasta hace pocos años, con pocas excepciones (por ejemplo, véanse las referencias revisadas en [7]).

La comunidad científica se ha percatado recientemente del uso subóptimo de la información contextual, por el que dicha información no se utiliza directamente para tomar mejores decisiones teniendo en cuenta el problema de optimización. Esta toma de consciencia ha impulsado nuevos esfuerzos de investigación sobre métodos basados en datos que utilizan la información contextual para tomar decisiones más eficientes y rentables. A continuación, revisamos los trabajos recientes que aprovechan la información contextual para mejorar el rendimiento promedio de la toma de decisiones, tema principal de esta tesis. En [7], los autores proponen utilizar una regla de decisión lineal para traducir directamente la información contextual en decisiones en el contexto de un clásico problema de inventario. El trabajo desarrollado en [56] refina el subóptimo marco “predecir y optimizar”, desarrollando una función objetivo alternativa al error cuadrático, teniendo en cuenta el problema de optimización lineal posterior. Mientras que el trabajo de [56] mapea la información contextual en una estimación de la fuente de incertidumbre, el enfoque de [7] traduce la información contextual directamente al espacio de decisión. Sin embargo, ambos trabajos codifican sus respectivas relaciones a través de un mapeo lineal. Además, estos dos trabajos están relacionados en que estos mapeos lineales son estimadores globales, es decir, estimadores que aprovechan todas las muestras disponibles para inferir el mapeo. Por último, el trabajo [17] es de naturaleza distinta ya que estudia estimadores locales, es decir, técnicas que solo utilizan muestras en una vecindad del estimador. En efecto, los autores de [17] se inspiran en varios modelos de aprendizaje automático para desarrollar técnicas que calculan una distribución empírica condicional de un parámetro incierto ponderando las observaciones pasadas en función de las similitudes de su información contextual.

Esta tesis se inspira en estos trabajos con un doble propósito, a saber: i) proponer nuevos marcos que mejoren el uso de la información contextual en problemas de toma de decisiones bajo incertidumbre, y ii) aplicar estos marcos a problemas de toma de decisiones relevantes pertenecientes a los mercados eléctricos. En este sentido, esta tesis está estrechamente alineada con los trabajos de [7], y [56]. En el curso de esta investigación, el trabajo de [7] fue ampliado y aplicado al problema de un productor de energía eólica, ofertando en un mercado diario de electricidad, dando lugar a la publicación [101] y abordado en el Capítulo 3. Además, el trabajo [102], que forma parte de esta tesis, propuso un método de programación matemática binivel para producir estimadores mejorados similares en espíritu a los de [56], dando lugar a otra aplicación presentadas en el Capítulo 4.

Tareas de decisión iterativas

La mayor parte de la teoría sobre la que se construye los paradigmas de decisión clásicos, como la programación estocástica o distribucionalmente robusta, se basan en el supuesto de que las distribuciones de probabilidad que gobiernan los parámetros inciertos son fijas y que las muestras de dichas variables se comportan como variables aleatorias *independientes e idénticamente distribuidas* (i.i.d.) [25]. En algunos casos, esta es una suposición razonable. Por ejemplo, consideremos que unos amigos están jugando una partida de cartas. En este juego hay varias cartas sobre la mesa en cada ronda, visibles para todos los jugadores. En este punto, el lector puede haber adivinado ya que las cartas sobre la mesa son información contextual. En efecto, el jugador (decisor) puede utilizar las cartas que están a la vista para ayudar a determinar su próximo movimiento (decisión). En este tipo de situación, podemos recoger cada movimiento y su resultado como parte de una muestra i.i.d. en la que el momento en el que se realizó la jugada es irrelevante. Esto es así ya que cada vez que las mismas cartas están sobre la mesa, se reproducen las mismas probabilidades y decisiones óptimas.

Sin embargo, esta situación es casi una excepción, que se da en tareas específicas típicamente relacionadas con juegos e invenciones diseñados por humanos. En la mayoría de las situaciones, el entorno en el que se toman las decisiones iterativas es similar pero evolutivo. Por ejemplo, cada día, el responsable de la toma de decisiones se encuentra con patrones climáticos similares, competidores similares, un comportamiento similar de los clientes y una realidad económica similar. Al mismo tiempo, el tiempo cambia cada minuto, los clientes no son idénticos y la situación geopolítica y económica cambia lenta pero constantemente, por nombrar algunos. Esta naturaleza causal pero evolutiva del mundo en que vivimos justifica que podamos inferir algunas relaciones entre la información contextual y los parámetros inciertos para un momento determinado y la necesidad de actualizar estas relaciones para mantener su eficacia. Esto significa que la suposición de que las muestras son i.i.d. en un conjunto de datos registrados

durante largos períodos puede ser no válida. Para afrontar este problema, en esta tesis investigamos una técnica conocido en la literatura como *ventana móvil* que puede combinarse con los marcos de decisión clásicos introducidos en este resumen para aprovechar conjuntos de datos históricos y abordar, de forma práctica, tareas de toma de decisiones iterativas en un entorno cambiante.

Resumen de los capítulos de esta tesis

En las secciones anteriores se han introducido los elementos fundamentales sobre los que se construye esta tesis. A continuación, se resume el contenido principal de los capítulos y apéndices que componen esta tesis.

El **Capítulo 1** comienza con una breve evolución histórica de la toma de decisiones en los mercados eléctricos, destacando la oportunidad de oro que tienen los agentes que operan en ellos para mejorar sus operaciones a través de la información contextual. Al igual que en este resumen, el capítulo resalta las contribuciones de esta tesis y avanza la estructura general del documento.

El **Capítulo 2** recoge el testigo, discutiendo formalmente los paradigmas clásicos de toma de decisiones que acabamos de introducir. El capítulo continúa discutiendo el potencial de la información contextual y cómo incorporar este valioso recurso en la toma de decisiones. Partiendo del problema estocástico contextual canónico, confrontamos las ventajas y desventajas de diferentes marcos de decisión, representativos del estado del arte y diseñados para abordar este tipo de problemas. Contribuimos a este esfuerzo científico con un marco matemático binivel con notables características y alcance general. El último bloque del capítulo está dedicado a abordar las particularidades de las tareas de toma de decisiones iterativas y trata dos temas principales relacionados: el entorno de la ventana móvil y el paradigma del aprendizaje “en línea”. En cuanto al primer tema, destacamos las ventajas de la configuración de la ventana móvil, que, en combinación con los marcos anteriormente descritos en el capítulo, permite abordar tareas iterativas en la práctica. En cuanto al segundo tema, revisamos las conexiones del aprendizaje en línea con la ventana móvil y los demás marcos de decisión y proponemos un nuevo algoritmo en línea especialmente diseñado para tareas iterativas con información contextual.

El **Capítulo 3** es el primero de los dos capítulos dedicados a presentar varias aplicaciones de los marcos de decisión contextual discutidos anteriormente en el contexto de los mercados eléctricos. En este capítulo se trata el problema del productor eólico desde dos perspectivas distintas.

La primera aplicación propone un método interpretable y computacionalmente eficiente para mejorar tanto las tareas de predicción como las de oferta a mercado de las energías renovables. Este método se basa en dos variantes de un modelo de optimización basado en datos, desarrollado recientemente, que aprovecha la información contextual

disponible para producir una predicción mejorada de energía renovable y para mejorar la rentabilidad de las ofertas del productor en el mercado diario de electricidad, respectivamente. La eficacia de nuestro enfoque se pone a prueba en un caso de estudio realista en el que pretendemos, por un lado, mejorar la predicción emitida por el operador del sistema eléctrico danés para la producción de energía eólica terrestre en la zona de oferta DK1 del mercado eléctrico paneuropeo y, por otro, formular una oferta de mercado competitiva para dicha producción. Para ello, simulamos una ventana móvil que imita los procesos reales de predicción y oferta y explota la información disponible en el momento en que debe emitirse la predicción o presentarse la oferta. El porcentaje de mejora alcanzado en las métricas de las predicciones y de la rentabilidad de la oferta señalan el valor intrínseco de explotar información adicional como por ejemplo las predicciones correlacionadas espacialmente. En esta línea, hemos observado que el uso (como información contextual) de las predicciones de energía eólica terrestre y marina en áreas geográficamente cercanas a la zona a la que pertenece la producción de energía eólica objetivo son valiosas. Esto parece ser especialmente cierto si esas zonas pertenecen al mismo país o al dominio del mismo operador del sistema.

La segunda aplicación discute un mercado eléctrico conceptual con una oferta iterativa en el que el tiempo entre la oferta y la entrega de energía es muy reducido. En esta aplicación, particularizamos el algoritmo en línea capaz de tener en cuenta la información contextual propuesto en el Capítulo 2 para mejorar las ganancias obtenidas por un productor de energía eólica en dicho escenario. Según la mejor información de que disponemos, esta es la primera vez que se aplican algoritmos en línea basados en gradientes a este problema. El resultado muestra ganancias económicas sustanciales con respecto a varios métodos de referencia, incluidos los que resuelven un problema de optimización sobre un conjunto de entrenamiento de muchas muestras. Esto es, en parte, debido a la rápida capacidad de adaptación de este algoritmo, especialmente útil en ambientes dinámicos, que le permite seguir patrones obviados por otros métodos basados en problemas de optimización con conjuntos de entrenamiento. Además, estas ganancias van acompañadas de una drástica reducción del coste computacional, lo que permite la aplicación de este novedoso algoritmo incluso en los mercados computacionalmente más desafiantes. El efecto combinado de este algoritmo y del mercado descrito en esta aplicación promete un significativo aumento de la rentabilidad de la energía eólica y una mayor participación de esta tecnología en el mercado.

El **Capítulo 4** discute dos aplicaciones que estiman inteligentemente los parámetros inciertos considerando el problema de optimización subyacente, es decir, teniendo en cuenta la región factible y el impacto que los errores sobre la función objetivo. En ambas aplicaciones, los estimadores se construyen mediante modelos que toman como entrada datos históricos e información contextual.

En la primera aplicación, aplicamos el enfoque contextual binivel, presentado en

la Sección 2.2.4, al problema de un productor estratégico de energía que gestiona una central térmica. El productor ofrece la generación de dicha central en un mercado eléctrico mayorista modelado a través de una función de demanda residual inversa incierta. Este enfoque produce estimadores prescriptivos de los parámetros inciertos que conforman la demanda residual, teniendo en cuenta la función objetivo y la región factible del problema subyacente en su estimación. Bajo supuestos de convexidad, el programa de optimización binivel resultante puede reformularse como un programa regularizado no lineal y un programa cuadrático entero mixto. El primer problema de optimización se resuelve iterativamente para valores decrecientes de un parámetro de regularización, alcanzando soluciones óptimas locales en un tiempo mínimo. El programa entero mixto es computacionalmente más costoso, pero, dadas las propiedades del problema, puede resolverse hasta optimalidad global.

El rendimiento de este enfoque y su relevancia práctica ha sido evaluado a través de un caso de estudio realista de un productor estratégico que participa en el mercado eléctrico ibérico. En concreto, los resultados numéricos muestran que el marco binivel no solo aumenta significativamente los ingresos del productor en general, sino que resulta crítico para las unidades de generación punta. En efecto, los ingresos de mercado de una central de generación punta son especialmente sensibles a la incertidumbre en la función de demanda residual inversa. Por lo tanto, en este caso, el productor estratégico puede poner en riesgo la mayor parte de sus ingresos de mercado al quedar fuera del mercado o al operar en déficit. Nuestro enfoque, sin embargo, es, por construcción, capaz de detectar dicha sensibilidad y, por tanto, de retener la mayor parte de los beneficios que el productor obtendría bajo una función de demanda inversa perfectamente predecible.

Bajo los supuestos de convexidad, hemos proporcionado dos reformulaciones de un solo nivel del programa binivel, a saber, un problema de optimización no lineal regularizado rápido de resolver y una reformulación no lineal entera mixta que puede alcanzar la solución óptima. En comparación con los enfoques alternativos disponibles en la literatura técnica, el nuestro presenta dos ventajas principales: garantiza la viabilidad en problemas de toma de decisiones con restricciones, y su solución puede abordarse directamente utilizando paquetes de optimización estándar.

La segunda aplicación propone un modelo de programación matemática basado en datos para prescribir el valor de la demanda neta que debe utilizarse para liquidar un mercado de electricidad de dos etapas con el fin de minimizar el coste total esperado de la explotación del sistema eléctrico subyacente. Para ello, hemos formulado un programa lineal entero mixto que modifica la predicción de la demanda mediante un mapeo afin teniendo en cuenta las características técnicas y económicas de las reservas de las centrales.

Los experimentos numéricos realizados en un modelo basados en el sistema eléctrico europeo revelan que el ahorro de costes que suponen los mapeos afines estimados es

sustancial. Además, partiendo de la base de que la estructura de costes de un sistema eléctrico depende en gran medida de su punto de funcionamiento y, por tanto, del nivel de demanda neta, hemos ideado una estrategia de partición de la muestra de datos basada en clústers para entrenar diferentes mapeos afines para distintos regímenes de demanda neta. La utilización de esta estrategia ha demostrado tener un doble efecto positivo en forma de un ahorro de costes sustancialmente mayor y una notable disminución de la carga computacional del modelo de programación entera mixta propuesto.

Por último, el **Capítulo 5** concluye esta tesis resaltando los aspectos principales de esta investigación y discute una serie de vías abiertas para posibles trabajos futuros en relación con las contribuciones de esta tesis.

Adicionalmente, el **Apéndice A** proporciona material complementario específico del marco contextual binivel desarrollado en el Capítulo 2. En concreto, buena parte del apéndice desarrolla cómo aplicar dicho método a problemas de programación estocástica de dos etapas con variables de recurso e ilustra este procedimiento con dos problemas clásicos de la literatura de la programación matemática. Adicionalmente, se proporciona una prueba formal de la convergencia del método binivel a la solución óptima en la aplicación del productor estratégico.

Contribuciones de esta tesis

Las principales contribuciones de esta tesis son:

1. La revisión del estado del arte de la toma de decisiones bajo incertidumbre utilizando información contextual, comparando varios marcos recientemente propuestos en la literatura. Además, esta revisión presta especial atención a las aplicaciones en los mercados eléctricos.
2. El desarrollo de modelos de optimización y marcos matemáticos basados en datos que aprovechan la información contextual en tareas de toma de decisiones afectadas por la incertidumbre y la aplicación de estos modelos a problemas clásicos del mercado eléctrico. Más concretamente, esta tesis ha resultado en:
3. Dos modelos de programación matemática interpretables y computacionalmente eficientes basados en reglas de decisión lineales. El primero mejora la predicción de energía eólica del operador del sistema danés mediante el uso de predicciones geográficamente correladas de áreas de oferta vecinas. El segundo aprovecha esta predicción mejorada junto con datos históricos del mercado para aumentar la rentabilidad de un portfolio de generación eólica en un mercado diario de electricidad con penalizaciones por desvío;
4. Un algoritmo en línea basado en gradientes y diseñado expresamente para tareas iterativas con información contextual disponible. Este algoritmo destaca por su

baja carga computacional y su habilidad para adaptarse a ambientes dinámicos, siendo la primera vez que se aplican algoritmos de este tipo en este problema. Los resultados obtenidos en el caso de estudio prueban su potencial para mejorar la rentabilidad y facilitar la integración de la energía eólica en los mercados eléctricos;

5. El desarrollo de un marco general basado en datos para la toma de decisiones bajo incertidumbre que resulta en modelos de programación matemática binivel. Estos modelos aprovechan la información contextual para producir estimadores de los parámetros inciertos teniendo en cuenta la región factible y la función objetivo de la tarea de decisión abordada. Este modelo se aplica al problema de un productor convencional (térmico) de energía eléctrica que oferta su generación de forma estratégica en el mercado diario, obteniendo notables beneficios.
6. El diseño de un modelo de programación matemática entero mixto para construir, a partir de los datos históricos disponibles, una estimación mejorada de la demanda neta utilizada en la liquidación de un mercado eléctrico de dos etapas. Este estimador inteligente produce ahorros sustanciales gracias a que el modelo de programación matemática tiene en cuenta la asimetría de los costes de reserva del sistema eléctrico subyacente.
7. Además, se extraen una serie de conclusiones técnicas a partir de ejemplos ilustrativos y casos de estudio analizados que son relevantes para los mercados de electricidad, junto con posibles líneas de investigación futuras.

Contents

1	Introduction, contributions and thesis outline	2
1.1	Decision making under uncertainty in electricity markets	4
1.2	Contributions of this thesis	6
1.3	Thesis outline	7
2	Contextual decision making under uncertainty	10
2.1	Classical paradigms for decision making under uncertainty	12
2.2	Decision making with contextual information	16
2.2.1	Conditional distribution	19
2.2.2	Decision rule	21
2.2.3	Smart predict, then optimize	22
2.2.4	Contextual bilevel framework	22
2.3	Iterative decision making	26
2.3.1	The world is not i.i.d.	26
2.3.2	Rolling-window setting and its elements	27
2.3.3	Online learning	28
2.4	Summary	32
3	Contextual optimization via decision rules	36
3.1	The trading problem of a wind power producer	38
3.1.1	Problem description	39
3.1.1.1	Renewable Energy Forecasting	43
3.1.1.2	Renewable Energy Trading	45
3.1.2	Experiment Design and Model Training	46
3.1.2.1	Data and Features	46
3.1.2.2	Performance Metrics	49
3.1.2.3	Model Training	50
3.1.3	Results	52
3.1.3.1	Improvements in Wind Power Forecasting	52
3.1.3.2	Improvements in Wind Power Trading	54

3.2	Online wind power producer	56
3.2.1	Problem description	58
3.2.2	The online newsvendor algorithm	58
3.2.3	Regularization through average penalty anchoring	61
3.2.4	Performance evaluation	62
3.2.5	Illustrative examples	64
3.2.5.1	Comparing the smooth and subgradient objective	64
3.2.5.2	Dynamic behavior	66
3.2.6	Case study	69
3.2.6.1	Data and experimental setup	69
3.2.6.2	Benchmark methods and implementation details	71
3.2.6.3	Numerical results	72
3.3	Summary	74
4	Contextual optimization via prescriptive estimation	77
4.1	Contextual strategic bidding	79
4.1.1	Problem description	80
4.1.2	Illustrative example	85
4.1.3	Case study	88
4.1.3.1	Experimental setup	88
4.1.3.2	Impact of the generation portfolio	90
4.1.3.3	Impact of parameter c_2	92
4.1.3.4	Impact of the residual demand elasticity	93
4.1.3.5	Computational results	93
4.2	Contextual economic dispatch	95
4.2.1	Problem description	96
4.2.2	The contextual dispatch model	99
4.2.3	Example	102
4.2.3.1	Impact of power regulation costs	104
4.2.3.2	Impact of grid congestion	106
4.2.3.3	Impact of the peak demand	106
4.2.3.4	Impact of the net demand regime	107
4.2.4	Data clustering and partitioning	108
4.2.5	Case Study	109
4.3	Summary	112
5	Closure	115
5.1	Summary and conclusions	117
5.2	Future work	120

A Contextual decision making via bilevel programming	124
A.1 Solving the bilevel approach with recourse variables	126
A.2 Applications of BL with and without full recourse	128
A.2.1 Newsvendor problem	128
A.2.2 Product placement problem	130
A.3 Asymptotic consistency of the bilevel approach applied to the strategic producer problem	133
References	136

List of Figures

2.1	Illustration of the rolling-window setting for three subsequent decision tasks.	28
3.1	Illustration of the rolling-window approach.	50
3.2	Illustration of the forecasts issued by the Danish TSO (BN) and model FM3 for the interval 01/01/16 to 01/08/16 (mm/dd/yyyy).	53
3.3	Box plot of the coefficients obtained for FM4 in the simulation period 02/04/16 to 04/22/2019.	54
3.4	Histogram of the values taken on by the decision-rule parameter w^T in model TM for the interval 11/30/16 to 04/22/19.	55
3.5	Evolution of decision-rule parameter w^T in TM and ratio R for the interval 11/30/16 to 04/22/19.	55
3.6	Accumulated opportunity-loss reduction of TM for the interval 11/30/16 to 04/22/19 for a installed capacity of 3669 MW.	56
3.7	Sample of the (sub-)gradients τ_t of NV_t and NV_{t20} computed in the dataset of the illustrative example.	65
3.8	Different instances of the original NV_t and smooth $NV_{t0.3}$ objective function with $\alpha = 0.3$ and $u = E_t - \mathbf{w}^T \mathbf{x}_t$	66
3.9	Example of the evolution of the coefficient w for different implementations of OLVN.	67
3.10	Evolution of w produced by five models over the test set. The blue and orange shaded periods correspond to the penalty scenarios $\psi_t^+ = 1, \psi_t^- = 3$ and $\psi_t^+ = 3, \psi_t^- = 1$, respectively. The entry w^* corresponds to the best single value for each penalty scenario.	68
3.11	Average dynamic regret R_T^d/T for $l = 3, 6, 12$, months and static regret R_T^s/T updated every 3 months (denoted as s) of the OLVN method. . .	73
4.1	Decision quantity q versus feature x for the illustrative example.	87
4.2	Inverse residual demand curve $p(r)$ (solid) and fitted inverse demand function $p_i(q)$ (dashed) in the interval $[0, \delta]$. The intercept and slope of the fitted line are α_i and $-\beta_i$, respectively.	89

4.3	Three-bus power system with one random demand and two thermal generators.	102
4.4	Prescribed affine transformation of the day-ahead net-demand forecast (aggregated system-wise). Demand is given in GW.	111

List of Tables

2.1	Average out-of-sample predictive error (RMSE) and objective function value \hat{v} by a model that minimizes the in-sample RMSE (predictive) and another that take into account the feasible region (prescriptive).	19
3.1	MAE reduction in percentage (%) with respect to the benchmark for different lengths of the training set T (months of data).	51
3.2	AOL reduction in percentage (%) of model TM with respect to the benchmark for different lengths of the training set T (months of data).	52
3.3	MAE and RMSE reduction in percentage (%) with respect to the benchmark.	52
3.4	Average absolute value $ \hat{\tau} $ and standard deviation σ of the (sub-) gradients and the metric AOL(%) computed for three smooth (α) and one subgradient (∂) implementations of the OLVN.	65
3.5	Out-of-sample AOL (%) obtained in the test set of the illustrative example. 68	
3.6	Installed capacity in MW by bidding zone and technology.	69
3.7	Average RMSE (MWh) of the original forecast, the persistent (naive 1h lag) and improved 1h-ahead forecast computed on the out-of-sample period 07/01/2015 to 06/04/2021 with a normalized generation capacity of 100 MW.	70
3.8	Out-of-sample AOL (%) for different combinations of parameters μ and η_0 over the span 07/01/2015 to 12/31/2015. Highlighted in black are shown the best result and parameters selected.	72
3.9	Out-of-sample AOL (%) and execution time (s) over the span 07/01/2016 to 06/04/2021.	73
4.1	Data sample S for the illustrative example.	86
4.2	Optimal offer and income for the unconstrained illustrative example (in-sample results). Parameter vectors w are: $w_{\alpha,0}^{\text{FO}} = 5.000, w_{\alpha,1}^{\text{FO}} = 1.000, w_{\beta,0}^{\text{FO}} = 12.298, w_{\beta,1}^{\text{FO}} = -0.878, w_{\gamma,0}^{\text{BL}} = -0.138, w_{\gamma,1}^{\text{BL}} = 0.341, w_{q0}^{\text{DR}} = -0.069, w_{q1}^{\text{DR}} = 0.170$	86

4.3	Optimal offer and income for the constrained illustrative example (in-sample results). Parameter vectors w are: $w_{\alpha,0}^{\text{FO}} = 5.000$, $w_{\alpha,1}^{\text{FO}} = 1.000$, $w_{\beta,0}^{\text{FO}} = 12.298$, $w_{\beta,1}^{\text{FO}} = -0.878$, $w_{\gamma,0}^{\text{BL}} = -1.300$, $w_{\gamma,1}^{\text{BL}} = 0.750$, $w_{q0}^{\text{DR}} = 0.158$, $w_{q1}^{\text{DR}} = 0.094$	88
4.4	Generation technology data.	90
4.5	Impact of generation technology.	91
4.6	Income distribution for the peak generating unit.	92
4.7	Operating regime of a medium generating unit ($c_1 = 35\text{€}/\text{MWh}$, $\bar{q} = 500\text{MW}$).	92
4.8	Impact of parameter c_2 on a medium generating unit.	93
4.9	Impact of residual demand elasticity	93
4.10	Comparison of BL-M and BL-R.	94
4.11	Average computing time.	94
4.12	Illustrative example: Technical and economic specifications of power plants.	103
4.13	Cost savings in percentage under different values of G_2 's power regulation costs C_2^{u} and C_2^{d}	104
4.14	Cost savings in percentage under different values of G_2 's power regulation costs C_2^{u} and C_2^{d} . Constraints (4.22e)–(4.22h) have been dropped from the training model (4.22).	104
4.15	Impact of grid congestion on cost savings.	106
4.16	Impact of peak demand.	107
4.17	Impact of the net-demand regime.	108
4.18	Base and peak generation capacity (GW) installed per node of the European network.	109
4.19	Uniform distributions from which the marginal production, up- and down-regulation costs of the units in the European system have been sampled.	110
4.20	Average cost savings in percentage (%) and average time (s) to solve the estimation problem (4.22) for a number K of partitions and various levels r of reduction in the size of the original training sets (out-of-sample results).	111

Chapter 1

Introduction, contributions and thesis outline

The subject matter of this thesis is the development of new data-driven frameworks for decision making under uncertainty applied to electricity markets. This chapter provides some background on the evolution of decision making in the context of electricity markets, paving the way for a more formal discussion of the subject in the following chapters. The contribution of this thesis and the structure of the document close this chapter.

1.1 Decision making under uncertainty in electricity markets

Thrilling yet challenging times lie ahead for the energy sector. The liberalization of the electricity markets resulted in many individual agents who have to compete with each other to remain in business [75]. To this end, agents' decisions must achieve certain objectives, e.g., producing revenues, reducing the carbon footprint, or managing risk [136]. Determining the most appropriate set of actions to achieve an agent's targets is a decision-making problem. Typical examples of decision-making problems that agents routinely face are unit commitment, managing water reservoirs, or determining a profit-maximizing bid/offer in wholesale markets [62]. Unfortunately, the day-to-day operation of these agents faces a fundamental challenge: uncertainty plagues most of the decisions they have to make [41]. In effect, many of the parameters that unambiguously define the problems that agents must deal with daily are only revealed after the decision has been made, for example, total energy demand, seasonal rainfall or wind energy production.

The techniques employed by agents to address uncertainty have matured in parallel with the increasing randomness that electricity markets have experienced in their history. The degree of uncertainty that pervaded electricity markets in the last century was significantly lower compared to the current situation [55]. Dispatchable power plants made up the portfolio of the generating units which comprised the electricity markets in those days, i.e., energy production was certain except for uncommon failures [135]. Thus, the main source of uncertainty originated from variables such as energy demand, which followed relatively predictable patterns, and electricity prices, which were highly dependent on the cost of fossil fuels [32]. At this stage, the techniques used by agents to address uncertainty in their decision-making problems were mostly based on *simple* forecasting tools and deterministic mathematical programs, enough to provide a reliable operation.

The aforementioned landscape changed dramatically with the successful integration of wind energy into the mix of generation [49]. This change was motivated for two reasons: the wind power production is completely dependent on whether conditions, and therefore hinder generation planning, and, at the same time, high volumes of this energy can influence the electricity price in wholesale markets [38]. The combined effect of these two features led to a substantial increase in the randomness affecting electricity markets

and triggered the search for alternative formulations of decision-making problems that formally addressed uncertainty.

As a result of this effort, stochastic programming (SP) was introduced in electricity markets [9]. Stochastic programming considers the full probability distribution of the uncertain parameters. The introduction of SP in electricity markets resulted in a vast research corpus with many notable applications [137], such as stochastic unit commitment and economic dispatch to accommodate wind energy [33, 10, 133], stochastic management of water reservoirs [52], and stochastic methods for trading electricity [14, 41]. However, this paradigm is not exempt from inconveniences, as it typically results in mathematical programs with heavy computational requirements [53, 93]. In addition to the problematic computational tractability of SP, the concern for other properties of the outcome, e.g., the return in less favorable scenarios or the variability of returns, resulted in many models being developed under the application of more robust decision-making paradigms [40]. Notable examples of these paradigms are robust optimization (RO) [89, 88] and distributionally robust optimization (DRO) [144, 145, 58].

These are not the only decision-making paradigms that are used in electricity markets. Originating from a different scientific community, the online learning (OL) paradigm focuses on decision tasks that are repetitive in nature and characterized by low or moderate investment requirements. This type of task, which we refer to as *iterative decision making* in this thesis, can also be tackled by SP, RO and DRO. However, their treatment by OL is specific and the conceptual framework substantially different. The application of OL to electricity markets is more recent but equally successful with applications to the optimal power flow [61, 70], real-time markets [67] or demand response [85, 84]. Notwithstanding the advances achieved, further effort is still required to mature new models that can cope with the higher share of renewable energy required to decarbonize the energy sector and to handle the complexity generated by new technologies such as electric vehicles, flexible demand, and storage facilities.

Parallel to the transformations produced by renewable energy and the introduction of new decision-making approaches, the development of smart grids and information technologies led to an explosion in the amount of raw data available [115]. This is not a minor change. Rather, the massive availability of data has caused a paradigm shift in which data are now understood as the engine that must drive decisions, creating a new thrust in research that leverages mathematical programming and statistical and machine-learning techniques to develop new data-driven frameworks for decision-making problems [99]. To understand the key points that underpin the new data-centric paradigm, it is necessary to comprehend the different sources that generate the data. There are streams of samples taken directly from the uncertain parameters that shape the problem of interest, whose use to guide decisions is already common in the literature [15, 95]. On the contrary, other pieces of information are not directly involved in the

decision-making problem but have value in explaining the randomness of the relevant uncertain parameters. We refer to the latter as *contextual information*.

In effect, the *context* in which markets operate includes a wealth of potentially relevant sources, e.g., satellite data, behavior patterns, or stock prices, which can help explain the source of uncertainty affecting an agent's decision-making problem [30, 65, 128]. A small example follows to better illustrate the role of contextual information in a decision-making problem. Consider a retailer who has to determine the energy to buy in a wholesale electricity market to satisfy an uncertain demand the next day. The price of electricity in each hour and the total energy demand are the main parameters that affect her decision, only revealed after the decision has been made (the offer on the market). Hopefully, the retailer has a dataset with historical electricity prices and demands that can be used, together with weather forecasts, the bank holiday calendar, and the price of financial derivatives to reduce the uncertainty in the decision-making problem and thus determine a cost-effective offer.

Contextual information is also known as covariate information, side information, auxiliary information, or features, [27, 8, 148] depending on the area of expertise, and its use in decision-making problems is promising and very recent. This thesis is framed within this new data-centric paradigm and aims to develop new mathematical models that leverage contextual information to produce efficient decisions and apply them to problems that agents in electricity markets routinely face.

Next, Section 1.2 formulates the main contribution of this thesis and Section 1.3 outlines the structure of the following chapters.

1.2 Contributions of this thesis

The main contributions of this thesis are:

1. The review of the current landscape of decision making under uncertainty using contextual information, comparing several state-of-the-art frameworks recently proposed in the literature. Furthermore, this review pays special attention to the applications to electricity markets.
2. The development of data-driven mathematical models and frameworks that leverage contextual information in decision making tasks affected by uncertainty and the application of these models to classical operational problems of electricity markets. More specifically, this thesis achieves:
3. Two computationally efficient and interpretable linear programming models based on linear decision rules that leverage contextual information in the short-term trading problem of a wind power producer. The first improves the Danish system operator's wind power forecast by using geographically correlated wind predictions

from neighboring bidding zones. The second leverages this enhanced forecast together with historical market data to increase the profitability of a wind generation portfolio in a realistic day-ahead electricity market with imbalance penalties;

4. A fully online gradient descent algorithm specifically designed to leverage contextual information in iterative decision-making tasks. This algorithm stands out for its low computational cost and its adaptability to dynamic environments. To the best of our knowledge, this is the first time that online gradient methods are applied to this problem. The numerical results obtained showcase its potential to improve profitability and facilitate the integration of wind energy into electricity markets;
5. The development of a general data-driven framework for decision making under uncertainty, resulting in bilevel optimization models. These models leverage contextual information to produce estimators of the uncertain parameters taking into account the feasible region and the objective function of the decision task addressed. The framework is applied, among others, to the problem of a strategic thermal producer offering in a day-ahead market, highlighting the crucial benefit of this strategy in peak generation units strongly dependent on uncertain market conditions;
6. The design of a mixed-integer mathematical programming model to construct, from available historical data, an improved estimate of the net demand to be used in the market clearing of a two-step electricity market. This strategy yields substantial savings as a consequence of taking into account the cost asymmetry of the underlying power system.
7. A number of technical conclusions are drawn from illustrative examples and realistic case studies that are relevant to electricity markets, together with prospective directions for future research.

1.3 Thesis outline

The structure of this thesis is outlined as follows:

Chapter 2 provides the mathematical background and tools to be used in the applications presented in the following chapters. In particular, Chapter 2 provides a formal introduction to the classical decision making paradigms under uncertainty and thoroughly discusses the use of contextual information in stochastic problems, reviewing several state-of-the-art frameworks for this purpose. As one of the main methodological contributions, this chapter proposes a new bilevel mathematical framework for decision making under uncertainty with contextual information, highlighting its wide applicability. This chapter also addresses the particularities of iterative decision-making tasks and

how to approach them from different paradigms, introducing a new online algorithm specially designed to leverage contextual information in iterative decision making.

Chapter 3 presents two applications of the contextual decision-making frameworks discussed in Chapter 2 to the problem of a wind power producer participating in a wholesale electricity market with a dual-price settlement for imbalances. The first application proposes two models based on decision rules to produce both an enhanced forecast of the wind energy production and a more profitable market offer. The second application demonstrates the tracking capability and inexpensive computational cost of online gradient-based algorithms in the wind power producer problem. We envision a conceptual wholesale market to facilitate the integration of wind energy and maximize the benefits in combination with the proposed online algorithm. The result shows dramatic improvements against standard industry practices and a substantial performance increase with respect to state-of-the-art methods, facilitating the integration of wind energy in electricity markets.

Chapter 4 presents two applications that smartly estimate the uncertain parameters, taking into account the optimization problem and the available contextual information. The first application applies the bilevel framework, introduced in Chapter 2, to the problem of a strategic thermal power producer offering in a wholesale electricity market, where the source of uncertainty comes from the unknown market conditions. The resulting bilevel problem is reformulated as a single-level optimization problem and solved using commercially available solvers. A second application follows, investigating alternative procedures for the market clearing of a two-stage electricity market compatible with current industrial practices. We propose a mixed-integer program that leverages the problem structure to construct, from the available contextual information and historical data, a *prescription* of the net demand, which does take into account the power system's cost asymmetry.

Finally, **Chapter 5** concludes this thesis and discusses a number of avenues for future work.

Additionally, **Appendix A** provides specific supplementary material for the contextual bilevel framework developed in Chapter 2.

Chapter 2

Contextual decision making under uncertainty: Mathematical Framework

This chapter provides the mathematical tools and framework to be used in the applications for electricity markets discussed in Chapter 3 and 4. Starting with the formal presentation of the classical paradigms used in decision making under uncertainty in Sections 2.1, this chapter continues reviewing the use of contextual information in decision making and presents four state-of-the-art approaches for contextual optimization in Section 2.2. Then, Section 2.3 addresses several topics related to iterative decision-making tasks, including their treatment within the online learning paradigm. Finally, Section 2.4 closes the chapter, highlighting the main ideas and establishing connections with successive chapters.

Given that the tools and frameworks introduced in this chapter are applicable to decision making tasks in general, we avoid the terms specific to electricity markets for the sake of a general presentation. A significant part of this chapter is based on the work in [102], product of this research.

2.1 Classical paradigms for decision making under uncertainty

There are many situations in which a decision maker has to determine the best actions needed to achieve certain objectives. The actions that best fulfill such objectives can be achieved by solving an optimization problem. In its simplest form, an optimization problem consists of finding the decision vector \mathbf{z} within a compact nonempty feasible set $\mathbf{z} \in Z \subseteq \mathbb{R}^n$ that minimizes a cost function $f(\mathbf{z})$, $f : Z \rightarrow \mathbb{R}$, known as the objective function, and through which we evaluate the fulfillment of the goal. Mathematically, we can write

$$\min_{\mathbf{z} \in Z} f(\mathbf{z}). \quad (2.1)$$

The aforementioned optimization problem is constructed based on the knowledge that the decision maker has regarding the cost function to be minimized and the constraints to be satisfied. This knowledge is introduced through a vector $\mathbf{y} \in \mathbb{R}^m$ that defines a particular instance of the optimization problem. Note that in this thesis, we focus on problems where Z is independent of the parameter \mathbf{y} . We can emphasize the dependence of the objective function on the parameter \mathbf{y} by rewriting the problem (2.1) as follows:

$$\min_{\mathbf{z} \in Z} f(\mathbf{z}; \mathbf{y}), \quad (2.2)$$

where $\mathbf{y} \in \mathcal{Y} \subseteq \mathbb{R}^m$ and we have redefined the objective function accordingly $f : Z \times \mathcal{Y} \rightarrow \mathbb{R}$. Often, the parameter vector \mathbf{y} is not known with certainty. This happens when \mathbf{y} refers to events that will occur in the future and are therefore uncertain at the time of making a decision. Thus, the parameter vector \mathbf{y} can be modeled as a random variable \mathbf{Y} governed by a probability distribution \mathbb{P} with several fundamental implications. First

of all, the objective function inherits the randomness of \mathbf{Y} and must also be treated as a random variable [123]. To minimize a cost function that depends on a random variable, we must therefore introduce a risk measure ρ on \mathbb{P} that transforms the random variable outcome into a real-valued function, which can be minimized according to

$$\min_{\mathbf{z} \in Z} \rho^{\mathbb{P}}(f(\mathbf{z}; \mathbf{Y})). \quad (2.3)$$

Although the feasible region Z is known with certainty, it should be clarified that \mathbf{Y} can affect the feasibility of recourse variables, that is, the variables to be optimized after the realization of the uncertainty to produce an optimal reaction. The paradigm that addresses problems in the form of (2.3) is known in the literature as Stochastic Programming (SP) [118, 25]. When the main concern of the decision maker is to minimize costs, the most widely used measure of risk is undoubtedly the expected value $\mathbb{E}[\cdot]$, which returns the mean value of the random cost $f(\mathbf{z}; \mathbf{Y})$ for a fixed decision \mathbf{z} . Replacing the generic risk measure with the expected value, problem (2.3) becomes

$$\min_{\mathbf{z} \in Z} \mathbb{E}_{\mathbb{P}}[f(\mathbf{z}; \mathbf{Y})]. \quad (2.4)$$

Therefore, the decision maker obtains the vector \mathbf{z} that minimizes the expected value of the outcome by solving the above problem. However, the distribution \mathbb{P} of the parameter vector \mathbf{y} is not known in most practical cases. The only known information usually reduces to a finite set of observations of the random parameter(s) in question, $\mathcal{Y}_N = \{\mathbf{y}_1, \mathbf{y}_2, \dots, \mathbf{y}_N\} = \{\mathbf{y}_i\}_{i=1}^N$. Attempts have been made to construct approximations of (2.4) through the observation set \mathcal{Y}_N , which offer results close, in a probabilistic sense, to those that would be obtained from such a stochastic optimization problem. A method to approximate \mathbb{P} proceeds by assuming a family of parametric distributions to model the uncertain parameter from which the best fit is obtained using the maximum likelihood criterion [3]. Given that the data do not contain perfect information of the random variable \mathbf{Y} , the result of this process is an estimator $\hat{\mathbb{P}}$ of the true distribution. With this estimator, we can alternatively solve the following problem

$$\min_{\mathbf{z} \in Z} \mathbb{E}_{\hat{\mathbb{P}}}[f(\mathbf{z}; \mathbf{Y})]. \quad (2.5)$$

Among other disadvantages, this approximation can introduce a fundamental bias when the family of parametric distributions is wrongly selected. Alternatively, the outcome distribution can be approximated using scenarios constructed based on the dataset \mathcal{Y}_N [73, 41]. Thus, the expected value operator reduces to a summation of finitely-many

discrete scenarios, yielding

$$\min_{\mathbf{z} \in Z} \sum_{w=1}^{\Omega} \pi_w f(\mathbf{z}; \mathbf{y}_w), \quad (2.6)$$

where $\pi_w \in [0, 1]$ is the probability of scenario $w \in \{1, \dots, \Omega\}$ characterized by a vector of uncertain parameters $\mathbf{y}_w \in \mathcal{Y}$. A special case for the construction of scenarios, which is also a straightforward way to construct the estimator $\hat{\mathbb{P}}$, proceeds by assigning an equal probability mass to the samples in \mathcal{Y}_N , resulting in an estimate of the probability distribution known as *empirical distribution*. Replacing the empirical distribution in (2.6) now renders

$$\min_{\mathbf{z} \in Z} \frac{1}{N} \sum_{i=1}^N f(\mathbf{z}; \mathbf{y}_i). \quad (2.7)$$

The problem above is the *sample average approximation* (SAA) of (2.4). Sample average approximation is a well-known data-driven solution strategy in Stochastic Programming [82, 118, 80], also known as *empirical risk minimization* in the realm of machine learning. More interestingly, the summation over equiprobable scenarios based on a dataset is a key ingredient that many of the frameworks in this chapter share.

The models inspired by the stochastic programs introduced in the preceding paragraph produce solutions with *good performances on average*. However, the concern for other properties of the outcome, e.g., the variability of such returns or the return in the less favorable scenarios, have motivated research into alternative approaches that differ from the prototypical expected-value problem (2.4). One of the most straightforward ways to reflect these concerns is to replace the risk-neutral expected value with another risk measure, such as the variance or the conditional value at risk (CVaR) [151, 116, 28].

Using alternative risk measures is not the only way to address other decision maker's goals. Conversely, there are several other completely different paradigms designed to protect the decision maker against harmful realizations of the uncertain parameter. Let $\mathbf{z}^S \in \arg \min_{\mathbf{z} \in Z} \mathbb{E}[f(\mathbf{z}; \mathbf{Y})]$ and $v^S = \mathbb{E}[f(\mathbf{z}^S; \mathbf{Y})]$. Although v^S is optimal in expectation, the value $f(\mathbf{z}^S; \mathbf{y}_i)$ can still be very large for a particular realization of the random parameter $(\mathbf{y}_i \in \mathcal{Y}) \sim \mathbf{Y}$. Therefore, a decision maker could be legitimately interested in being protected against the worst-case outcome of the random variable \mathbf{Y} from among a set of possible values $\Lambda \subseteq \mathcal{Y}$, known in the literature as the *uncertainty set* [130]. If that is the case, the decision maker can alternatively solve the robust optimization (RO) counterpart of problem (2.4):

$$\min_{\mathbf{z} \in Z} \max_{\mathbf{y} \in \Lambda} f(\mathbf{z}; \mathbf{y}). \quad (2.8)$$

Let $\varphi(\mathbf{z}) = \max_{\mathbf{y} \in \Lambda} f(\mathbf{z}; \mathbf{y})$. The optimal robust decision can be obtained solving $\mathbf{z}^R \in \arg \min_{\mathbf{z} \in Z} \varphi(\mathbf{z})$. As in the previous case, the expected cost of this choice can be calculated as $v^R = \mathbb{E}[f(\mathbf{z}^R; \mathbf{Y})]$. Thus, we can define the *price of robustness* as $\varrho = v^R - v^S$. By construction of problem (2.3), we have $\varrho \geq 0$ assuming perfect information on the probability distribution of \mathbf{Y} . Therefore, producing robust solutions \mathbf{z}^R , which protect against harmful realizations of the uncertainty, typically implies paying a price in the performance on average [18]. However, in many applications the support \mathcal{Y} is certain but the knowledge about the true probability distribution is limited, null, or imprecise, resulting in robust decisions that can outperform the risk-neutral counterparts, achieving a lower expected value (negative price of robustness) in practice [20].

Distributionally Robust Optimization (DRO) is similar in spirit but follows a different approach. This paradigm does not protect the decision maker against the worst realization of the uncertainty but rather against the worst possible distribution among a set of candidate distributions $\hat{\mathbb{Q}}$ of the uncertainty vector [83]. The key ingredient of this approach is to define an *ambiguity set* in which the worst distribution lies [139], e.g., a ball Θ centered around the empirical distribution of \mathbf{Y} , whose design is based on the dataset \mathcal{Y}_N . With these ingredients, the distributionally robust problem can be written as

$$\min_{\mathbf{z} \in Z} \max_{\hat{\mathbb{Q}} \in \Theta} \mathbb{E}_{\hat{\mathbb{Q}}} [f(\mathbf{z}; \mathbf{Y})]. \quad (2.9)$$

When Θ only includes the empirical distribution, the solution to this problem coincides with the solution of (2.7). In contrast, when the ball Θ has an infinite radius, the outcome of problem (2.8) can be recovered under some conditions. Therefore, balls with a finite radius can potentially produce solutions with an intermediate degree of coverage against risk. This is also possible in RO, designing uncertainty sets that satisfy $\Lambda \subset \mathcal{Y}$ [15]. Equally interesting is the fact that RO and DRO can produce more tractable mathematical problems than their stochastic counterparts, resulting in reformulations with more favorable time complexities [64, 57, 16]. For a more in-depth discussion of the innumerable robust variants found in the literature and their properties, we refer the reader to the monographs [23, 60, 13, 130] and the references therein.

The use of robust paradigms is prominent when the knowledge regarding the uncertain phenomenon is limited. However, in many tasks, there is *good* information available on the random distribution, e.g., in the form of abundant and reliable data, and the same decision tasks are faced periodically. In the remainder of this thesis, we focus specifically on those tasks where the performance on average gains importance, and therefore, we are interested in data-driven approaches closer to problem (2.7). Next, Section 2.2 discusses the potential of contextual information in this setting and presents

several state-of-the-art frameworks that leverage contextual information.

2.2 Decision making with contextual information

As discussed in Chapter 1, the adoption and development of new information technologies has dramatically increased the amount of data available to decision makers [111, 31]. These data come not only from samples of the uncertain parameters affecting the decision-making task, but are also produced by other potentially related phenomena within the task's context, resulting in what we know as contextual information [30, 29]. Contextual information is a valuable resource that can boost decision making and is present today in almost every situation where a decision has to be made. Historically, none of the methodologies introduced in previous sections considered contextual information directly, ignoring the benefits that this resource can provide to reduce uncertainty and improve decision making. This section addresses contextual information in more detail, discussing its potential to enhance previous paradigms and reviewing the state-of-the-art papers on the subject.

Before discussing how to leverage this new resource, it is best to describe the nature of contextual information in more detail. Some contextual information takes the form of a realization of a random variable or vector, which may lie in a discrete or continuous domain and whose relation to the uncertain parameters is governed by a (most likely unknown) joint probability distribution. Conversely, many pieces of contextual information do not exhibit random behavior, such as the day of the week or the hour of the day related to the decision to be made. Regardless of its nature, any piece of information to be used as contextual information must be available before making the decision. When some relevant contextual information $(\mathbf{x} \in \mathcal{X} \subseteq \mathbb{R}^p) \sim \mathbf{X}$ is available, one can reformulate problem (2.4) as follows:

$$\min_{\mathbf{z} \in \mathcal{Z}} \mathbb{E}[f(\mathbf{z}; \mathbf{Y}) | \mathbf{X} = \mathbf{x}]. \quad (2.10)$$

In practice, neither the *joint* distribution of \mathbf{X} and \mathbf{Y} , nor the conditional distribution of \mathbf{Y} given $\mathbf{X} = \mathbf{x}$ are known and therefore problem (2.10) cannot be solved. In addition, even if the true distribution were known and decision \mathbf{z} was fixed, problem (2.10) would typically require computing the expectation of a function of a continuous random vector (i.e., a multivariate integral), which is, in itself, a hard task in general [68]. Instead of the true distribution, the only information that the decision maker typically has is a sample $S = \{(\mathbf{y}_i, \mathbf{x}_i), \forall i \in \mathcal{N}\}$, where $\mathbf{y}_i \in \mathcal{Y} \subseteq \mathbb{R}^m$ is a realization of the random variable \mathbf{Y} recorded together with or related to the context $\mathbf{x}_i \in \mathcal{X} \subseteq \mathbb{R}^p$, and \mathcal{N} denotes the set of available samples.

Against this background, problem (2.10) is alternatively replaced with a *surrogate* optimization problem, in the hope that the solution to the latter is good enough for the

former. In this direction, different approaches have been proposed to construct such a surrogate optimization problem. For instance, the traditional *modus operandi* follows the rule “first predict, then optimize,” which results in the following *surrogate problem* to approximate the solution to (2.10)

$$\min_{\mathbf{z} \in Z} f(\mathbf{z}; \hat{\mathbf{y}}), \quad (2.11)$$

where $\hat{\mathbf{y}} \in \mathbb{R}^m$ denotes an estimate of the outcome of the uncertainty \mathbf{Y} under a particular piece of contextual information \mathbf{x} . The surrogate problem (2.11) is attractive for several reasons. First and foremost, it is much simpler and faster to solve than (2.10). Actually, it is a *deterministic* optimization problem which, as opposed to (2.10), only requires evaluating the cost function $f(\mathbf{z}; \cdot)$ at the single value or scenario $\hat{\mathbf{y}}$. Furthermore, problem (2.11) seems intuitive and natural, especially when $\hat{\mathbf{y}}$ represents “the most likely value” for \mathbf{Y} given $\mathbf{X} = \mathbf{x}$. Indeed, the single scenario $\hat{\mathbf{y}}$ is often chosen as an estimate of the expected value of the uncertainty \mathbf{Y} conditional on $\mathbf{X} = \mathbf{x}$, that is, $\hat{\mathbf{y}} \approx \mathbb{E}[\mathbf{Y}|\mathbf{X} = \mathbf{x}]$, where, logically, the approximation is built from the available sample S . In the realm of forecasting, the estimate $\hat{\mathbf{y}}$ is usually referred to as a *point prediction* and we refer to this approach as FO from forecasting.

To build the estimate $\hat{\mathbf{y}} \approx \mathbb{E}[\mathbf{Y}|\mathbf{X} = \mathbf{x}]$, a function $g^{\text{FO}} : \mathcal{X} \times \mathbb{R}^q \rightarrow \mathbb{R}^m$ is normally chosen from a \mathbf{w} -parameterized family G^{FO} , with $\mathbf{w} \in \mathbb{R}^q$, to construct the forecasting model $\hat{\mathbf{y}} = g^{\text{FO}}(\mathbf{x}; \mathbf{w})$. The goodness of a certain parameter vector \mathbf{w} is quantified in terms of a loss function $l^{\text{FO}}(\mathbf{y}, \hat{\mathbf{y}}) : \mathcal{Y} \times \mathbb{R}^m \rightarrow \mathbb{R}$ that measures the accuracy of the estimate. Then, given the sample $S = \{(\mathbf{y}_i, \mathbf{x}_i), \forall i \in \mathcal{N}\}$, the choice of \mathbf{w} is driven by the minimization of the *in-sample* loss, yielding

$$\mathbf{w}^{\text{FO}} \in \arg \min_{\mathbf{w} \in \mathbb{R}^q} \sum_{i \in \mathcal{N}} l^{\text{FO}}(\mathbf{y}_i, g^{\text{FO}}(\mathbf{x}_i; \mathbf{w})). \quad (2.12)$$

Note that when the mapping is a linear function $g^{\text{FO}}(\mathbf{x}_i; \mathbf{w}) = \mathbf{w}^\top \mathbf{x}_i$ and the root mean square error is chosen as the loss function, problem (2.12) reduces to the classical linear regression $\mathbf{w}^{\text{FO}} = \arg \min_{\mathbf{w} \in \mathbb{R}^q} \sum_{i \in \mathcal{N}} (\mathbf{y}_i - \mathbf{w}^\top \mathbf{x}_i)^2$. In this framework, the optimal decision \mathbf{z}^{FO} under the context $\mathbf{X} = \mathbf{x}$ is thus obtained by solving the following deterministic problem

$$\mathbf{z}^{\text{FO}}(\mathbf{x}) \in \arg \min_{\mathbf{z} \in Z} f(\mathbf{z}; g^{\text{FO}}(\mathbf{x}; \mathbf{w}^{\text{FO}})). \quad (2.13)$$

Thus, this approach relies on a forecast of the uncertainty variable \mathbf{Y} , in particular, a *good* estimate of $\mathbb{E}[\mathbf{Y}|\mathbf{X} = \mathbf{x}]$. Even though this approach is intuitive and may perform relatively well in many situations, it is fundamentally flawed for the following two basic reasons. First, since $\hat{\mathbf{y}} \approx \mathbb{E}[\mathbf{Y}|\mathbf{X} = \mathbf{x}]$ in FO, the surrogate problem (2.11) works as a

proxy of the problem

$$\min_{\mathbf{z} \in Z} f(\mathbf{z}; \mathbb{E}[\mathbf{Y}|\mathbf{X} = \mathbf{x}]), \quad (2.14)$$

which, in general, is not equivalent to (2.10). Second, even in those cases where these two problems are indeed equivalent, for example, when f is linear, the loss function l^{FO} , which is used to compute \mathbf{w}^{FO} (e.g., the squared error), is only intended to obtain a statistically good estimate of $\mathbb{E}[\mathbf{Y}|\mathbf{X} = \mathbf{x}]$ and does not account for the objective function f and the feasible set Z . For instance, approach (2.12)-(2.13) is unable to capture that overestimating $\mathbb{E}[\mathbf{Y}|\mathbf{X} = \mathbf{x}]$ could worsen the objective function f much more than underestimating it. Next, we give an example to illustrate this phenomenon and to clarify some of the elements introduced so far in the chapter.

An illustrative example

The example described in the following paragraphs demonstrates the fact that a model trained for a prediction task might not always be the best option to use in a decision-making problem. To this end, we consider a series of decision tasks characterized by the underlying optimization problem

$$\min_{3 \leq z \leq 8} |z - y|, \quad (2.15)$$

where $y \in \mathbb{R}$ is a parameter that unequivocally determines the problem. The decision maker cannot solve (2.15) directly because the parameter y is governed by a random variable $y \sim Y$ and the realization of this variable is unknown when the decision $z \in [3, 8]$ must be made. The random variable Y follows a quadratic model $Y = 0.6X^2 + 0.7X + \epsilon$ where $X \sim U(1, 4)$ is a contextual random variable and $\epsilon \sim U(-1, 1)$ is a random noise. Unfortunately, this true mapping is also unknown to the decision maker. Instead, a collection of samples $S = \{(y_i, x_i), i \in \mathcal{N}\}$ is available with $\mathcal{N} = \{1, \dots, N\}$. Equipped with S , the decision maker has to face a collection of new / future decision tasks represented by the dataset $\tilde{S} = \{(y_j, x_j), j \in \tilde{\mathcal{N}}\}$ with $\tilde{\mathcal{N}}$ defined analogously to \mathcal{N} . In this demonstrative example, we set $N = \tilde{N} = 5000$. In the literature, the sets S and \tilde{S} are known as *training set* and *test set*, respectively. We also use the terms *in-sample* and *out-of-sample* to refer to decisions or metrics related to S and \tilde{S} .

The traditional way in which FO is applied proceeds first selecting a family g^{FO} . In this case, we consider a linear model of the form $\hat{y} = g^{\text{FO}}(x) = w_1x + w_0$ to produce point forecasts $\hat{y}_j^{\text{FO}}(x_j)$ that we then plug in problem (2.15). The parameters $w_1^{\text{FO}}, w_0^{\text{FO}}$, which minimize the root mean square error (RMSE) on the set S are calculated using a standard linear regression. Although the model $\hat{y}_j^{\text{FO}} = w_1^{\text{FO}}x_j + w_0^{\text{FO}}$ is general and can be used for other purposes, the FO approach does not guarantee that the coefficients

$w_1^{\text{FO}}, w_0^{\text{FO}}$ produce the collection of estimates \hat{y}_j that obtain the minimum average value of the objective function. To demonstrate this, we compare a second linear model whose parameters $w_1^{\text{PR}}, w_0^{\text{PR}}$ (we use PR from prescriptive) are selected taking into account the feasible region of problem (2.15). We take the occasion to clarify that those methods, which consider properties of the underlying decision-making problems are sometimes referred to in the literature as *prescriptive* approaches as opposed to the *predictive* approaches such as FO. In this example, $w_1^{\text{PR}}, w_0^{\text{PR}}$ are inferred performing a linear regression in the subset $\{(y_i, x_i) : 3 \leq y_i \leq 8\}$, inspired by the boundaries of the underlying problem.

	Predictive	Prescriptive
Prediction error (RMSE)	0.49	0.64
Objective value (\hat{v})	1.01	0.96

Table 2.1: Average out-of-sample predictive error (RMSE) and objective function value \hat{v} by a model that minimizes the in-sample RMSE (predictive) and another that take into account the feasible region (prescriptive).

The RMSE and average objective function value \hat{v} , defined $\hat{v} = 1/\tilde{N} \sum_{j=1}^{\tilde{N}} |z_j - y_j|$, obtained by the predictive and prescriptive linear models are collated in Table 2.1. As the reader may have already suspected, the RMSE achieved by the predictive linear model used in FO is the lowest since it is designed to minimize this type of error. However, the fact that the prescriptive model obtains a higher RMSE does not prevent it from scoring the lowest average objective function value \hat{v} , improving on its counterpart by 5.5% and showing room to enhance this strategy.

The prescriptive strategy used in this example was for illustration purposes only. The following sections introduce four formal data-driven frameworks that leverage contextual information in expected value problems in the form of (2.10). The first three, reviewed in Sections 2.2.1-2.2.3, are state-of-the-art frameworks already present in the literature, while the fourth framework, introduced in Section 2.2.4, is developed within this thesis and proposes a bilevel formulation to overcome some of the weaknesses of its counterparts.

2.2.1 Conditional distribution

The first of the approaches follows from the observation that problem (2.10) can be equivalently recast as

$$\min_{\mathbf{z} \in Z} \mathbb{E}[f(\mathbf{z}; \mathbf{Y}) | \mathbf{X} = \mathbf{x}] = \min_{\mathbf{z} \in Z} \mathbb{E}_{\mathcal{Q}_{|\mathbf{x}}} [f(\mathbf{z}; \mathbf{Y})], \quad (2.16)$$

where $\mathcal{Q}_{|\mathbf{x}}$ represents the conditional probability distribution of \mathbf{Y} given $\mathbf{X} = \mathbf{x}$. Thus, a family of surrogate decision-making models can be introduced with the following general

form

$$\min_{\mathbf{z} \in Z} \mathbb{E}_{\hat{\mathcal{Q}}_{|\mathbf{x}}} [f(\mathbf{z}; \mathbf{Y})], \quad (2.17)$$

where $\hat{\mathcal{Q}}_{|\mathbf{x}}$ is an approximation of the unknown probability measure $\mathcal{Q}_{|\mathbf{x}}$ that is constructed from the available sample $S = \{(\mathbf{y}_i, \mathbf{x}_i), \forall i \in \mathcal{N}\}$. For the surrogate problem (2.17) to be computationally tractable, the proxy $\hat{\mathcal{Q}}_{|\mathbf{x}}$ is often built as a discrete probability distribution supported on a finite number of points, more specifically, on the \mathbf{y} -locations of the sample, i.e., $\{\mathbf{y}_i, \forall i \in \mathcal{N}\}$. This way, the solution to (2.17) under context $\mathbf{X} = \mathbf{x}$ can be generically expressed as

$$\mathbf{z}^{\text{ML}}(\mathbf{x}) \in \arg \min_{\mathbf{z} \in Z} \sum_{i \in \mathcal{N}} g^{\text{ML}}(\mathbf{x}, \mathbf{x}_i; \mathbf{w}) f(\mathbf{z}; \mathbf{y}_i), \quad (2.18)$$

with $\{g^{\text{ML}}(\mathbf{x}, \mathbf{x}_i; \mathbf{w}), \forall i \in \mathcal{N}\}$ being the probability masses that the specific proxy $\hat{\mathcal{Q}}_{|\mathbf{x}}$ places on $\{\mathbf{y}_i, \forall i \in \mathcal{N}\}$, generally computed through machine learning techniques (ML stands for Machine Learning). These masses or weights are determined as a function $g^{\text{ML}} : \mathcal{X} \times \mathcal{X} \times \mathbb{R}^q \rightarrow \mathbb{R}$ of the historical contextual information \mathbf{x}_i , the current context \mathbf{x} , and some parameters \mathbf{w} .

In essence, this scheme adapts the SAA to the case of *conditional* stochastic programs. It was first formalized in [17] and, since then, has been subject to a number of improvements (e.g., regularization procedures for bias-variance reduction [129]; robustification [19]; and algorithmic upgrades [47]) and extensions, e.g., to a dynamic decision-making setting [21]. Recently, the work in [100] introduced a bilevel formulation to optimally tune the parameters \mathbf{w} that determine the weights $g^{\text{ML}}(\mathbf{x}, \mathbf{x}_i; \mathbf{w})$. Using our notation, the method proposed in [100] can be formulated as follows:

$$\mathbf{w}^{\text{ML}} \in \arg \min_{\mathbf{w} \in \mathbb{R}^q; \hat{\mathbf{z}}_i} \sum_{i \in \mathcal{N}} f(\hat{\mathbf{z}}_i; \mathbf{y}_i) \quad (2.19a)$$

$$\text{s.t. } \hat{\mathbf{z}}_i \in \arg \min_{\mathbf{z} \in Z} \sum_{i' \in \mathcal{N}: i' \neq i} g^{\text{ML}}(\mathbf{x}_i, \mathbf{x}_{i'}; \mathbf{w}) f(\mathbf{z}; \mathbf{y}_{i'}), \quad \forall i \in \mathcal{N}, \quad (2.19b)$$

where the function $g^{\text{ML}} : \mathcal{X} \times \mathcal{X} \times \mathbb{R}^q \rightarrow \mathbb{R}$ used to compute the weights can be chosen from a catalog of several classical machine learning algorithms G^{ML} such as k -nearest neighbors, Nadaraya-Watson kernel regression or Random Forest. The author of [100] resorts to tailor-made approximations and greedy algorithms for each machine learning technique that is used to construct function g^{ML} , but the paper does not provide a general-purpose solution strategy valid for any function g^{ML} . After solving (2.19), the optimal decision $\mathbf{z}^{\text{ML}}(\mathbf{x})$ under context $\mathbf{X} = \mathbf{x}$ is obtained by solving (2.18) with $\mathbf{w} = \mathbf{w}^{\text{ML}}$.

The surrogate problems (2.11) and (2.17) are, by design, different, in part because

they are the result of distinct frameworks to address the conditional stochastic program (2.10). The surrogate problem (2.11) is based on the assumption that it is possible to find a good decision \mathbf{z} in terms of the conditional expected cost $\mathbb{E}[f(\mathbf{z}; \mathbf{Y})|\mathbf{X} = \mathbf{x}]$ by optimizing that decision for a single scenario $\hat{\mathbf{y}}$ of the uncertainty \mathbf{Y} . Naturally, all the complexity of this approach lies in how to infer, from the data sample S , the single scenario $\hat{\mathbf{y}}$ that unlocks the best decision \mathbf{z} . This inference process uses global methods that consider all data points in the sample to obtain more robust decision mappings. In contrast, all the difficulty of the surrogate problem (2.17) resides in how to retrieve a good approximation of the true conditional distribution $\mathcal{Q}_{|\mathbf{x}}$ from the sample S . Such an approximation is performed using local machine learning methods that only employ data close to the given context \mathbf{x} and consequently, a large amount of data is required to avoid overfitting. In more practical terms, embedding local machine learning methods into the estimation problem (2.19) makes this problem computationally intractable in most cases. Besides, the surrogate problem (2.11) is computationally less demanding than (2.17), because the latter requires evaluating the cost function $f(\mathbf{z}; \cdot)$ for multiple values of the uncertainty \mathbf{Y} .

2.2.2 Decision rule

A second class of surrogate decision-making models arises from the idea of using the sample S to directly learn the optimal decision \mathbf{z} as a function of the context \mathbf{x} , thereby bypassing the need for constructing the estimate $\hat{\mathbf{y}}$ or the proxy distribution $\hat{\mathcal{Q}}_{|\mathbf{x}}$. Following this logic, we seek a decision rule or mapping $g^{\text{DR}} : \mathcal{X} \times \mathbb{R}^q \rightarrow \mathbb{R}^n$ from a family G^{DR} so that $\hat{\mathbf{z}} = g^{\text{DR}}(\mathbf{x}; \mathbf{w}) \approx \arg \min_{\mathbf{z} \in Z} \mathbb{E}[f(\mathbf{z}; \mathbf{Y})|\mathbf{X} = \mathbf{x}]$. Particularizing for the empirical distribution of the data, this approach renders

$$\mathbf{w}^{\text{DR}} \in \arg \min_{\mathbf{w} \in \mathbb{R}^q} \sum_{i \in \mathcal{N}} f(g^{\text{DR}}(\mathbf{x}_i; \mathbf{w}); \mathbf{y}_i) \quad (2.20a)$$

$$\text{s.t. } g^{\text{DR}}(\mathbf{x}_i; \mathbf{w}) \in Z, \quad \forall i \in \mathcal{N}. \quad (2.20b)$$

One clear advantage of directly learning the optimal decision policy is that, after solving (2.20), the decision \mathbf{z}^{DR} to be implemented under context $\mathbf{X} = \mathbf{x}$ is efficiently computed as follows:

$$\mathbf{z}^{\text{DR}}(\mathbf{x}) = g^{\text{DR}}(\mathbf{x}; \mathbf{w}^{\text{DR}}). \quad (2.21)$$

In effect, the mapping (2.21) constitutes the surrogate decision-making model itself. This method, which aims to determine an optimal decision rule, is denoted by DR (acronym of Decision Rule). Nevertheless, feasibility issues may arise as this approach does not necessarily guarantee that the resulting \mathbf{z}^{DR} obtained through (2.21) belongs to Z in any context \mathbf{x} when the sample set S is finite. The authors of [7] propose and

investigate this approach for the popular newsvendor problem, for which they consider a linear decision rule. Their newsvendor formulation does not involve any constraint and therefore, decisions yielded by (2.21) are always valid. If feasibility issues arise in a particular application of this framework, one can circumvent this issue by adding a projection step onto the feasible set Z at the expense of a significant increase in the computational burden, in general.

2.2.3 Smart predict, then optimize

In view of FO's design flaws, a number of approaches have proposed replacing the problem-agnostic l^{FO} , which is generally used in (2.12) with a problem-aware loss function $l^{\text{SP}}(\mathbf{y}, \hat{\mathbf{y}}) = f(\hat{z}(\hat{\mathbf{y}}); \mathbf{y})$, where $l^{\text{SP}} : \mathbb{R}^m \times \mathbb{R}^m \rightarrow \mathbb{R}$ and $\hat{z} : \mathcal{Y} \rightarrow Z$ defined as $\hat{z}(\mathbf{y}) = \arg \min_{\mathbf{z} \in Z} f(\mathbf{z}; \mathbf{y})$. Therefore, function l^{SP} evaluates the loss of optimality associated with the decision $\hat{z}(\hat{\mathbf{y}})$ that is prescribed by the surrogate decision-making problem (2.11) for the single value $\hat{\mathbf{y}}$. Accordingly, the optimal parameter vector \mathbf{w}^{SP} is obtained as the one that minimizes the *in-sample* optimality loss, i.e.,

$$\mathbf{w}^{\text{SP}} \in \arg \min_{\mathbf{w} \in \mathbb{R}^q} \sum_{i \in \mathcal{N}} f(\hat{z}(g^{\text{SP}}(\mathbf{x}_i; \mathbf{w})); \mathbf{y}_i), \quad (2.22)$$

where the function $g^{\text{SP}} : \mathcal{X} \times \mathbb{R}^q \rightarrow \mathbb{R}^m$ is chosen from a family of functions G^{SP} . We use the acronym SP, which stands for “Smart Predict”, to refer to this setup. Solving problem (2.22) using descent optimization methods requires computing the gradient of the loss function $l^{\text{SP}}(\mathbf{y}, \hat{\mathbf{y}})$ with respect to \mathbf{w} . This may not be feasible, since it involves the differentiation of the discontinuous function $\hat{z}(\mathbf{y})$ [90]. To overcome this difficulty, a great deal of research has been devoted to finding methods to approximate the gradient of (2.22) for particular instances. The work developed in [76], for example, describes a procedure to solve (2.22) under the following three conditions: i) f is quadratic, ii) the uncertainty is only present in the coefficients of the linear terms of f , and iii) no constraints are imposed on the decision \mathbf{z} , which means $Z = \mathbb{R}^n$. Some years later, the authors [50] proposed a heuristic gradient-based procedure to solve (2.22) for strongly convex problems with deterministic equality constraints and inequality chance constraints. Almost concurrently, reference [56] discusses the difficulties of solving (2.22) in the case of linear problems, since such a formulation may lead to an uninformative loss function. To overcome this issue, they successfully develop a convex surrogate that allows $g^{\text{SP}}(\mathbf{x}_i; \mathbf{w})$ to be efficiently trained in the linear case. Finally, the authors in [140] suggest a similar approach to that of [50] in combinatorial problems with a regularized linear objective function.

2.2.4 Contextual bilevel framework

The three aforementioned approaches are part of the most recent efforts found in the literature to address conditional stochastic programs in the form of (2.10). This section

presents a forth framework, developed within this thesis and published in [102], which is one of the main methodological contributions of this thesis.

The last four references reviewed in Section 2.2.3 propose ad-hoc gradient methods for specific instances of (2.22). However, to the best of our knowledge, the technical literature lacks a general-purpose procedure to solve this problem using available optimization solvers. To fill this gap, we propose the following bilevel program [44] as a generic mathematical formulation of (2.22):

$$\mathbf{w}^{\text{BL}} \in \arg \min_{\mathbf{w} \in \mathbb{R}^q; \hat{\mathbf{z}}_i} \sum_{i \in \mathcal{N}} f(\hat{\mathbf{z}}_i; \mathbf{y}_i) \quad (2.23a)$$

$$\text{s.t. } \hat{\mathbf{z}}_i \in \arg \min_{\mathbf{z} \in \mathcal{Z}} f(\mathbf{z}; g^{\text{BL}}(\mathbf{x}_i; \mathbf{w})), \quad \forall i \in \mathcal{N}, \quad (2.23b)$$

where $g^{\text{BL}} : \mathcal{X} \times \mathbb{R}^q \rightarrow \mathbb{R}^m$ is selected similarly to g^{FO} and g^{SP} . Problem (2.23) is formulated as a bilevel optimization model commonly used to mathematically characterize non-cooperative and sequential Stackelberg games in which the *leader* makes her decisions while anticipating the reaction of the *follower* [36]. In this sense, the upper-level problem determines the optimal parameter vector \mathbf{w} anticipating the decision provided by each lower-level problem (2.23b) if the value $\hat{\mathbf{y}}_i$ is given by $g^{\text{BL}}(\mathbf{x}_i; \mathbf{w})$. We denote this approach based on bilevel programming by BL (acronym for BiLevel). Later in this section, we discuss the assumptions that problem (2.10) must satisfy so that problem (2.23) can be reformulated as a single-level optimization problem to be solved using off-the-shelf optimization solvers. Although solving the bilevel problem (2.23) may be computationally expensive, this is a task that can be performed offline. Once \mathbf{w}^{BL} has been determined, the optimal decision \mathbf{z}^{BL} under context $\mathbf{X} = \mathbf{x}$ is computed by solving the following problem:

$$\mathbf{z}^{\text{BL}}(\mathbf{x}) \in \arg \min_{\mathbf{z} \in \mathcal{Z}} f(\mathbf{z}; g^{\text{BL}}(\mathbf{x}; \mathbf{w}^{\text{BL}})). \quad (2.24)$$

The bilevel program (2.23) computes the value of the parameter vector \mathbf{w} that maximizes the *in-sample* performance of the surrogate decision-making model (2.24). For this estimation to be of use, it must be guaranteed that under two contexts $\mathbf{x}_i, \mathbf{x}'_i$, such that $\mathbf{x}_i = \mathbf{x}'_i$, it holds $\hat{\mathbf{z}}_i = \hat{\mathbf{z}}'_i$, i.e., under equal contexts, equal decisions. This is a condition that is reminiscent of the notion of *non-anticipativity* in Stochastic Programming. Importantly, this condition is automatically satisfied if the solution to the lower-level problem (2.23b) is unique for any value of \mathbf{w} . Otherwise, the bilevel program (2.23) would choose the $\hat{\mathbf{z}}_i$ from the optimal solution set of (2.23b) that minimizes the upper-level objective function (2.23a) *given*—i.e., by anticipating—the uncertainty outcome \mathbf{y}_i . This is so, because the bilevel program (2.23), as we have formulated it, delivers the optimistic Stackelberg solution [45]. For instance, let us assume that there

exists a value $\tilde{\mathbf{w}}$ such that $f(\mathbf{z}; g^{\text{BL}}(\mathbf{x}_i; \tilde{\mathbf{w}})) = \vartheta$ for all $i \in \mathcal{N}$, where ϑ is a constant. In this case, the lower-levels (2.23b) boil down to feasibility problems imposing that $\mathbf{z} \in Z$ and therefore, $\hat{\mathbf{z}}_i$ can violate non-anticipativity and adapt to realization \mathbf{y}_i for all $i \in \mathcal{N}$. More importantly, using $\tilde{\mathbf{w}}$ in (2.24) would lead to degenerate and highly suboptimal decisions under any context $\mathbf{X} = \mathbf{x}$. This issue is reported in [56] for linear objective functions, where the authors propose a convex surrogate function of l^{SP} to train meaningful instances of model $g^{\text{SP}}(\cdot; \mathbf{w}^{\text{SP}})$.

Next, we discuss the procedure to solve (2.23) using off-the-shelf optimization solvers. Suppose that the lower-level problem (2.23b) is strongly convex in \mathbf{z} and satisfies a Slater condition [43], then the classical approach to solve (2.23) is to replace the lower level (2.23b) with its equivalent Karush-Kuhn-Tucker (KKT) conditions [28]. To illustrate this, let us assume that the feasible set Z is defined by the following constraints:

$$h_k^{\text{in}}(\mathbf{z}) \leq 0, \quad k = 1, \dots, K, \quad (2.25)$$

$$h_l^{\text{eq}}(\mathbf{z}) = 0, \quad l = 1, \dots, L, \quad (2.26)$$

where $h_k^{\text{in}} : Z \rightarrow \mathbb{R}$ are convex functions and $h_l^{\text{eq}} : Z \rightarrow \mathbb{R}$ are affine functions. After this particularization, the single-level KKT reformulation of problem (2.23) renders:

$$\mathbf{w}^{\text{BL}} \in \arg \min_{\mathbf{w}, \hat{\mathbf{z}}_i, \lambda_{ki}, v_{li}} \sum_{i \in \mathcal{N}} f(\hat{\mathbf{z}}_i; \mathbf{y}_i) \quad (2.27a)$$

$$\begin{aligned} \text{s.t. } & \nabla f(\hat{\mathbf{z}}_i, g^{\text{BL}}(\mathbf{x}_i; \mathbf{w})) + \sum_{k=1}^K \lambda_{ki} \nabla h_k^{\text{in}}(\hat{\mathbf{z}}_i) \\ & + \sum_{l=1}^L v_{li} \nabla h_l^{\text{eq}}(\hat{\mathbf{z}}_i) = 0, \quad \forall i \in \mathcal{N} \end{aligned} \quad (2.27b)$$

$$h_k^{\text{in}}(\hat{\mathbf{z}}_i) \leq 0, \quad \forall k, \quad \forall i \in \mathcal{N} \quad (2.27c)$$

$$h_l^{\text{eq}}(\hat{\mathbf{z}}_i) = 0, \quad \forall l, \quad \forall i \in \mathcal{N} \quad (2.27d)$$

$$\lambda_{ki} \geq 0, \quad \forall k, \quad \forall i \in \mathcal{N} \quad (2.27e)$$

$$\lambda_{ki} h_k^{\text{in}}(\hat{\mathbf{z}}_i) = 0, \quad \forall k, \quad \forall i \in \mathcal{N}, \quad (2.27f)$$

where $\lambda_{ki}, v_{li} \in \mathbb{R}$ are, respectively, the Lagrange multipliers related to constraints (2.25) and (2.26) for each lower-level problem, (2.27a) is the objective of the upper level, and constraints (2.27b), (2.27c) and (2.27d), (2.27e), (2.27f), are the stationarity, primal feasibility, dual feasibility and slackness conditions, respectively. As discussed in [121], problem (2.27) violates the Mangasarian-Fromovitz constraint qualification at every feasible point and therefore, interior-point methods fail to find even a local optimal solution to this problem. To overcome this issue, a regularization approach was first introduced in [122] and further investigated in [114]. This method replaces all complementarity

constraints (2.27f) by:

$$-\sum_{ki} \lambda_{ki} h_k^{in}(\hat{\mathbf{z}}_i) \leq \epsilon, \quad (2.28)$$

where ϵ is a small non-negative scalar that allows reformulating (2.27) as a parametrized non-linear optimization problem, which typically satisfies constraint qualifications and can therefore be efficiently solved by standard non-linear optimization solvers. From hereon, we refer to this approach as BL-R. Authors of [122] prove that, as ϵ tends to 0, the solution of the parametrized problems tends to a *local* optimal solution of problem (2.27).

An alternative procedure to find *global* solutions can be used if problem (2.27) satisfies the following additional conditions: i) f is quadratic and convex, that is, $f(\mathbf{z}; \mathbf{y}, \mathbf{Q}) = \mathbf{z}^\top \mathbf{Q} \mathbf{z} + \mathbf{y}^\top \mathbf{z}$ where $\mathbf{Q} \in \mathbb{R}^{n \times n}$ is a known positive semidefinite matrix and $\mathbf{y} \in \mathbb{R}^n$ is the only uncertain parameter vector, ii) the forecasting model $g^{\text{BL}}(\mathbf{x}_i; \mathbf{w})$ is linear on the feature vector \mathbf{x}_i , and iii) functions h_k^{in}, h_l^{eq} are linear with $h_k^{in}(\mathbf{z}_i) = \mathbf{a}_k^\top \mathbf{z}_i + b_k$ and $h_l^{eq}(\mathbf{z}_i) = \mathbf{d}_l^\top \mathbf{z}_i + e_l$ where $\mathbf{a}_k, \mathbf{d}_l \in \mathbb{R}^n$ and $b_k, e_l \in \mathbb{R}$. After particularizing for these conditions and linearizing the complementarity slackness conditions according to Fortuny-Amat [59], problem (2.27) can be reformulated as the following mixed-integer quadratic programming problem:

$$\mathbf{w}^{\text{BL}} \in \arg \min_{\mathbf{w}, \hat{\mathbf{z}}_i, \lambda_{ki}, v_{li}, u_{ki}} \sum_{i \in \mathcal{N}} \hat{\mathbf{z}}_i^\top \mathbf{Q} \hat{\mathbf{z}}_i + \mathbf{y}_i^\top \hat{\mathbf{z}}_i \quad (2.29a)$$

$$\text{s.t. } \mathbf{Q} \hat{\mathbf{z}}_i + g^{\text{BL}}(\mathbf{x}_i; \mathbf{w}) + \sum_{k=1}^K \lambda_{ki} \mathbf{a}_k + \sum_{l=1}^L v_{li} \mathbf{d}_l = 0, \quad \forall i \in \mathcal{N} \quad (2.29b)$$

$$\mathbf{a}_k^\top \hat{\mathbf{z}}_i + b_k \leq 0, \quad \forall k, \quad \forall i \in \mathcal{N} \quad (2.29c)$$

$$\mathbf{d}_l^\top \hat{\mathbf{z}}_i + e_l = 0, \quad \forall l, \quad \forall i \in \mathcal{N} \quad (2.29d)$$

$$\lambda_{ki} \geq 0, \quad \forall k, \quad \forall i \in \mathcal{N} \quad (2.29e)$$

$$\lambda_{ki} \leq u_{ki} M^{\text{D}}, \quad \forall k, \quad \forall i \in \mathcal{N} \quad (2.29f)$$

$$\mathbf{a}_k^\top \hat{\mathbf{z}}_i + b_k \geq (u_{ki} - 1) M^{\text{P}}, \quad \forall k, \quad \forall i \in \mathcal{N} \quad (2.29g)$$

$$u_{ki} \in \{0, 1\}, \quad \forall k, \quad \forall i \in \mathcal{N}, \quad (2.29h)$$

where u_{ki} are binary variables, and $M^{\text{P}}, M^{\text{D}} \in \mathbb{R}^+$ are large enough constants whose values can be determined as proposed in [109]. The resulting model (2.29) is a single-level Mixed-Integer Quadratic Problem (MIQP) that can be solved using off-the-shelf optimization solvers such as CPLEX or Gurobi to global optimality. We denote this method by BL-M.

It is worth mentioning that if $\mathbf{Q} = \mathbf{0}$ and the objective function is thus linear, i.e. $f(\mathbf{z}_i) = \mathbf{y}^\top \mathbf{z}_i$, then optimization problem (2.29) has an incentive to provide the degenerate solution $\mathbf{w}^{\text{BL}} = \mathbf{0}$, as discussed in [56]. To address this issue, we can use

the following modified objective function $f(\mathbf{z}_i) = \mathbf{y}^\top \mathbf{z}_i + \rho \|\mathbf{z}_i\|_2^2$, with $\rho \in \mathbb{R}^+$, which includes a penalty proportional to the squared norm of the decision vector and allows us to reformulate (2.29) as a strongly convex quadratic program [140].

2.3 Iterative decision making

In this thesis, we investigate the performance of the approaches introduced in Sections 2.2 in realistic case studies based on the operational decision-making tasks that agents face in electricity markets. The underlying decision-making tasks share common ingredients in all applications: i) they are due periodically, and ii) do not imply large investments compared to those that determine the construction of new assets. In this thesis, we refer to these tasks as *iterative decision-making tasks*. This section addresses several practical considerations required to successfully apply the frameworks of Sections 2.2 to iterative decision-making tasks.

2.3.1 The world is not i.i.d.

Most of the theory on top of which stochastic programming is built relies on the assumption that the probability distributions that govern \mathbf{X} and \mathbf{Y} are fixed and that the samples of such variables behave as *independent and identically distributed* (i.i.d.) random variables [25]. In some cases, this is a reasonable assumption. For example, consider that some friends are playing a card game. In this game, several cards are on the table in each round, visible to all players. At this point, the reader may have already guessed that the cards on the table are contextual information. In effect, the player (decision maker) can use the cards on display to help determine her next move (decision). In this kind of situation, we can collect every move and its outcome as part of an i.i.d. sample. In this setting, the timestamp of the move is irrelevant since each time the same cards are on the table, the same probabilities and optimal decisions are replicated.

However, this situation is almost an exception, which happens in specific tasks typically related to games and inventions designed by humans. In most situations, the environment in which iterative decisions are made is similar but evolving. For example, every day, the decision maker encounters similar climate patterns, similar competitors, similar customer behavior and a similar economic reality. At the same time, the weather changes every minute, customers are not identical and the geopolitical and economic situation is slowly but constantly changing, to name a few.

The causal and evolving nature of the world in which we live justifies the fact that we can infer some relationships between contextual information and the uncertain parameters for a particular point in time and the need to update these relationships to maintain their effectiveness. Using a mathematical analogy, the linearization of a non-linear function (dynamic reality) computed at a point (current moment) is valid within a neighborhood, usually deteriorating as we move away (in time) from it. Thus, the

relationships or mappings between contextual information and uncertain parameters that hold in two independent periods are typically similar but generally different. This means that the assumption that samples are i.i.d. in a dataset recorded over long periods may not hold. Against this background, the next section is devoted to discussing a setting known in the literature as *rolling window* that can be combined with the frameworks presented in this chapter to tackle, in a practical way, iterative decision-making tasks that face an evolving uncertainty.

Before moving to the next section, it should be clarified that by iterative decision making, we are not referring to the type of problem addressed by multistage programming in which future decisions are conditioned by the decisions and realization of the uncertainty of previous stages. Rather, this thesis addresses classical two-stage stochastic problems that are faced sequentially. Recall that two-stage stochastic problems are characterized by a single stage / vector of decisions prior to the realization of the uncertainty, with possibly a set of recourse actions adopted *a posteriori*. Therefore all problems are independent of each other, without any intertemporal constraint binding them.

2.3.2 Rolling-window setting and its elements

As introduced in the previous section, the evolving nature of reality limits the value of the oldest information. This means that utilizing the whole set of samples collected over, for example, many years may not always be the best strategy to infer the target variables of the frameworks presented in Section 2.2 for two main reasons, namely i) the oldest samples may encode different relationships that could hide and distort the patterns in the most recent information and ii) additional samples may result in significant increases in the computational effort with little or null performance gains.

If either of these two conditions is fulfilled, it is more sensible to use only a portion of the available data that includes the most recent information. This subset of data, used to solve the optimization problem, is known in the literature as the *training set* and was already introduced in the example presented in Section 2.2. Furthermore, in iterative decision-making tasks, we typically have available a constant stream of new data that we can use to replace the oldest points belonging to our training set in a gradual update. This setting is usually called a *rolling-window* update [11]. New samples are not only useful for updating the training set, but are of capital importance for evaluating the performance of a model. The collection of samples used for that purpose is known as a *test set*, regardless of whether or not they are, at some point, also incorporated as part of the training set in a rolling-window update.

When samples are linked to specific points in time it is customary to use t instead of the generic subscript i . If this is the case, the symbol used to denote the training set \mathcal{N} is typically replaced with \mathcal{T} . In a rolling-window setting, we denote by $\mathcal{T}(t)$ the training

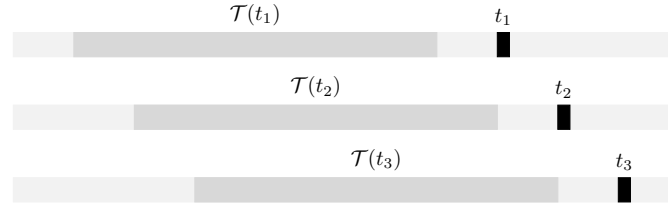


Figure 2.1: Illustration of the rolling-window setting for three subsequent decision tasks.

set linked with an element t of the test set $\tilde{\mathcal{T}}$. Therefore, for a sequence $t_1, t_2, t_3, \dots \in \tilde{\mathcal{T}}$ we can define the same number of different training sets $\mathcal{T}(t_1), \mathcal{T}(t_2), \mathcal{T}(t_3), \dots$. Note that the samples of the uncertain parameters attached to t_1 may only be available after some time and may not be ready to be incorporated into $\mathcal{T}(t_2)$. Figure 2.1 provides a graphic example that illustrates this setting. Furthermore, it is also possible that the training set is not updated in each time step but rather at fixed intervals due to technical restrictions or to ease the computational burden.

Under the current abundance of data, it is common for the decision maker to have lengthy datasets with many samples not even used to build the first training set of the rolling window $\mathcal{T}(t_1)$. Although this old data may not be used directly to estimate future relationships, it can still be valuable to the decision maker in other ways. For example, one can simulate the performance of different rolling windows to determine the optimal length $T = |\mathcal{T}|$, this is, the number of samples that produce the best results following the particular performance versus computational effort criterion of the decision maker. The dataset used for this target is known as *validation set* and can additionally or alternatively be leveraged to determine the best value of the model's *hyper-parameters*, i.e., parameters that do not appear in the underlying decision-making task but appear in the model or optimization problem due to the particular framework or algorithm employed in its resolution.

This section summarizes the most important elements related to the rolling-window setting. Next, we address an additional decision-making paradigm, closely related to this setting.

2.3.3 Online learning

In this chapter, we have introduced several decision-making paradigms that can be used to assist in iterative decision tasks. In this respect, we can establish connections and overlaps between these frameworks and the online learning literature. Online learning (OL) is characterized by two main features, namely i) it gathers techniques to assist with iterative decision-making tasks, as evidenced by the word *online* in its very name, and ii) its objective is to design algorithms that minimize the average long-term regret metric that we discuss later in this section. Online learning is a broad field and it is not within the scope of this section to address it fully. For a more detailed introduction to

the subject, we refer the reader to the monographs [124, 72, 107].

Algorithm 1 Online learning setting

```

1: for  $t = 1, \dots, T$  do
2:   Select  $\mathbf{z}_t \in Z \subseteq \mathbb{R}^n$ 
3:   Receive  $f_t : Z \rightarrow \mathbb{R}$ 
4:   Pay  $f_t(\mathbf{z}_t)$ 
5: end for
  
```

Online learning, as understood within the context of this thesis, considers a minimal setting where a decision maker has to decide $\mathbf{z}_t \in Z \subseteq \mathbb{R}^n$ for a period of time t after which a loss function $f_t : Z \rightarrow \mathbb{R}$ becomes known, forcing the decision maker to incur a cost $f_t(\mathbf{z}_t)$. Note that the formulation $f_t(\mathbf{z})$ is more general than $f(\mathbf{z}; \mathbf{y}_t)$, introduced in Section 2.1 as it does not even request the objective function to maintain the same structure across time intervals. Thus, the decision maker can use the full knowledge of f_t to update \mathbf{z}_t and deliver \mathbf{z}_{t+1} . This setting is summarized in Algorithm 1. The main strength of the OL paradigm is that it frees the decision maker from most assumptions that typically hamper other theories, such as requiring the samples to be i.i.d., and therefore is widely applicable in many contexts. Moreover, many families of algorithms developed within OL are relatively inexpensive in terms of computational burden and offer notable performance in dynamic environments.

As mentioned at the start of this section, in online learning, the *de facto* metric to evaluate the performance of a series of decision vectors $\mathbf{z}_1, \dots, \mathbf{z}_T$ produced by an algorithm is the regret $\mathcal{R}_T \in \mathbb{R}$. The regret \mathcal{R}_T provides a versatile and, in a sense, normalized metric to compare an algorithm through different problems with the advantage that little assumption is made about the oracle that generates the decisions. Traditionally, the benchmark used in online learning to compute \mathcal{R}_T is the best single action in hindsight $\mathbf{z}^{\mathcal{H}}$ that can be obtained as the solution of an offline optimization problem under perfect information $\mathbf{z}^{\mathcal{H}} \in \min_{\mathbf{z} \in Z} \sum_{t=1}^T f_t(\mathbf{z})$, yielding

$$\mathcal{R}_T = \sum_{t=1}^T f_t(\mathbf{z}_t) - \sum_{t=1}^T f_t(\mathbf{z}^{\mathcal{H}}). \quad (2.30)$$

Then, the classical target of the work developed within online learning is to design algorithms that achieve asymptotic sublinear regret as the number of rounds T increase or mathematically $\lim_{T \rightarrow \infty} \mathcal{R}_T/T \leq 0$. We discuss in more detail the regret in Section 3.2.4.

Within online learning, online convex optimization (OCO) focuses on online problems where the losses f_t are requested to be convex functions. An interesting family of OCO algorithms are based on the *Follow-the-Leader* (FTL) algorithm [107], which resembles the stochastic SAA introduced in Section 2.1. Although the theoretical foun-

dations of the two approaches are different, their implementation is very similar. The FTL computes every \mathbf{z}_t as follows:

$$\mathbf{z}_t = \arg \min_{\mathbf{z} \in Z} \sum_{i=1}^{t-1} f_i(\mathbf{z}). \quad (2.31)$$

The differences between FTL and SAA are inherent to the paradigms in which they are developed. While in the case of SAA we talk about empirical scenarios $f(\cdot; \mathbf{y}_t)$ with equal probability $1/T$, in FTL we have available historical records of f_t . Furthermore, while in a rolling-window SAA the oldest scenarios may be completely disregarded, in FTL all elements in the collection $\{f_i : i = 1, \dots, t-1\}$ intervene in shaping \mathbf{z}_t .

Although FTL is an online algorithm by right, the most popular and recognizable online algorithms are those based on gradients of f_t such as the online gradient descent (OGD) and its variants. First introduced by [152], OGD has proven to be very effective and versatile [61, 104, 69, 106, 141]. Starting from an initial value \mathbf{z}_1 , the OGD performs iterative updates of \mathbf{z}_t based on gradients of f_t , denoted $\boldsymbol{\tau}_t = \nabla f_t$. The magnitude of the update is controlled by a variable learning rate $\eta_t > 0$, which normally encourages a smooth update. In each round, the updated vector is forced to lie within the feasible region Z through the Euclidean projection $\Pi_Z : \mathbb{R}^n \rightarrow Z$ and $\Pi_Z(\mathbf{o}) = \arg \min_{\mathbf{z} \in Z} \|\mathbf{o} - \mathbf{z}\|_2$. Assembling all the steps together, it yields Algorithm 2.

Algorithm 2 Online Gradient Descent (OGD)

Require: $\mathbf{z}_1 \in Z \subseteq \mathbb{R}^n$, $\eta_1, \dots, \eta_T > 0$

- 1: **for** $t = 1, \dots, T$ **do**
 - 2: Output \mathbf{z}_t
 - 3: Receive $f_t : Z \rightarrow \mathbb{R}$
 - 4: Pay $f_t(\mathbf{z}_t)$
 - 5: Compute $\boldsymbol{\tau}_t = \nabla f_t(\mathbf{z}_t)$
 - 6: Update $\mathbf{z}_{t+1} = \Pi_Z(\mathbf{z}_t - \eta_t \boldsymbol{\tau}_t) = \arg \min_{\mathbf{z} \in Z} \|\mathbf{z}_t - \eta_t \boldsymbol{\tau}_t - \mathbf{z}\|_2$
 - 7: **end for**
-

The selection of the learning rate sequence η_1, \dots, η_T is of paramount importance, dramatically changing the long-term performance of OGD. The original proposal by [152] presents two main alternatives, namely, a variable $\eta_t \propto 1/\sqrt{t}$ and a fixed learning rate $\eta_t = \eta$, providing regret guarantees in both cases. However, in practice the variable choice $\eta_t \propto 1/\sqrt{t}$ results in almost neglectable updates for high values of t , hindering the adaptation to changing environments in late stages. The fix option $\eta_t = \eta$ enables the algorithm to keep learning limitless, although a fixed learning rate is not the best choice when facing changing environments, motivating the development of many OGD variants [71, 147, 81].

One of the most remarkable features of OGD is that it relies on just the last sample collected by the decision maker to update \mathbf{z}_t , resulting in a computationally inexpensive

method, especially if the gradient and projection steps can be computed through closed-form expressions (which happens in several useful cases). This is in sharp contrast with FTL, SAA and the rest of the approaches presented in this chapter where the decision is either fixed or re-optimized from scratch in each round t through a training set made up of many samples.

Motivated by this interesting property, we propose a variant of the original OGD to leverage contextual information in the following paragraphs. As in the case of DR, introduced in Section 2.2.2, in this thesis, we propose to replace the original decision variable in OGD with $z(\mathbf{x}) = g^{\text{OL}}(\mathbf{x}; \mathbf{w})$, $g^{\text{OL}} : \mathcal{X} \times \mathcal{W} \rightarrow \mathbb{R}^n$, $\mathbf{w} \in \mathcal{W} \subseteq \mathbb{R}^q$. Two main considerations should be observed in this transformation. Firstly, the known feasibility problems of DR force the introduction of a new euclidean projection to ensure that the resulting \mathbf{z}_t belongs to Z . Secondly, the gradient is now calculated on the composite function $\boldsymbol{\tau}_t = \nabla f_t(g^{\text{OL}}(\mathbf{x}_t; \cdot))$ (recall \mathbf{w}_t is now the variable) which can hinder obtaining a closed-form to compute it. Although these changes may require attention, normally they do not prevent the successful application of the resulting algorithm, as shown in Chapter 3.

When \mathbf{z}_t is a vector, the scalar choice η_t proposed in early approaches disregards the fact that each component may benefit from different learning rates for several reasons, e.g., because the scale or the dynamics of each component is different. Therefore, we incorporate a multidimensional learning rate $\boldsymbol{\eta}_t \in \mathbb{R}^q$ that enables independent updates as proposed in [147]. The last remaining aspect is how to update the vector $\boldsymbol{\eta}_t$. As discussed in the paragraph above, the classical choices for the learning rate attain poor performances in dynamic environments and in long-term iterative tasks. To improve this aspect of the original OGD algorithm, we follow the ideas in [147] once more. Let “ $\circ n$ ” denote the n -th Hadamard power with $n \in \mathbb{R}$ so that $\boldsymbol{\tau}_t^{\circ 2} = [\tau_{t1}^2, \dots, \tau_{tq}^2]^\top$. We start the derivation of the update by adding a variable that accumulates the running average of the Hadamard squared gradient, yielding

$$\bar{\boldsymbol{\tau}}_t^{\circ 2} = \rho \bar{\boldsymbol{\tau}}_{t-1}^{\circ 2} + (1 - \rho) \boldsymbol{\tau}_t^{\circ 2}, \quad (2.32)$$

where $\rho \in [0, 1)$ is a decay constant and $\bar{\boldsymbol{\tau}}_0 = \mathbf{0}$. Once we have available a component-wise running average of the gradient, each component of the learning rate can be updated following

$$\boldsymbol{\eta}_t = \eta (\bar{\boldsymbol{\tau}}_t^{\circ 2} + \epsilon \mathbf{1})^{\circ -1/2}, \quad (2.33)$$

where $\epsilon \in \mathbb{R}^+$ helps better condition the denominator and $\eta > 0$ is a constant. Finally, the update of \mathbf{w}_t yields

$$\mathbf{w}_{t+1} = \Pi_{\mathcal{W}}(\mathbf{w}_t - \boldsymbol{\eta}_t \circ \boldsymbol{\tau}_t), \quad (2.34)$$

where \circ denotes the element-wise product and $\Pi_{\mathcal{W}}$ the Euclidean projection over the set \mathcal{W} .

Algorithm 3 Contextual Online Gradient Descent (COGD)

Require: $\mathbf{w}_1 \in \mathcal{W} \subseteq \mathbb{R}^n$, $\eta > 0$, $\rho \in [0, 1)$, $\epsilon \in \mathbb{R}^+$

- 1: Initialize $\bar{\boldsymbol{\tau}}_0^{\circ 2} = \mathbf{0}$
 - 2: **for** $t = 1, \dots, T$ **do**
 - 3: Output \mathbf{w}_t
 - 4: Receive \mathbf{x}_t
 - 5: Compute $\mathbf{z}_t = \Pi_Z(g^{\text{OL}}(\mathbf{x}_t; \mathbf{w}_t))$
 - 6: Receive $f_t : Z \rightarrow \mathbb{R}$
 - 7: Pay $f_t(\mathbf{z}_t)$
 - 8: Compute $\boldsymbol{\tau}_t = \nabla f_t(g^{\text{OL}}(\mathbf{x}_t; \mathbf{w}_t))$
 - 9: Accumulate $\bar{\boldsymbol{\tau}}_t^{\circ 2} = \rho \bar{\boldsymbol{\tau}}_{t-1}^{\circ 2} + (1 - \rho) \boldsymbol{\tau}_t^{\circ 2}$
 - 10: Compute $\boldsymbol{\eta}_t = \eta(\bar{\boldsymbol{\tau}}_t^{\circ 2} + \epsilon \mathbf{1})^{\circ -1/2}$
 - 11: Update $\mathbf{w}_{t+1} = \Pi_{\mathcal{W}}(\mathbf{w}_t - \boldsymbol{\eta}_t \circ \boldsymbol{\tau}_t)$
 - 12: **end for**
-

The resulting contextual online gradient descent (COGD) algorithm is outlined in Algorithm 3. We highlight that COGD can leverage contextual information directly at the same time that it maintains the interesting properties of OGD. Furthermore, COGD promises a nice performance in dynamic environments through an adaptive component-wise update of the learning rate.

2.4 Summary

The classical decision-making paradigms, e.g., SP, RO, or DRO, presented in Section 2.1 did not formally address contextual information until just recently. On the contrary, contextual information has been extensively used in supervised Machine Learning (ML) to forecast an uncertain (typically single) quantity but disregarding the particularities of the subsequent tasks in which such predictions are used. Therefore, the traditional way contextual information was used, if at all, was far from taking full advantage of this currently abundant resource. The realization of this fact has recently spurred a wave of research on data-driven models that use contextual information to make more efficient decisions.

In this regard, Section 2.2 has presented four frameworks that follow different strategies to utilize contextual information, the last of which has been developed within this thesis. The first framework, proposed by [17] and reviewed in Section 2.2.1, presents a data-driven framework that approximates the empirical conditional distribution using several methods inspired by classical ML algorithms. Section 2.2.2 reviews a completely different framework, denoted DR. The decision rule approach (DR), proposed by [7], uses a linear decision rule to translate feature vectors into decisions in a straightforward procedure. The third framework presented in [56] focuses on linear problems for

which the authors refine the suboptimal FO framework by developing an alternative loss function to replace the classical root mean squared error, taking into account the subsequent linear optimization problem. The fourth contextual framework, thoroughly discussed in Section 2.2.4, is one of the main methodological contributions of this thesis. This framework proposes a generic procedure based on bilevel optimization, whereby a parametric model is estimated by taking into account the impact of its output on the feasibility and objective value of the decision.

Although the frameworks summarized above can be used in several settings, this thesis focuses on decision tasks that are due periodically and characterized by low or moderate risk (as opposed to those capital-intensive tasks that are related to the construction of new assets). These tasks are named within this thesis as iterative decision-making tasks and are addressed in Section 2.3. The first two parts of Section 2.3 discussed a *rolling-window* setting to be combined with the frameworks presented in Section 2.2 in practical situations where the samples are not *independent and identically distributed*. The last part of the section addresses the connection of this setting with the literature on online learning and proposes a new version of the online gradient descent (a classical online algorithm) that leverages features, which we have named contextual online gradient descent (COGD).

Next, we briefly outline the content of the remaining chapters. Chapter 3 investigates DR and COGD, which share the use of a linear decision rule as a common ingredient. Furthermore, both methods are applied to two instances of the problem of a wind power producer offering in a wholesale electricity market. In the first case, the DR method is used to produce an enhanced estimator of wind energy production and a more profitable bid, demonstrating improved economic and computational results compared to several benchmarks in a realistic case study based on data from the European transmission system operators. The second application envisions an hourly cleared market, demonstrating the notable capabilities of COGD and the benefits of this combination in order to achieve higher shares of wind energy in the market. To the best of our knowledge, this is the first time that online gradient methods are applied to this problem.

Then, Chapter 4 gathers two applications that smartly estimate the uncertain parameters, taking into account the optimization problem. The first application concerns a strategic producer who manages a thermal units, offering in a day-ahead electricity market. We apply the contextual bilevel approach, introduced in Section 2.2.4, to prescribe the uncertain parameters of an inverse residual demand function through which the market is modeled. A second application follows, investigating alternative procedures for the market clearing of a two-stage electricity market compatible with current industrial practices. We propose a mixed-integer program that leverages the problem structure to construct, from the available contextual information and historical data, a

prescription of the net demand, which does take into account the power system's cost asymmetry.

Chapter 3

Contextual optimization via decision rules

Chapter 3 is dedicated to the problem of a wind power producer offering in a wholesale electricity market. This is a clear example of an iterative decision task, discussed in Section 2.3, where the target is to determine a sequence of offers that tries to maximize the returns on average. The difficulty of this problem is that the amount of wind energy produced and the corresponding deviation penalties are uncertain when the market offer has to be decided. We analyze two different applications where we leverage some of the mathematical tools introduced in Chapter 2.

The first application analyzes a wholesale electricity market cleared daily. Based on the DR method, introduced in Section 2.2.2, two data-driven models are produced to improve the forecasting and trading of wind energy using contextual information. The focus of the second application is to show the benefits that online methods, such as COGD (see Section 2.3.3) can bring to electricity markets, envisioning a setting where a wholesale electricity market is cleared every hour. To the best of our knowledge, this is the first time that an online gradient method is applied to the problem of a wind power producer trading in a wholesale electricity market.

3.1 The trading problem of a wind power producer

The application presented in this section is based on the published manuscript [101]. In this application, we study the problem of a wind power producer offering in a day-ahead electricity market. Furthermore, the application presented in this section builds on the work by [7] where the DR method, discussed in Section 2.2.2, is proposed and applied to the *newsvendor* problem [113]. The work in [7] neatly fits the setup of the wind power producer problem, providing an easy-to-implement and effective procedure. However, as explained further on, our decision task exhibits some peculiarities that make it especially challenging, requiring additional effort for a successful application of DR. Among the most interesting aspects of this application, we highlight the fact that the model resulting from applying DR to the *newsvendor* problem can be used with a twofold purpose, namely, to produce an enhanced forecast of the wind energy production, and to improve the gains of trading this energy in the market. We combine both steps in a fully data-driven procedure, demonstrating its performance in a case study based on real data of the European TSOs. Next, we review recent work related to both wind power forecasting and trading.

The technical literature on wind power forecasting and trading is tremendously vast. Mentioning all of the many relevant references on both topics in this introduction would be, therefore, an infeasible and purposeless task. We refer, instead, to monographs [77, 97], which offer a comprehensive treatment of both topics, and then highlight those approaches which we believe, are most closely related to ours. In the realm of wind power prediction, this would mean those that either seek to model the spatial correlations among wind sites (see, e.g., [95, 132, 143, 149]) or to adaptively combine alternative

wind power forecasts for the same site so as to produce a better one (see, for example, [105, 119, 120]). In our case, however, we are not aiming to develop a better forecasting model. What we propose, instead, is a general mathematical framework to improve the forecasts delivered by any *existing* method by leveraging available power system data, for example, spatially correlated wind energy forecasts.

On the other hand, there also exists a wealth of methods to determine the optimal energy bid that a wind power producer should place in a day-ahead electricity market (see, for instance, [110, 94, 26, 153, 91, 12, 46]). To this end, these methods all make explicit use of stochastic models for wind power production and/or market prices, for example, in the form of scenario forecasts or predictive densities. Additionally, other strategies have also been proposed to cope with the inherent uncertainty in wind power production, such as the purchase of power reserves [51] or by means of a combined portfolio of wind and hydropower generation [131]. What distinguishes our work from these others is that we directly derive a wind power day-ahead bid from available *point* forecasts and other relevant data, thus avoiding the need to generate *scenarios* or *probabilistic* forecasts for electricity prices and wind power production.

We particularly draw attention to [92] and [35] as being the approaches that are probably closest to ours. In [92], a reinforcement learning algorithm is built to compute and follow the nominal level of the profit-maximizing quantile forecast of wind power that should be bid into the day-ahead market. While their algorithm is designed to learn and track the expected marginal opportunity costs directly from market data, they assume that a good estimate of the wind power predictive density is available (as in the other references mentioned above). Our approach, to the contrary, is free from this classical assumption.

In [35], the authors propose two data-driven approaches to reduce the imbalance costs incurred by renewable energy producers. In their first approach, they formulate a meta-optimization problem whereby the hyper-parameters of all the forecasting models involved in the decision-making process are tuned to minimize the imbalance costs. In their second approach, they directly train an artificial neural network to that very same end. In contrast with our proposal, which boils down to a linear programming problem, the complexity of theirs is such that they need to resort to heuristic optimization algorithms. Furthermore, our way of producing market bids is somewhat different: we do not seek a bidding model that overrides the need for forecasts (understood in a classical statistical sense), but rather we collect those forecasts, among other features, and combine them to produce profit-maximizing bids.

3.1.1 Problem description

Consider an electricity market for short-term energy transactions that consists of a day-ahead market and a *dual-price* balancing market. In the former, energy offers and bids

are typically submitted between 12 and 36 hours in advance of the actual delivery of electricity. In the latter, deviations of market participants concerning their day-ahead dispatch are financially settled at a price that depends on the sign of the total system imbalance [97, Ch. 7].

In such a context, the market revenue ρ of a renewable energy producer in a dual-price balancing market is given by

$$\rho = \lambda^D E - (\psi^-(E^D - E)^+ + \psi^+(E - E^D)^+), \quad (3.1)$$

where $(a)^+ = \max(a, 0)$, and λ^D , E^D , ψ^- , ψ^+ , and E represent the day-ahead market price, the day-ahead renewable energy bid, the marginal opportunity costs for under- and overproduction, and the eventual renewable energy production, respectively. In (3.1), the first term accounts for the incomes the renewable power producer would obtain from partaking in the day-ahead market if perfect information on eventual production was known to said producer, while the second is the opportunity cost the producer incurs in deviating from the day-ahead bid E^D . Logically, parameters ψ^- , ψ^+ , and E are uncertain to the renewable energy producer at the moment of offering in the day-ahead market. Besides, the term $\lambda^D E$ is beyond the power producer's control. As a result, the optimal offer E^D that a (price-taker) risk-neutral renewable energy producer should place in the day-ahead market is given as the solution to the following linear programming problem, whereby the renewable energy producer seeks to minimize the expected opportunity cost for under- and overproduction:

$$\min_{E^D \in [0, \bar{E}]} \mathbb{E} [\psi^-(E^D - E)^+ + \psi^+(E - E^D)^+]. \quad (3.2)$$

In problem (3.2), the expectation is taken over the stochastic input parameters E , ψ^- and ψ^+ . Actually, the way the solution to problem (3.2) is addressed depends on the information we have about these parameters. Furthermore, this problem must be (independently) solved in each trading period comprising the day-ahead market horizon (typically the 24 hours of a day). For simplicity, though, we have dropped the time index from the problem formulation. We will introduce that index in a later stage of our exposition.

The marginal opportunity costs for under- and overproduction, i.e., ψ^- and ψ^+ , are defined as:

$$\psi^- = \lambda^- - \lambda^D, \quad (3.3)$$

$$\psi^+ = \lambda^D - \lambda^+, \quad (3.4)$$

where, in turn, the prices for under- and overproduction, i.e., λ^- and λ^+ are given by

$$\lambda^- = \begin{cases} \lambda^B & \text{if } \lambda^B \geq \lambda^D, \\ \lambda^D & \text{if } \lambda^B < \lambda^D, \end{cases} \quad (3.5)$$

$$\lambda^+ = \begin{cases} \lambda^D & \text{if } \lambda^B \geq \lambda^D, \\ \lambda^B & \text{if } \lambda^B < \lambda^D. \end{cases} \quad (3.6)$$

In (3.5) and (3.6), λ^D and λ^B denote the day-ahead and the balancing market prices, in that order. Therefore, according to the rules (3.3)–(3.6) of a dual-price imbalance settlement, the overproduction of a renewable energy producer is always rewarded at a price lower than or equal to the day-ahead market price, while their underproduction is always penalized at a price higher than or equal to the day-ahead market price. This settlement is, at least, used in some European countries such as Spain and Denmark [138].

Problem (3.2) takes the form of the classical *newsvendor* problem [113], for which an analytical solution exists. Indeed, the optimal solution to this problem (that is, the optimal bid E^{D*}), is given by

$$E^{D*} = F_E^{-1} \left(\frac{\bar{\psi}^+}{\bar{\psi}^+ + \bar{\psi}^-} \right), \quad (3.7)$$

where F_E is the cumulative distribution function (cdf) of the renewable energy production corresponding to the time period of the market horizon for which the day-ahead bid must be submitted, and the overbar character denotes the *expected value* of the random variable underneath.

Despite its apparent simplicity, the application of formula (3.7) is quite demanding, as it requires models to produce a probabilistic forecast of E (i.e., an estimate of its cdf) and point forecasts of ψ^- and ψ^+ . In the first approach proposed in [35], for example, those models are tuned (by way of what they call a meta-optimization problem) to produce a good estimate of (3.7). Our goal, though, is to sidestep the need for those models and directly use available data instead. This motivates our data-driven approach, which we gradually build next.

Suppose that the renewable energy producer is to place a bid into the day-ahead market and that measurements of her renewable energy production at past periods are available. We can then directly use the *empirical* cdf of these data, namely, \hat{F}_E , in lieu of F_E in (3.7), which thus becomes

$$\hat{E}^D = \inf \left\{ e : \hat{F}_E(e) \geq \frac{\bar{\psi}^+}{\bar{\psi}^+ + \bar{\psi}^-} \right\}, \quad (3.8)$$

where the infimum is required due to the discrete nature of \hat{F}_E . Naturally, \hat{E}^D in (3.8) and E^{D*} in (3.7) are generally different, and therefore, \hat{E}^D is usually suboptimal in (3.2). Actually, \hat{E}^D is the solution to the following *sample average approximation* (SAA) of (3.2)

$$\min_{E^D \in [0, \bar{E}]} \frac{1}{T} \sum_{t \in \mathcal{T}} \bar{\psi}^-(E^D - E_t)^+ + \bar{\psi}^+(E_t - E^D)^+, \quad (3.9)$$

where $t \in \mathcal{T}$ is a timestamp index that labels the realizations E_t with $\mathcal{T} = \{1, \dots, T\}$. From the equivalence between (3.8) and (3.9), we can infer that if we (artificially) set $\bar{\psi}^- = \bar{\psi}^+ = 1$ in (3.9), we get an estimate of the *median* of the renewable energy production. We will leverage this fact later on to develop a straightforward method to enhance the quality of renewable energy forecasts.

Problem (3.9), however, is likely to deliver poor bids \hat{E}^D , because it overlooks the fact that, at the moment of bidding, the renewable power producer may have available a vector of contextual information \mathbf{x} made up of p features with some predictive power on future production. Accordingly, to get a better bid \hat{E}^D , we need to reformulate the SAA problem (3.9) to account for and take advantage of that information. For this purpose, we consider the enriched dataset $\{(E_t, \mathbf{x}_t), \forall t \in \mathcal{T}\}$, where \mathbf{x}_t is the p -dimensional vector of contextual information \mathbf{x} observed at time t . The features in \mathbf{x} may include measures of potentially explanatory variables available at time period t or forecasts of these variables issued for that time period. We then follow the DR approach proposed in [7] (see Section 2.2.2) and consider the following linear decision rule

$$\mathcal{L} = \left\{ E^D : \mathcal{X} \rightarrow \mathbb{R} : E^D(\mathbf{x}) = \mathbf{w}^\top \mathbf{x} \right\}, \quad (3.10)$$

which, inserted into (3.9), renders

$$\min_{\mathbf{w}} \frac{1}{T} \sum_{t \in \mathcal{T}} \bar{\psi}^-(\mathbf{w}^\top \mathbf{x}_t - E_t)^+ + \bar{\psi}^+(E_t - \mathbf{w}^\top \mathbf{x}_t)^+ \quad (3.11a)$$

$$\text{s.t. } 0 \leq \mathbf{w}^\top \mathbf{x}_t \leq \bar{E}, \quad \forall t \in \mathcal{T}. \quad (3.11b)$$

Note that (3.11) is a particularization of (2.20), introduced in Section 2.2.2, where the linear decision rule (3.10) corresponds to the model $g^{\text{DR}}(\mathbf{x}; \mathbf{w}) = \mathbf{w}^\top \mathbf{x}$. Nonetheless, problem (3.11) still requires further elaboration to become a fully data-driven model. Indeed, while in the technical literature on the data-driven newsvendor problem (see, for instance, [7] and [74]), the marginal opportunity costs $\bar{\psi}^-$ and $\bar{\psi}^+$ are assumed to be known with certainty, in our case, these costs are unknown to the renewable energy producer at the moment of bidding into the day-ahead market. Consequently, problem (3.11) still needs the support of a forecasting model that provides it with an estimate of $\bar{\psi}^-$ and $\bar{\psi}^+$. To circumvent this hurdle, we propose to work with the even

more enriched dataset $\{(E_t, \psi_t^-, \psi_t^+, \mathbf{x}_t), \forall t \in \mathcal{T}\}$, where the pair (ψ_t^-, ψ_t^+) represents the marginal costs of under- and overproduction that were observed at time t , and solve instead the following optimization problem:

$$\min_{\mathbf{w}} \frac{1}{T} \sum_{t \in \mathcal{T}} \psi_t^- (\mathbf{w}^\top \mathbf{x}_t - E_t)^+ + \psi_t^+ (E_t - \mathbf{w}^\top \mathbf{x}_t)^+ \quad (3.12a)$$

$$\text{s.t. } 0 \leq \mathbf{w}^\top \mathbf{x}_t \leq \bar{E}, \quad \forall t \in \mathcal{T}, \quad (3.12b)$$

where we have replaced $\bar{\psi}^-$ and $\bar{\psi}^+$ with ψ_t^- and ψ_t^+ , respectively. Model (3.12) is, in effect, fully data-driven.

Finally, to recast problem (3.12) as a linear program, we introduce the auxiliary variables o_t and u_t to equivalently reformulate the positive-part function as follows:

$$\min_{\mathbf{w}, \mathbf{u}, \mathbf{o}} \frac{1}{T} \sum_{t \in \mathcal{T}} \psi_t^- u_t + \psi_t^+ o_t \quad (3.13a)$$

$$\text{s.t. } u_t \geq \mathbf{w}^\top \mathbf{x}_t - E_t, \quad \forall t \in \mathcal{T} \quad (3.13b)$$

$$o_t \geq E_t - \mathbf{w}^\top \mathbf{x}_t, \quad \forall t \in \mathcal{T} \quad (3.13c)$$

$$0 \leq \mathbf{w}^\top \mathbf{x}_t \leq \bar{E}, \quad \forall t \in \mathcal{T} \quad (3.13d)$$

$$u_t, o_t \geq 0, \quad \forall t \in \mathcal{T}. \quad (3.13e)$$

The result is an inexpensive program, which can be solved to optimality with any commercial optimization solver. As discussed in Section 2.2.2, we can use the optimal coefficient vector \mathbf{w}^* obtained after solving problem (3.13) and a vector of contextual information \mathbf{x}_t to produce an estimate of the wind energy production E_t^D as follows:

$$E_t^D = (\mathbf{w}^*)^\top \mathbf{x}_t. \quad (3.14)$$

Note that in certain cases, e.g., when the number of training samples T is low or when \mathbf{x}_t belongs to an unbounded set, the resulting estimator E_t^D can be outside the interval $[0, \bar{E}]$. This issue can be easily circumvented by replacing (3.14) with the inexpensive projection

$$E_t^D = \max(0, \min(\bar{E}, (\mathbf{w}^*)^\top \mathbf{x}_t)). \quad (3.15)$$

Next, we explain how we use the linear program (3.13) and the subsequent step (3.15) to improve the tasks of renewable energy forecasting and trading.

3.1.1.1 Renewable Energy Forecasting

Problems (3.13) and (3.15) provides us with a simple, yet effective procedure to enhance the quality of a given renewable energy forecast by exploiting contextual infor-

mation. For this purpose, first we need to set $\psi_t^- = \psi_t^+ = 1, \forall t \in \mathcal{T}$, in (3.13). This results in the following linear programming problem:

$$\min_{\mathbf{w}, \mathbf{u}, \mathbf{o}} \frac{1}{T} \sum_{t \in \mathcal{T}} u_t + o_t \quad (3.16a)$$

$$\text{s.t. } u_t \geq \mathbf{w}^\top \mathbf{x}_t - E_t, \quad \forall t \in \mathcal{T} \quad (3.16b)$$

$$o_t \geq E_t - \mathbf{w}^\top \mathbf{x}_t, \quad \forall t \in \mathcal{T} \quad (3.16c)$$

$$0 \leq \mathbf{w}^\top \mathbf{x}_t \leq \bar{E}, \quad \forall t \in \mathcal{T} \quad (3.16d)$$

$$u_t, o_t \geq 0, \quad \forall t \in \mathcal{T}. \quad (3.16e)$$

Then, we have to include the renewable energy forecast we wish to improve as one of the features in the linear decision rule. The remaining features will then correspond to that extra contextual information we want to take advantage of to enhance the quality of the renewable energy forecast. This extra information may be of a very different nature. For example, some of the features could correspond to categorical variables (hour of the day, day of the week ...) and others could be forecasts of potentially related stochastic variables. As a matter of fact, several features in vector \mathbf{x} could represent forecasts on the renewable energy production of interest, but issued by different entities. The only condition for a piece of information to be treated as a feature is that it must be available at the time when the enhanced renewable energy forecast is to be generated.

Finally, once we obtain \mathbf{w}^F solving (3.16) an estimator of the wind energy production \hat{E}_t can be obtained through an expression analogous to (3.15), which in this case yields

$$\hat{E}_t = \max(0, \min(\bar{E}, (\mathbf{w}^F)^\top \mathbf{x}_t)). \quad (3.17)$$

Below, in this application, we seek to improve the onshore wind power production forecast of the DK1 bidding zone belonging to the pan-European electricity market, which is issued every day by the Danish TSO. To this end, we use, as additional features, the forecasts of the wind power production in neighboring zones, which are produced by the respective TSOs in charge of those zones. We also introduce a fix feature equal to one and the corresponding component of the linear decision rule that acts as an intercept to correct for possible offsets. Note that the onshore DK1-wind power forecast issued by the Danish TSO is produced by the tool known as *WindFor*¹, a state-of-the-art software for forecasting wind power production at different scales that leverages numerical weather predictions (wind speed and direction), statistics and artificial intelligence. Given the presumed quality of this forecast, we also use it as a benchmark for our method. This benchmark model, which only comprises the onshore DK1-wind power forecast, is referred to as BN (from benchmark) throughout the rest of the application.

¹WindFor. See <https://enfor.dk/services/windfor/>.

3.1.1.2 Renewable Energy Trading

In principle, model (3.13) could be directly used for renewable energy trading without further elaboration. To this aim, we would just need to solve this problem for the enriched dataset $\{(E_t, \psi_t^-, \psi_t^+, \mathbf{x}_t), \forall t \in \mathcal{T}\}$ and thus, obtain the optimal coefficient vector \mathbf{w}^* defining the linear decision rule (this is what we call *model training*). Then, the bid E_t^D , to be submitted by the renewable energy producer to the day-ahead market for time period t of the market horizon, would be computed as in (3.15).

Unfortunately, what we observe in practice is that the direct application of model (3.13) does not produce, in general, a bid more profitable than the expected-value bid (that is, the bid consisting in submitting the quality point forecast of the benchmark method BN). The reason for this has to do with the limited predictability of the marginal opportunity costs ψ^- and ψ^+ (i.e., the absence of repeating patterns in the series of these costs). In effect, as shown in Figure 2 of [126], the most sophisticated models for predicting ψ^- and ψ^+ deliver forecasts that are completely uninformative or misleading for lead times beyond several hours into the future. However, the lead times required for partaking in the day-ahead market are usually longer than 12-14 hours. This empirical observation is, besides, supported by economic theory: the balancing market price λ^B represents a marginal cost for system imbalances in real time, which should be purely random. Consequently, the balancing market price should behave as a noise around the spot price λ^D . As a result, there is little in ψ^- and ψ^+ that can be predicted for lead times longer than several hours. In this situation, the model flexibility introduced by the features in problem (3.13) tends to produce overfitted linear decision rules, that is, rules that capture “fictitious” patterns of ψ^- and ψ^+ in the historical/training dataset, not repeated beyond that set.

Against this background, in lieu of model (3.13), we propose to solve the following optimization problem:

$$\min_{w \in \mathbb{R}, \mathbf{u}, \mathbf{o}} \frac{1}{T} \sum_{t \in \mathcal{T}} \psi_t^- u_t + \psi_t^+ o_t \quad (3.18a)$$

$$\text{s.t. } u_t \geq w \hat{E}_t - E_t, \quad \forall t \in \mathcal{T} \quad (3.18b)$$

$$o_t \geq E_t - w \hat{E}_t, \quad \forall t \in \mathcal{T} \quad (3.18c)$$

$$u_t, o_t \geq 0, \quad \forall t \in \mathcal{T}, \quad (3.18d)$$

where the single feature of this model, namely, \hat{E} , represents the improved renewable energy forecast obtained from model (3.16). What we suggest for renewable energy trading is, therefore, a two-step procedure in which we first improve the renewable energy forecast by way of (3.16) and then we correct such a forecast for trading by means of the substantially less flexible model (3.18).

As reported in [74], in newsvendor problems (similar to the renewable energy trading problem we address here), the bulk of the economic gains we attain from data-driven procedures are linked to the improvement of the estimate of E that we get. Following this rationale, we first use (3.16) to enhance this estimate as much as possible, and then employ (3.18) to account for mid-term patterns of ψ^- and ψ^+ (the little that we can explain about these costs) in the market bid. Therefore, we compute the bid to be submitted to the day-ahead market for time period t as

$$E_t^D = \max(0, \min(\bar{E}, w^T \hat{E}_t)), \quad (3.19)$$

with $w^T \in \mathbb{R}$ being the optimal decision-rule coefficient delivered by (3.18).

In the following section, we elaborate on the application of this two-step procedure on a real experiment.

3.1.2 Experiment Design and Model Training

Next, we detail the experiment conducted to assess the performance of the data-driven models introduced in Sections 3.1.1.1 and 3.1.1.2 for renewable energy forecasting and trading, respectively. As mentioned, we focus on the *onshore wind power produced in the DK1 area of the pan-European electricity market*.

This section is divided into three parts. In the first, we present the data gathered and the different trained and tested models. In the second and third, we introduce the metrics used to quantify the performance of those models and elaborate on how we train them.

3.1.2.1 Data and Features

The data employed in this research span from 01/08/2015 to 04/22/2019 (date format mm/dd/yyyy) and are fully published and freely available for download from the website of the Danish TSO² and the ENTSO-e Transparency Platform³ (ETP), which facilitates the reproducibility of our results. These data pertain to various features that either relate to the hour of the day and day of the week, or to day-ahead predictions about a number of potentially relevant variables, specifically, the total load, scheduled generation and solar power production in DK1, and wind power productions (onshore, offshore or both) in market zones adjacent to DK1, namely, zone 2 of Denmark (DK2), zone 2 of Norway (NO2), zones 3 and 4 of Sweden (SE3 and SE4, respectively), and the bidding zone of Germany, Austria and Luxembourg (DE-AT-LU). According to the Manual of Procedures⁴ (MoP) of the ETP, these predictions should be made available in

²Energinet. See <https://energinet.dk/>.

³ENTSO-e Transparency Platform. See <https://transparency.entsoe.eu/>.

⁴ENTSO-e's Manual of Procedure v3.1 (2013). See <https://www.entsoe.eu/data/transparency-platform/mop/>.

the platform by the different TSOs no later than 18:00 h of day $D - 1$ and span the 24 hours of the following day D . However, some TSOs are temporarily failing to faithfully comply with the ETP's MoP. This is the case, for example, of the Danish TSO, which has a tendency to upload the day-ahead forecasts pertaining to DK1 and DK2 several hours late (in the early morning of day D). In addition, the day-ahead forecasts are not accompanied with their issuance time stamp, which makes it impossible to determine the exact time in day D at which those forecasts were generated. This implies that we cannot guarantee that all the forecasts we use as features in our models below are time-consistent, that is, that have been issued at the same time. Directly after presenting our models, we explain how we deal with this time-consistency issue in order to guarantee a rigorous analysis and evaluation of the proposed approach.

On a different front, the categorical features named as “hour of the day” and “day of the week” each comprise a group of 0/1 time series, specifically, 24 time series for the case of “hour of the day” and seven for “day of the week.” These series, besides, take on a value of one for all the time periods that correspond to the label of the feature, and zero otherwise. For example, for every hour of “Monday”, only one of the seven series of the feature “day of the week” takes on the value one, whereas the value of the other six is set to zero.

We build and train seven models of the type of (3.16). The first five of these models differ from one another by the number of features they exploit. More precisely,

Forecasting Model 1 (FM1), which only includes the day-ahead predictions of the on- and offshore wind power production in DK1.

Forecasting Model 2 (FM2), which results from adding the categorical variables “hour of the day” and “day of the week”, and the day-ahead forecasts of solar power production, scheduled generation and total load in DK1 to model FM1.

Forecasting Model 3 (FM3), which is derived from model FM1 by adding the day-ahead forecasts of the on- and offshore wind power production in DK2.

Forecasting Model 4 (FM4), which results from model FM3 by adding the day-ahead forecasts of the onshore wind power production in NO2, DE-AT-LU, SE3 and SE4, and the day-ahead forecasts of offshore wind power production in DE-AT-LU.

Forecasting Model 5 (FM5), which includes all the previous features.

Utopian Model 1 (UM1), which is analogous to FM4, but uses the realized values of all the features that represent forecasts (that is, the actual outcomes of the associated stochastic processes), except, logically, for the DK1-onshore wind power forecast, which is what we seek to improve.

Utopian Model 2 (UM2), which is also similar to model FM4, but uses the realized values of wind power production in SE3, SE4, NO2 and DE-AT-LU.

Models UM1 and UM2 are unrealizable in practice, as they assume perfect information on some of the features (instead of forecasts). However, their analysis is worthwhile to assess the impact of the aforementioned time-consistency issue. Models FM1-FM5 can be divided into two groups, namely:

1. Models FM1, FM2 and FM3 only use information relative to DK1 and/or DK2, and therefore, we can ensure that these models exploit time-consistent information as the information pertaining DK1 and DK2 is issued and uploaded to the ETP by the same entity, i.e., the Danish TSO.
2. Models FM4 and FM5 also make use of information relative to the rest of bidding zones. Hence, we cannot guarantee that these models employ time-consistent information. However, the performance comparison between models FM3, FM4 and UM2 allows us to measure the impact of this possible time inconsistency. In fact, this impact is concluded to be negligible in Section 3.1.3.1 (around 0.25-0.30 percentage points in terms of prediction performance).

Finally, model UM1 provides us with an upper bound on how much the DK1-onshore wind power forecast issued by the Danish TSO could be improved with our methodology by enhancing the information on the features. More precisely, it allows us to quantify how much we would gain in prediction performance if we could use the actual realized values of the features that our models exploit instead of their forecasts.

As we have said, the benchmark model BN, which we use for comparison and evaluation, is the raw onshore DK1-wind power forecast issued by the Danish TSO. Note that this forecast is a feature (that is, an input) common to all the models listed above. This way, the ultimate goal of these models is to enhance the Danish TSO's forecast by exploiting the information carried by the other features considered. In selecting those other features that may be potentially most relevant to enhancing the onshore DK1-wind power forecast issued by the Danish TSO, we have limited ourselves to information that: i) pertains to DK1 and/or neighbouring bidding zones and ii) is published either in the ETP or on Energinet.dk's website.

For trading the onshore DK1-wind power production in the pan-European day-ahead market, we construct an eighth model TM (trading model) of the type of (3.18) that receives as input the wind power forecast \hat{E}_t from model FM3. This is because it is the simplest among the proposed models for wind power forecasting, which exhibits the best overall prediction performance over the test set. Furthermore, in Section 3.1.3.2, we compare the market performance of the bid produced by model TM with that of the trading strategies consisting in directly bidding the point forecast given by models BN and FM3 into the day-ahead market.

The wind power forecasts for the market zone DE-AT-LU are available on a 15-min time resolution, while the rest are given in hourly resolutions. Consequently, we compute the hourly average values of the DE-AT-LU data series. A different issue is that some of the series have missing values, although the proportion of gaps in the data series relative to their length is negligible. We fill these gaps with a linear interpolation of the values in their extremes. Last but not least, in models FM1–FM5, UM1 and UM2, each non-categorical feature is dynamically scaled by the maximum value of the feature that is observed in the training dataset. The target variable, that is, the onshore wind power production in DK1 is also scaled by the most up to date value of the wind power capacity installed in that zone, and is available in the ETP, which is 3669 MW. For convenience, all the data series are labeled using Coordinated Universal Time (UTC), which is also the time reference we use for our experiments.

3.1.2.2 Performance Metrics

To evaluate the performance of the various forecasting models stemming from (3.16), we use the *Mean Absolute Error* (MAE) and the *Root Mean Square Error* (RMSE), i.e.,

$$\text{MAE} = \frac{1}{|\tilde{T}|} \sum_{t \in \tilde{T}} |E_t - E_t^D|, \quad (3.20)$$

$$\text{RMSE} = \frac{1}{|\tilde{T}|} \sqrt{\sum_{t \in \tilde{T}} (E_t - E_t^D)^2}, \quad (3.21)$$

where \tilde{T} is the test set and $|\tilde{T}| = |\tilde{T}|$.

Recall that, when forecasting, the purpose of model (3.16) is to improve an existing renewable energy prediction. In our case, this prediction is the day-ahead forecast of the onshore wind power production in DK1, which is issued by the Danish TSO every day. For this reason, we are especially interested in the percentage improvement with respect to the same forecast in terms of MAE and RMSE.

Simultaneously, to assess the performance of the trading model that results from problem (3.18), we compute the *average opportunity loss* (AOL) linked to the onshore wind power production in DK1 over the test set, that is,

$$\text{AOL} = \frac{1}{|\tilde{T}|} \sum_{t \in \tilde{T}} \psi_t^-(E_t - E_t^D)^+ + \psi_t^+(E_t^D - E_t)^+. \quad (3.22)$$

The AOL gives us an idea of the monetary value lost by the onshore wind power production in DK1 due to its limited predictability. Therefore, rather than in the value of AOL *per se*, we are far more interested in the decrease in the AOL we attain by means

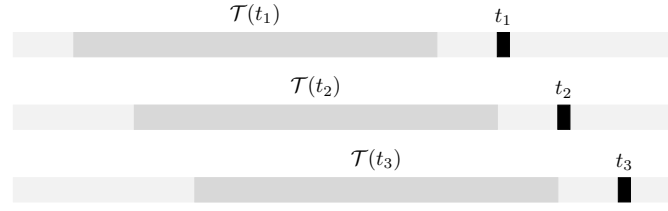


Figure 3.1: Illustration of the rolling-window approach.

of model (3.18) relative to the AOL delivered by submitting the Danish TSO's forecast to the day-ahead market. Finally, note that if ψ_t^- and ψ_t^+ are set to one for all t the AOL metric becomes equivalent to computing the MAE.

3.1.2.3 Model Training

Except for the categorical information “hour of the day” and “day of the week”, all the features we exploit in models (3.16) are forecasts of a variety of potentially informative variables for time t . All these forecasts pertain to the 24 hours of the following day. In actual practice, models (3.16) and (3.18) are trained using a rolling-window approach as discussed in Section 2.3.2 and therefore, the training set depends on each time period t of the test set $\tilde{\mathcal{T}}$. We denote $\mathcal{T}(t)$ the rolling training set linked with $t \in \tilde{\mathcal{T}}$ as illustrated in Figure 3.1. Note that the length of the training set is kept constant as time progresses. Furthermore, there is a gap between the time period t and its corresponding training set $\mathcal{T}(t)$. The reason for this gap is that the values of E , ψ^- and ψ^+ for the time interval between the moment the forecasts are made available and time t are still not known and consequently, such time periods cannot be used for the training of the models (3.16) or (3.18).

This rolling-window approach dynamically re-estimates the decision-rule parameters \mathbf{w}^F and w^T solving (3.16) and (3.18), respectively, as the information on the considered features is updated. Each time these parameters are re-estimated, equations (3.17) and (3.19) are used to issue improved forecasts and bids for time period t .

Critical to the training of models FM1–FM5 and TM is determining the length $T = |\mathcal{T}|$ of the training set. This length defines when the data linked to certain days in the past have become too old to be considered in the training process. We devote the first year of data to tune this length for models FM1–FM5. In this time interval, the piece of data spanning from 08/07/2015 to 02/02/2016 (180 days) is used as the validation subset. We then compute the MAE on this subset for each of the models FM1–FM5 and for different lengths of the training subset, which we vary from one to seven months. We remark that the length of the training set is the only hyper-parameter that needs to be tuned for our models, which represents an advantage in terms of ease of use and implementation.

T	FM1	FM2	FM3	FM4	FM5
1	11.67	7.40	10.37	4.57	-2.08
2	12.30	10.97	11.95	10.18	7.98
3	12.78	11.40	12.55	12.62	10.87
4	12.51	11.55	12.38	12.75	11.52
5	12.46	11.10	12.48	13.05	12.01
6	12.67	11.75	12.83	13.05	12.69
7	12.46	11.86	12.49	13.03	12.37

Table 3.1: MAE reduction in percentage (%) with respect to the benchmark for different lengths of the training set T (months of data).

Table 3.1 summarizes the results of this analysis, where the MAE linked to each model and length is expressed in percentage reduction with respect to the MAE associated with the benchmark, namely, the onshore DK1-wind power forecast issued by the Danish TSO. From this table, we see that the improvement in the performance of models FM1–FM5, which is initially observed as we increase the length of the training set, not only ends up saturating, but even reverses, as we extend the training set beyond several months (e.g., six months in the case of FM5). This is due to the fact that, at some point in time, the information contained in the oldest data becomes obsolete and thus, potentially misleading. In light of these results, we set the length of the training set for forecasting to six months.

We proceed in a similar fashion to establish the length of the dataset we use to train the trading model TM. In this case, we change the validation subset to 06/03/2016–11/29/2016 (180 days). This change is required because model TM is fed with the improved wind power forecast yielded by FM3 (the one exhibiting the best trade-off between simplicity, data reliability and forecasting performance). Consequently, training model TM involves generating a sufficient number of predictions from model FM3 first, which, in turn, is to be trained over a dataset spanning six months. Hence, we need to reserve a large chunk of data to study the impact of the length of the training set on the performance of model TM. Table 3.2 shows the results of this study for a length of the training set varying from one to ten months. The numbers in the table correspond to the AOL reduction of model TM in percentage with respect to the AOL given by the benchmark, that is, the trading strategy consisting in submitting the wind power prediction issued by the Danish TSO to the pan-European electricity market. In view of these results and for ease of implementation, we also set the length of the training set for trading to six months.

Next, we discuss the results obtained from the simulation conducted on all the remaining days in the full dataset that have not been used to determine the length of the training set.

T	1	2	3	4	5	6	7	8	9	10
TM	3.04	7.62	8.20	8.33	9.29	9.14	8.36	8.25	8.05	7.67

Table 3.2: AOL reduction in percentage (%) of model TM with respect to the benchmark for different lengths of the training set T (months of data).

	FM1	FM2	FM3	FM4	FM5	UM1	UM2
MAE	7.03	7.03	8.53	8.55	8.53	10.18	8.80
RMSE	6.04	6.22	7.16	7.33	7.46	9.14	7.46

Table 3.3: MAE and RMSE reduction in percentage (%) with respect to the benchmark.

3.1.3 Results

We divide this section into two parts. In the first one, we present and discuss the improvements in wind power forecasting brought about by the linear decision rule that results from (3.16). Subsequently, we elaborate on the improvements in wind power trading that we attain by means of model (3.18).

3.1.3.1 Improvements in Wind Power Forecasting

The first and last days in the test set are 02/04/2016 and 04/22/2019. That is, the test set in the simulation comprises 1174 days in total. Table 3.3 provides the MAE and the RMSE reductions (in percentage) with respect to the performance metrics of the benchmark, namely, the raw forecast issued by the Danish TSO.

We observe that model (3.16), which, in essence, is a computationally inexpensive and interpretable linear program, is able to substantially enhance the wind power forecasts made by Energinet.dk. In fact, most of the reduction can be achieved by linearly combining Energinet.dk’s predictions for the onshore and offshore DK1-wind power productions (model FM1). From these results, we infer that historical information of wind power forecasts pertaining to neighboring bidding zones is not currently being exploited by the Danish TSO. In contrast, the performance comparison of models FM1 and FM2, on the one hand, and of models FM4 and FM5, on the other, seems to signal the fact that the “hour of the day” and “day of the week”, and the day-ahead forecasts of solar power production, scheduled generation and total load in DK1 do not have predictive power on the targeted variable. Moreover, the comparison between FM1 and UM1 reveals that a significant improvement in the forecasting of the DK1-onshore wind power production can be attained by enhancing the quality of the forecasts in the areas adjacent to DK1. However, the comparison between FM1, FM3, FM4 and UM2 further indicates that the bulk of this potential improvement is to be attributed to the DK1 and DK2 wind-related features. The models of the type in (3.16) that exhibit the best forecasting performance are FM3, FM4 and FM5. Since FM3 is significantly simpler

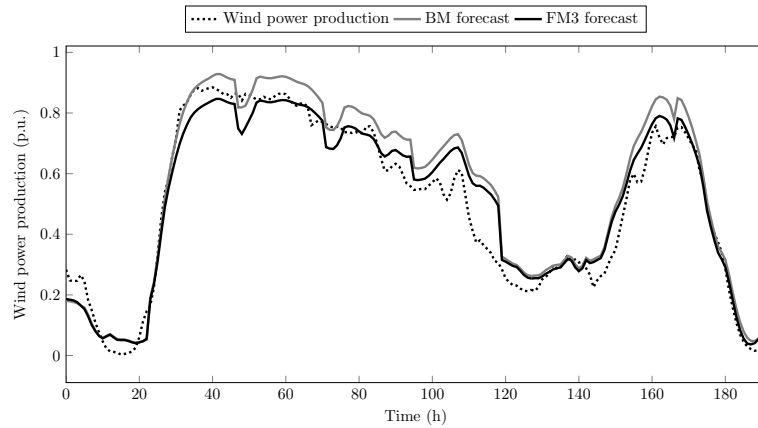


Figure 3.2: Illustration of the forecasts issued by the Danish TSO (BN) and model FM3 for the interval 01/01/16 to 01/08/16 (mm/dd/yyyy).

than the rest and offers the best guarantees in terms of data reliability⁵, we use FM3 to feed TM with the required wind power forecast. Interestingly, even though models FM2 and FM5 exploit a larger number of features than FM1 and FM4, respectively, their forecasting performance is not (or barely) improved.

For the sake of illustration, Figure 3.2 plots the actual realization of the wind power production in the time interval 01/01/16 to 01/08/16, together with the forecasts issued by Energinet.dk (BN) and the proposed model FM3. It can be observed that from hour 80 onwards, the forecast yielded by FM3 is always closer to the actual wind power production than the forecast used by the Danish TSO. On average, model FM3 produces forecasts that, over the simulation period, deviate 100.44 MW with respect to the true wind power values, whereas Energinet.dk's average deviation for this period amounts to 109.82 MW.

The simplicity of model (3.16) makes it more interpretable than other forecasting models based, for instance, on artificial neural networks. Not surprisingly, the coefficient corresponding to the onshore DK1-wind power forecast issued by the Danish TSO is the largest one for the FM and UM models. For example, its value in model FM4 ranges from 0.8335 to 1.0267 over the simulation period. The other coefficient values of model FM4 are depicted in a box plot in Figure 3.3. As observed, the forecasts for the offshore DK1-wind, the onshore and offshore DK2-wind, and the onshore SE4-wind are also significant.

⁵Model FM3 uses data simultaneously produced and uploaded to the ETP by the same entity, namely, the Danish TSO. One can expect, therefore, that the forecasts contained in these data have been built with the same past information available.

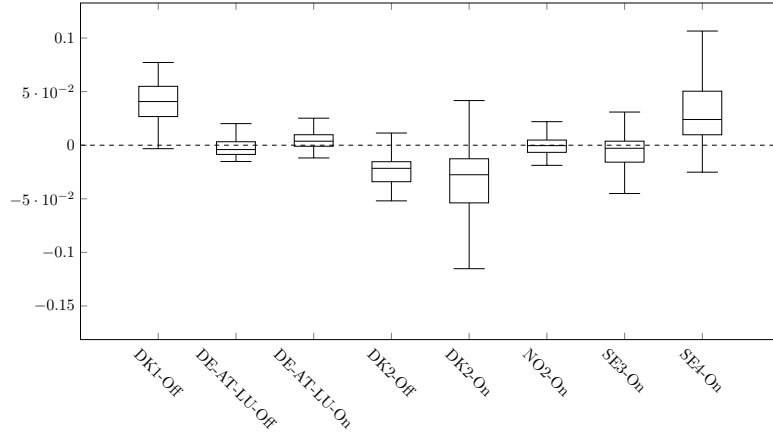


Figure 3.3: Box plot of the coefficients obtained for FM4 in the simulation period 02/04/16 to 04/22/2019.

3.1.3.2 Improvements in Wind Power Trading

The first and last days of the test set, in this case, are 11/30/2016 and 04/22/2019, in that order. This means that the test set in this simulation consists of 874 days. In this analysis we assume that the wind power point forecast issued by each model is directly bid into the day-ahead market and then we compute the average opportunity loss as in (3.22).

If the forecasts issued by FM3 are used as bids, the AOL is reduced by 1.30% with respect to the benchmark, which consists in bidding the raw wind power point forecast issued by the Danish TSO into the day-ahead market. Although model FM3 is tailored to forecasting, the reduction of the prediction error that it achieves is accompanied with an AOL decrease too.

If the mid-term dynamics of the marginal opportunity costs are accounted for through model TM, the AOL reduction increases up to 2.13%. In this regard, the histogram of the values taken on by the decision-rule parameter w^T over the simulation period is plotted in Figure 3.4. Interestingly, this parameter tends to take values above 1, so as to profit from the fact that, in the DK1 bidding zone, overproduction is, on average, more penalized than underproduction.

To further explain the AOL reduction achieved by TM, we define the empirical *critical fractile* estimated over the training set \mathcal{T} as

$$R = \frac{\frac{1}{T} \sum_{t \in \mathcal{T}} \psi_t^+}{\frac{1}{T} \sum_{t \in \mathcal{T}} \psi_t^- + \frac{1}{T} \sum_{t \in \mathcal{T}} \psi_t^+}. \quad (3.23)$$

The ratio R balances the marginal opportunity cost for overproduction and the marginal opportunity cost for either under- or overproduction, all of them averaged over \mathcal{T} . A value of R higher than 0.5 means that the opportunity cost for overproduction was

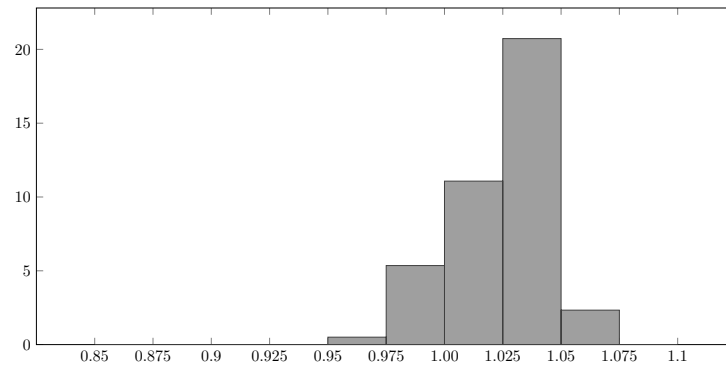


Figure 3.4: Histogram of the values taken on by the decision-rule parameter w^T in model TM for the interval 11/30/16 to 04/22/19.

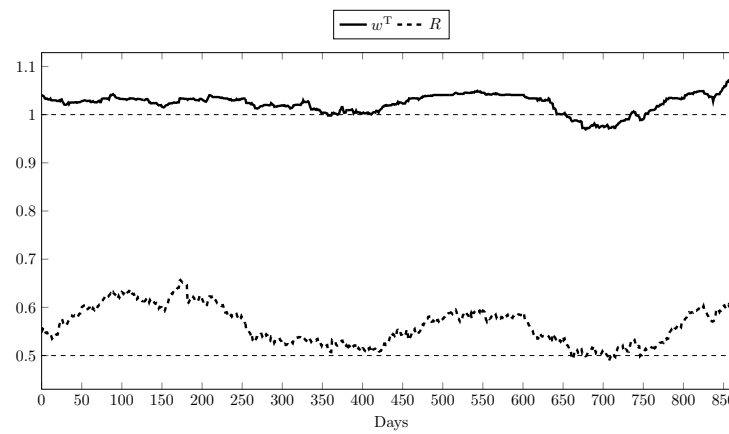


Figure 3.5: Evolution of decision-rule parameter w^T in TM and ratio R for the interval 11/30/16 to 04/22/19.

more significant than that for underproduction throughout the training period. In such a case, the optimal market bid should be higher than the forecast production in order to hedge against overproduction. Conversely, if R is lower than 0.5, the optimal market bid should be lower than the forecast production.

Figure 3.5 depicts the time evolution of the decision-rule parameter w^T in TM together with the ratio R over the simulation period 11/30/16-04/22/19. As observed, the value of w^T continuously adapts to the variations of R as the training period \mathcal{T} moves forward. This way, the bids provided by TM take into account the mid-term dynamics of ψ^- and ψ^+ to properly hedge against under or overproduction.

Finally, Figure 3.6 illustrates the accrued reduction in opportunity loss achieved by model TM with respect to the benchmark over the simulation period. Note that the plot is studded with time instants when the accrued improvement suddenly decreases. This is because the series of balancing prices is scattered with highly unpredictable spikes. Indeed, the limited predictability of balancing prices is what makes the trading strategy consisting in minimizing expected deviations so hard to beat. To finish this section, we

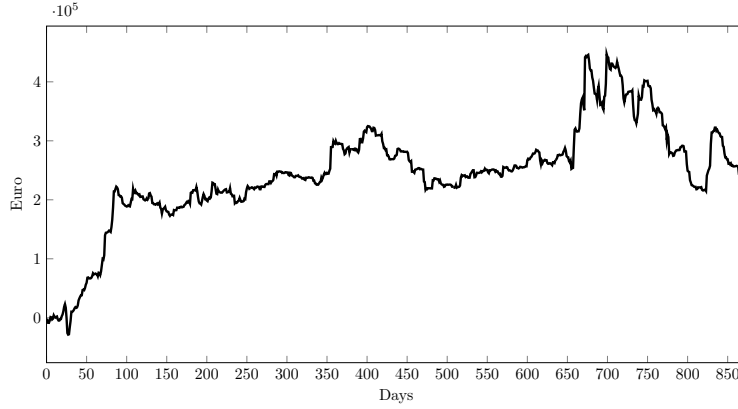


Figure 3.6: Accumulated opportunity-loss reduction of TM for the interval 11/30/16 to 04/22/19 for a installed capacity of 3669 MW.

note that a similar experiment could be conducted for a particular wind farm or a particular wind power producer. To illustrate the benefits of our approach, however, we have decided to work with the aggregate onshore DK1-wind power production for several reasons. First, there is a rich set of market data related to DK1 and surrounding bidding zones publicly available in ETP, while analogous datasets for specific wind farms or producers are usually kept confidential. Second, DK1 uses a dual-price balancing settlement, and last, the onshore installed wind power capacity in DK1 amounts to 3669 MW. Today, portfolios of similar size can easily be found in countries such as Spain, United Kingdom or Germany⁶.

3.2 Online wind power producer

Next, we present another strongly related application addressing the wind power producer problem in an online setting. As mentioned in the previous application, it is common that wholesale electricity markets require producers to make offers anywhere between 12 to 36 hours before, in the so-called day-ahead markets. It is clear that this requirement hinders the integration of variable renewable energy and wind energy in particular due to the significant lead time between the offer and the actual delivery of energy, which in turn dilutes the accuracy of the forecasts and the value of contextual information (see Section 3.1.1.2).

Aware of this and other issues, and backed by the development of information technologies and computation capabilities, there is a current trend that points towards a reduction in the lead time of electricity markets⁷. Inspired by this idea, we investigate a conceptual setting in which the daily wholesale electricity market (which usually closes at 12.00 the day before) is replaced by an hourly market that closes just before the start of the next energy delivery period. This setting has a threefold purpose, namely:

⁶The Wind Power. See https://www.thewindpower.net/owners_en.php.

⁷Increasing time granularity in electricity markets, innovation landscape brief, IRENA (2019).

i) it helps us to quantify the evident gains that avoiding the lead time could mean for wind power producers, ii) it enables the investigation of online algorithms, showcasing the benefits they bring to electricity markets, and iii) it allows us to use realistic data, obtained from the Danish TSO Energinet, from a market with a dual-price settlement for imbalances.

In this setting, two remarks should be made. Firstly, the production during the delivery period is still uncertain since wind energy exhibits fast dynamics and can significantly vary from one period to another. At the same time, those *predictive* approaches based on forecasts are obviously more precise than in the case of day-ahead markets, meaning that methods such as FO, described in Section 2.2, are stronger contestants to beat. Against this background, we particularize the contextual online gradient descent (COGD) algorithm, introduced in Section 2.2.2, to the wind power producer problem, comparing its performance with respect to other approaches that use contextual information in the previous application, such as FO and DR.

The COGD algorithm combines elements from the DR approach and the popular online gradient descent (OGD) [152]. For a review of the work closer, in a methodological sense, to COGD, we refer the reader to Section 2.3.3. Online algorithms have proved helpful in many relevant problems related to power systems and electricity markets with applications to the optimal power flow [61, 70], real-time markets [67], demand response [85, 84, 86] with several authors highlighting the connection between online learning and control theory [6, 39]. However, to the best of our knowledge, the problem of a wind power producer offering in a wholesale electricity market, as formulated in this chapter, has not yet being addressed using online gradient methods.

The wind power producer problem was already introduced in the previous application, and therefore we refer the reader to Section 3.1 for a general review of the literature on trading wind energy. For completeness, we address the most relevant work in connection with the current application emphasizing those aspects related to an online setting. As in the previous application, the work by [92] and [35] is related to ours. The reinforcement learning algorithm used in [92] to follow the optimal quantile is different from ours because, again, we do not require a wind power predictive density available and we do not track the optimal quantile but rather we focus on encoding the optimal offer as a linear decision rule of the features. Note that reinforcement learning includes a different set of techniques concerned with the repercussion of the decision in the future based on the current state rather than updating the decision based on the last information obtained as in the online setting. In [35], the authors propose a meta-optimization problem to optimize the forecasting hyper-parameters taking into account the decision task and an artificial neuronal network to minimize the imbalance cost. Both approaches are complex, involving several independent components to be implemented, and they are computationally more expensive than the continuous update

that COGD performs.

Evidently, the work in [101] (on which the previous application is based) is one of the closest to the application under discussion here. Both approaches replace the target variable with a linear decision rule dependent on contextual information. However, each approach tackles different market settings, resulting in different design characteristics. In the case of the previous application, the accuracy of the forecasts available to the producer is substantially lower, requiring a two-step procedure that involves forecasting and trading steps to prevent overfitting. Conversely, we can avoid the former in the current application. Another relevant distinction is that, in this application, the producer learns the performance of her offer before making the next one, enabling continuous feedback through the online COGD algorithm. Consequently, the COGD algorithm avoids the resolution of any mathematical program yielding a computationally inexpensive method suitable to produce offers in markets with reduced lead time.

3.2.1 Problem description

As explained in the introduction of this section, the setting addressed here is very close to the one described in Section 3.1.1. The main difference lies in that we consider an hourly wholesale electricity market that closes just before the start of the actual delivery of energy. This is a fundamental difference with respect to the day-ahead market addressed in the previous application, since it enables continuous feedback of the wind power producer's offer based on its performance during the last period and the reduced lead time increases the value of potentially informative samples. Other than that, the problem is very similar to the one presented in Section 3.1.1.

To avoid repetition, we refer the reader to Section 3.1.1 for a general introduction of the problem, observing the comments of the paragraph above. Note that in this application, we replace the nomenclature E_t^D by E_t^F to emphasize that we consider a different market setting (D comes from day-ahead market while F from forward market).

3.2.2 The online newsvendor algorithm

In this section, we particularize the contextual online gradient descent (COGD), introduced in Section 2.3.3, to the context of a wind power producer offering in a forward market. The result is an algorithm that we named OLNv (from online newsvendor). For the derivation of OLNv, we start recovering problem (3.12) that we reproduce here for completeness:

$$\min_{\mathbf{w}} \frac{1}{T} \sum_{t \in \mathcal{T}} \psi_t^- (\mathbf{w}^\top \mathbf{x}_t - E_t)^+ + \psi_t^+ (E_t - \mathbf{w}^\top \mathbf{x}_t)^+ \quad (3.24a)$$

$$\text{s.t. } 0 \leq \mathbf{w}^\top \mathbf{x}_t \leq \bar{E}, \quad \forall t \in \mathcal{T}. \quad (3.24b)$$

In this application, we refer to the approaches based on this model with the abbreviation DR (from decision rule). Recall that the update of the optimal solution to (3.24), denoted from hereon as \mathbf{w}^{DR} , is achieved by resolving from scratch problem (3.24) at each step. Then, an offer in the forward market can be computed as

$$E_t^{\text{F}} = \max(0, \min(\bar{E}, (\mathbf{w}^{\text{DR}})^{\top} \mathbf{x}_t)). \quad (3.25)$$

Instead, in OLVN, we start from an initial value \mathbf{w}_1 and perform continuous updates of this vector based on the information provided by the last realization of the objective function. The objective function of (3.24) when the set \mathcal{T} reduces to one sample yields

$$NV_t(\mathbf{w}) = \psi_t^+ (E_t - \mathbf{w}^{\top} \mathbf{x}_t)^+ + \psi_t^- (\mathbf{w}^{\top} \mathbf{x}_t - E_t)^+, \quad (3.26)$$

where NV_t (from newsvendor) refers to the newsvendor objective function in period t . The OLVN method requires computing a gradient of the objective function to perform the update, for which we analyze two alternative procedures in the following paragraphs.

The first approach is inspired by the work of [150] on the pinball loss, a particular case of the objective function found in newsvendor models. Since the pinball loss is not strictly differentiable, the authors propose an alternative smooth approximation to ensure that computing gradients is always possible. Note that the objective function (3.26) is not differentiable at $E_t = \mathbf{w}^{\top} \mathbf{x}_t$. We first propose to circumvent this issue extending the approach in [150] to the more general expression (3.26) that considers arbitrary (positive) penalties as

$$NV_{t\alpha}(\mathbf{w}) = \psi_t^+ (E_t - \mathbf{w}^{\top} \mathbf{x}_t) + \alpha(\psi_t^- + \psi_t^+) \log(1 + e^{-(E_t - \mathbf{w}^{\top} \mathbf{x}_t)/\alpha}), \quad (3.27)$$

where $\alpha > 0$ is a parameter that controls the approximation and where higher values result in smoother functions. Then, we derive a closed-form solution to obtain gradients of (3.27), yielding

$$\nabla NV_{t\alpha}(\mathbf{w}) = \left(-\psi_t^+ + (\psi_t^+ + \psi_t^-) \frac{1}{1 + e^{(E_t - \mathbf{w}^{\top} \mathbf{x}_t)/\alpha}} \right) \mathbf{x}_t. \quad (3.28)$$

The second approach deals directly with the objective function as formulated in (3.26). Even though the original objective is not strictly differentiable, a variant of the OLVN algorithm is readily applicable to subdifferentiable functions, provided that a subgradient can be computed instead [107]. In this case, the mapping that returns a subdifferential

of (3.26) is given by

$$\partial NV_t(\mathbf{w}) = \begin{cases} -\psi_t^+ \mathbf{x}_t, & E_t - \mathbf{w}^\top \mathbf{x}_t > 0, \\ \psi_t^- \mathbf{x}_t, & E_t - \mathbf{w}^\top \mathbf{x}_t < 0, \\ [-\psi_t^+ \mathbf{x}_t, \psi_t^- \mathbf{x}_t], & E_t - \mathbf{w}^\top \mathbf{x}_t = 0. \end{cases} \quad (3.29)$$

Note that, when $E_t - \mathbf{w}^\top \mathbf{x}_t = 0$, any value in the interval $[-\psi_t^+ \mathbf{x}_t, \psi_t^- \mathbf{x}_t]$ is a legitimate subgradient belonging to $\partial NV_t(\mathbf{w})$. For the sake of simplicity and reproducibility, the implementation of our algorithm returns zero whenever this condition is fulfilled.

Once a gradient as in (3.28) or a subgradient as in (3.29) has been computed, the key step of OLVN is to update \mathbf{w}_t using a multidimensional learning rate $\boldsymbol{\eta}_t \in \mathbb{R}^p$ (note that in this case the dimension of the learning rate is equal to the dimension of the contextual information vector) through

$$\mathbf{w}_{t+1} = \Pi(\mathbf{w}_t - \boldsymbol{\eta}_t \circ \boldsymbol{\tau}_t, \mathbf{x}_t), \quad (3.30)$$

where \circ denotes the element-wise product, $\boldsymbol{\tau}_t = \nabla NV_{t\alpha}(\mathbf{w}_t)$ or $\boldsymbol{\tau}_t = \partial NV_t(\mathbf{w}_t)$ depending on the implementation of OLVN, and Π is a projection operator defined as $\Pi : \mathbb{R}^p \times \mathcal{X} \rightarrow \mathbb{R}^p$. Precisely, Π maps its arguments into the solution of the following optimization problem:

$$\Pi(\mathbf{o}, \mathbf{x}) = \arg \min_{\mathbf{w} \in W(\mathbf{x})} \frac{1}{2} \|\mathbf{o} - \mathbf{w}\|_2. \quad (3.31)$$

The feasible set in (3.31) is defined by the set-valued mapping $W : \mathcal{X} \rightrightarrows \mathbb{R}^p$, $W(\mathbf{x}) = \{\mathbf{w} : 0 \leq \mathbf{w}^\top \mathbf{x} \leq \bar{E}\}$. Note that, for any input \mathbf{x} , the output of W is a convex region bounded by two parallel hyperplanes. As the Euclidean norm is used, a unique solution is guaranteed to exist for any instance of (3.31). Generally, the Euclidean projection of a point into a convex set requires solving a convex optimization problem, however, the definition of W allows us to find a closed-form expression, yielding

$$\Pi(\mathbf{o}, \mathbf{x}) = \begin{cases} \mathbf{o}, & 0 \leq \mathbf{o}^\top \mathbf{x} \leq \bar{E}, \\ \mathbf{o} + \frac{\bar{E} - \mathbf{o}^\top \mathbf{x}}{\|\mathbf{x}\|_2^2} \mathbf{x}, & \mathbf{o}^\top \mathbf{x} > \bar{E}, \\ \mathbf{o} + \frac{-\mathbf{o}^\top \mathbf{x}}{\|\mathbf{x}\|_2^2} \mathbf{x}, & \mathbf{o}^\top \mathbf{x} < 0. \end{cases} \quad (3.32)$$

This reduces the resolution of the optimization problem (3.31) to evaluating (3.32). Even though the operator Π guarantees the feasibility of \mathbf{w}_t under the realization \mathbf{x}_t , we need to resort to the projection

$$\pi(\mathbf{w}, \mathbf{x}) = \max(0, \min(\bar{E}, \mathbf{w}^\top \mathbf{x})), \quad (3.33)$$

setting $E_t^F = \pi(\mathbf{w}_t, \mathbf{x}_t)$ to ensure E_t^F remains feasible for any new piece of contextual information.

The last remaining aspect is to compute the vector $\boldsymbol{\eta}_t$ following the ideas in [147]. As introduced in Section 2.3.3, we use the update given by (2.32) and (2.33) in our OLN algorithm with the values $\epsilon = 10^{-6}$ and $\rho = 0.95$, following the recommendations in [147]. The benefit of this update is twofold. On the one hand, OLN adapts the learning rate vector to the scale of every feature. On the other, OLN is capable to track the most recent dynamic between the uncertain vector $[E_t, \psi_t^+, \psi_t^-]$ and the vector of contextual information \mathbf{x}_t . Finally, the complete OLN algorithm particularized for the feature-driven wind power producer problem is compiled in Algorithm 4. Recall that “ $\circ n$ ” denotes the n -th Hadamard power with $n \in \mathbb{R}$ so that $\boldsymbol{\tau}_t^{\circ 2} = [\tau_{t1}^2, \dots, \tau_{tq}^2]^\top$ and $\bar{\boldsymbol{\tau}}_t^{\circ 2}$ is the moving average vector of the former.

Algorithm 4 Online Newsvendor (OLNV)

Require: Initial values $\mathbf{w}_1 \in \mathbb{R}^p$, $\eta > 0$, $\rho \in [0, 1)$, $\epsilon \in \mathbb{R}^+$

- 1: Initialize $\bar{\boldsymbol{\tau}}_0^{\circ 2} = \mathbf{0}$
 - 2: **for** $t = 1$ to T **do**
 - 3: Output \mathbf{w}_t
 - 4: Receive \mathbf{x}_t
 - 5: Compute $E_t^F = \pi(\mathbf{w}_t, \mathbf{x}_t)$
 - 6: Receive NV_t and pay $NV_t(E_t^F)$
 - 7: Set $\boldsymbol{\tau}_t = \nabla NV_{t\alpha}(\mathbf{w}_t)$ or $\boldsymbol{\tau}_t = \partial NV_t(\mathbf{w}_t)$
 - 8: Accumulate $\bar{\boldsymbol{\tau}}_t^{\circ 2} = \rho \bar{\boldsymbol{\tau}}_{t-1}^{\circ 2} + (1 - \rho) \boldsymbol{\tau}_t^{\circ 2}$
 - 9: Compute $\boldsymbol{\eta}_t = \eta(\bar{\boldsymbol{\tau}}_t^{\circ 2} + \epsilon \mathbf{1})^{\circ -1/2}$
 - 10: Update $\mathbf{w}_{t+1} = \Pi(\mathbf{w}_t - \boldsymbol{\eta}_t \circ \boldsymbol{\tau}_t, \mathbf{x}_t)$
 - 11: **end for**
-

3.2.3 Regularization through average penalty anchoring

In a mature electricity market under a dual-price mechanism, it is common that $\psi_t^+ = \psi_t^- = 0$ for a significant number of hours [97], meaning that load and generation are close to equilibrium in the system. From (3.26), it is evident that, in this situation, a deviation from the forward market offer is not penalized since the imbalances and forward market offers are paid the same price. Moreover, the gradients computed through (3.26) are equal to zero and therefore the variable vector \mathbf{w}_t is not updated, wasting information about the relationship between E_t and \mathbf{x}_t . For their part, when penalties are different from zero, they typically exhibit random behavior with sharp spikes representing highly imbalanced scenarios which, in turn, yields destabilizing updates of the vector \mathbf{w}_t . To tackle both issues, we propose performing the following convex transformation of the original penalties:

$$\psi_t^{+'} = \mu \psi_t^+ + (1 - \mu) \bar{\psi}^+, \quad (3.34)$$

$$\psi_t^{-'} = \mu\psi_t^- + (1 - \mu)\bar{\psi}^-, \quad (3.35)$$

where $0 \leq \mu \leq 1$ and $\bar{\psi}^+, \bar{\psi}^- \in \mathbb{R}^+$ are the historical average penalties. This convex transformation is inspired by the concept of constraining the optimal offer around the point forecast developed in [153], but unlike them, we do not impose hard constraints on the decision vector \mathbf{w}_t . Instead, we smooth the objective function using as anchor the sample average optimal market quantile determined by the average market penalties $\bar{\psi}^+$ and $\bar{\psi}^-$. To do so, we consider a convex combination of the original objective function (3.26), which we denote NV_t^R , with an additional term that minimizes such a quantile,

$$\begin{aligned} NV_t^R = & \mu\psi_t^+ \left(E_t - \mathbf{w}^\top \mathbf{x}_t\right)^+ + \mu\psi_t^- \left(\mathbf{w}^\top \mathbf{x}_t - E_t\right)^+ \\ & + (1 - \mu)\bar{\psi}^+ \left(E_t - \mathbf{w}^\top \mathbf{x}_t\right)^+ + (1 - \mu)\bar{\psi}^- \left(\mathbf{w}^\top \mathbf{x}_t - E_t\right)^+. \end{aligned} \quad (3.36)$$

Then, by means of (3.34) and (3.35), we recover the original objective structure, i.e.,

$$NV_t^R = \psi_t^{+'} \left(E_t - \mathbf{w}^\top \mathbf{x}_t\right)^+ + \psi_t^{-'} \left(\mathbf{w}^\top \mathbf{x}_t - E_t\right)^+. \quad (3.37)$$

Therefore, by replacing ψ_t^+, ψ_t^- with $\psi_t^{+'}, \psi_t^{-'}$ in the original objective function, we regularize the learning procedure adding no extra computational cost. Thus, by selecting $\mu < 1$, provided that $\bar{\psi}^+, \bar{\psi}^- > 0$, the algorithm leverages the information contained in samples with both penalties equal to zero, potentially accelerating the convergence and obtaining smoother updates through the gradient. The same reasoning applies to the smooth objective function. Note that when the available samples are not sufficient to provide reliable estimators of the true $\bar{\psi}^+$ and $\bar{\psi}^-$, the producer can resort to assuming a balanced market with penalties $\bar{\psi}^+ = \bar{\psi}^- = 1$.

3.2.4 Performance evaluation

Consider that we have a sequence of offers E_1^F, \dots, E_T^F obtained by solving (3.24) or from Algorithm 4 after learning, one by one, the samples belonging to the test set $\tilde{\mathcal{T}}$. As in the previous application, we can evaluate the economic performance of this sequence through the *average opportunity loss* (AOL), which we reproduce here for completeness

$$\text{AOL} = \frac{1}{|\tilde{\mathcal{T}}|} \sum_{t \in \tilde{\mathcal{T}}} \psi_t^- (E_t - E_t^F)^+ + \psi_t^+ (E_t^F - E_t)^+, \quad (3.38)$$

where $\tilde{T} = |\tilde{\mathcal{T}}|$. The value of this metric alone provides limited information about how a particular method is performing. A natural benchmark is the score obtained when a forecast of the wind energy production (in the sense of minimizing the root mean square error) is directly used as an offer in the market. We refer to this method as FO (from

forecast). Let AOL^{FO} be the average opportunity loss incurred by FO. Leveraging this quantity, we redefine the original metric in relative terms, i.e.,

$$\text{AOL}(\%) = \frac{\text{AOL}^{\text{FO}} - \text{AOL}}{\text{AOL}^{\text{FO}}} \cdot 100. \quad (3.39)$$

In this manner, the metric is expressed as a percentage of the possible improvement, where a value of 100% means perfect performance with zero deviation cost. As in the previous application, we use this metric as the main tool to evaluate the economic performance in the case study presented in Section 3.2.6.

The regret is a metric very related to the definition of the AOL in (3.38). However, the regret places the focus on the performance against a benchmark instead of measuring the monetary returns *per se*. This metric is a central pillar of the online learning literature. Traditionally, in online learning, the regret compares a sequence of decision $\mathbf{w}_1, \dots, \mathbf{w}_T$ against the best single vector in hindsight $\mathbf{w}^{\mathcal{H}}$. The latter is computed *ex-post* solving a problem analogous to (3.24) once the whole collection of samples belonging to $\tilde{\mathcal{T}}$ is known. Let $W^{\mathcal{H}}$ be the intersection of all feasible sets $W(\mathbf{x}_t)$, more precisely $W^{\mathcal{H}} : \mathcal{X} \rightrightarrows \mathbb{R}^p$, $W^{\mathcal{H}} = \{\mathbf{w} : 0 \leq \mathbf{w}^\top \mathbf{x}_t \leq \bar{E}, t \in \tilde{\mathcal{T}}\}$. The *standard* regret, used in online learning [37, 107], renders

$$\mathcal{R}_T^s = \sum_{t \in \tilde{\mathcal{T}}} NV_t(\mathbf{w}_t) - \min_{\mathbf{w} \in W^{\mathcal{H}}} \sum_{t \in \tilde{\mathcal{T}}} NV_t(\mathbf{w}). \quad (3.40)$$

Outperforming $\mathbf{w}^{\mathcal{H}}$ can be a relatively easy task when the uncertain NV_t objective functions are produced by a non-stationary process, i.e., the assumption of a fixed probability distribution generating the points $(E_t, \psi_t^+, \psi_t^-)$ does not hold. This is true despite the fact that $\mathbf{w}^{\mathcal{H}}$ is determined under perfect information since the selection is limited to a single vector. On the other side of the spectrum, one may consider the *worst case* regret, as proposed by [22], interchanging the summation and the minimum, i.e.,

$$\mathcal{R}_T^w = \sum_{t \in \tilde{\mathcal{T}}} NV_t(\mathbf{w}_t) - \sum_{t \in \tilde{\mathcal{T}}} \min_{\mathbf{w} \in W(\mathbf{x}_t)} NV_t(\mathbf{w}), \quad (3.41)$$

where the second term of (3.41) computes the best individual decision $\mathbf{w}_t^{\mathcal{H}}$. The regret computed in this way can be highly pessimistic and unrealistic. Note that in the context of the wind power producer, it is always possible to find a value for \mathbf{w} such that $E_t - \mathbf{x}_t^\top \mathbf{w} = 0$, and therefore (3.41) reduces to the summation of the original objective function $\mathcal{R}_T^w = \sum_{t \in \tilde{\mathcal{T}}} NV_t(\mathbf{w}_t)$. Alternatively, [152] suggests to compare the performance of online algorithms against a sequence of arbitrary decisions $\mathbf{u}_1, \dots, \mathbf{u}_T$,

$\mathbf{u}_t \in W(\mathbf{x}_t)$, yielding

$$\mathcal{R}_T^d = \sum_{t \in \tilde{\mathcal{T}}} NV_t(\mathbf{w}_t) - \sum_{t \in \tilde{\mathcal{T}}} NV_t(\mathbf{u}_t). \quad (3.42)$$

We refer to this approach as *dynamic* regret. This formulation enables a metric to be defined, with an adjustable difficulty between the previous benchmarks. Note that (3.40) and (3.41) are special cases of (3.42) with $\mathbf{u}_t = \mathbf{w}^{\mathcal{H}} \forall t$ and $\mathbf{u}_t = \mathbf{w}_t^{\mathcal{H}} \forall t$, in that order.

Given the ability to create regret benchmarks with intermediate difficulty between the standard and worst-case options, we choose (3.42) as the definition of regret to be used in this application. Then, the question is how to choose a reasonable series of benchmark decisions \mathbf{u}_t to be used against OLNv. To this end, we propose dividing $\tilde{\mathcal{T}}$ in k adjacent partitions of equal length l , except possibly the last one. Without loss of generality, by assuming $T - kl = 0$, we have $\tilde{\mathcal{T}}_i = \{t : (i-1)l + 1 \leq t \leq il\}, \forall i$, with $i = 1, \dots, k$. Let us define the feasible sets $W_i^{\mathcal{H}} = \{\mathbf{w} : 0 \leq \mathbf{w}^\top \mathbf{x}_t \leq \bar{E}, t \in \tilde{\mathcal{T}}_i\}$. Accordingly, we can compute $\mathbf{w}_i^{\mathcal{H}} \in \arg \min_{\mathbf{w} \in W_i^{\mathcal{H}}} \sum_{t \in \tilde{\mathcal{T}}_i} NV_t(\mathbf{w})$.

Finally, the sequence of decisions to be used in this application, together with the dynamic definition of regret in (3.42), is $\mathbf{u}_t = \mathbf{w}_i^{\mathcal{H}}, \forall t \in \tilde{\mathcal{T}}_i$. We empirically investigate the dynamic regret performance of OLNv in the case study presented in Section 3.2.6.

3.2.5 Illustrative examples

This section analyzes several illustrative examples to gain insight into the behavior of OLNv. The first case compares the two alternative implementations introduced in Section 3.2.2 and discusses their main properties. As a result of this analysis, we select the subgradient objective function as the default procedure to perform the update of \mathbf{w}_t in OLNv. On a different front, one of the key features of online learning algorithms is their tracking ability. In the second illustrative example, we deal with a dynamic environment with alternating penalty scenarios where we compare the DR approach, based on a linear optimization problem and a training set of many samples, and the online OLNv algorithm, demonstrating the salient capabilities of the latter in this regard.

3.2.5.1 Comparing the smooth and subgradient objective

This illustrative example aims to elucidate whether the smooth approximation presented in (3.27) provides any computational advantage over the direct subgradient implementation of OLNv to select the implementation to be used in the rest of the case study.

To this end, we consider a simplified setting with a single feature, a forecast of the actual wind production, which we also use as the baseline of the method FO, and a single

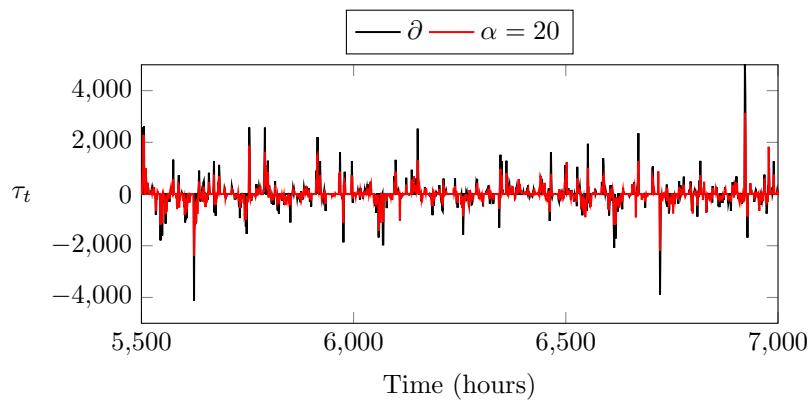


Figure 3.7: Sample of the (sub-)gradients τ_t of NV_t and NV_{t20} computed in the dataset of the illustrative example.

	∂	$\alpha = 0.05$	$\alpha = 5$	$\alpha = 20$
$ \bar{\tau} $	121.7	122.0	125.6	133.5
σ	380.8	379.7	310.4	293.3
AOL(%)	5.3	5.2	0.8	-14.5

Table 3.4: Average absolute value $|\bar{\tau}|$ and standard deviation σ of the (sub-) gradients and the metric AOL(%) computed for three smooth (α) and one subgradient (∂) implementations of the OLVN.

regressor $w_t \in \mathbb{R}$. No intercept is considered to ease the representation and analysis of w_t . We sample the feature from a uniform distribution $x_t \sim U(10, 90)$ (MW) and the true wind generation series is built adding a normal noise $E_t = x_t + \epsilon_t$ with $\epsilon_t \sim \mathcal{N}(0, 6)$ (MW). We produce a dataset of 1 year (8760 samples) through this process. Given that the penalties ψ_t^+ and ψ_t^- are difficult to simulate, we compute them based on real day-ahead and regulation prices of the Danish DK1 bidding zone. We retrieve data corresponding to the year 2017 from the data portal of the Danish TSO, Energinet⁸. Four implementations of Algorithm 4 are executed, three of them computing gradients of the smooth objective function through (3.28) with $\alpha = 0.05, 5$ and 20 , respectively, and the last one leveraging subgradients of the original cost mapping as in (3.29), to which we refer as ∂ . All instances are initialized with $w_1 = 1$, which means that the first offer produced by FO and OLVN are the same. In this section we do not use any convex transformation of the prices, i.e., $\mu = 1$, and we set $\eta = 0.005$. We run the OLVN algorithm throughout the dataset, performing updates of w_t every hour.

Figure 3.7 shows a sample of ∂NV_t and ∇NV_{t20} that correspond to the subgradient and gradient of the smooth objective function with $\alpha = 20$, respectively. Note that only NV_t and NV_{t20} are represented for the sake of clarity. We can observe that the maximum values of the spikes in the case of NV_{t20} are comparatively lower due to

⁸Energinet data service. See <https://www.energidataservice.dk/>

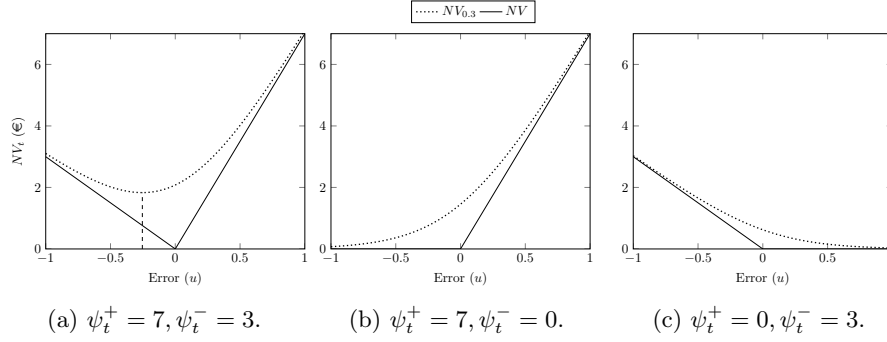


Figure 3.8: Different instances of the original NV_t and smooth $NV_{t0.3}$ objective function with $\alpha = 0.3$ and $u = E_t - \mathbf{w}^\top \mathbf{x}_t$.

the high smoothing effect obtained with $\alpha = 20$. This observation is aligned with the decreasing value of the standard deviation of the (sub-)gradients σ collated in Table 3.4 as α increases.

To the contrary, the mean absolute value of the (sub-)gradients, denoted as $|\dot{\tau}|$, follows the opposite evolution. To understand the rationale behind this evolution, we provide Figure 3.8 showing three instances of the original and smooth losses. In all cases, we corroborate that $NV_{t\alpha}$ asymptotically approaches the original newsvendor function. However, plot 3.8a evidences that the minimum of $NV_{t\alpha}$ is biased. This is valid whenever $\psi_t^+ \neq \psi_t^-$, a common situation in markets with a dual-price settlement for imbalances. Furthermore, when one penalty is equal to zero, the minimum is never attained. The imperfections of $NV_{t\alpha}$ distort the magnitude and even the sign of the gradients, causing a long-term drift of w_t that increases with α as shown in Figure 3.9.

Finally, the last row of Table 3.4 presents the AOL(%) obtained by each implementation, using the synthetic forecast FO as the baseline. In this table, it is clear that AOL(%) deteriorates when α increases. Thus, the smooth approach avoids some sharp changes in the decision vector but at the expense of a biased long-term evolution of the coefficient w_t and important economic losses. Therefore, we conclude that the smooth approximation does not provide any substantial advantage over the subgradient implementation in this application. As a result of this analysis, we use subgradients to implement the OLNv method throughout the rest of this application.

3.2.5.2 Dynamic behavior

In this illustrative example, we explore the tracking ability of the OLNv and DR approaches. Similar to the previous case, we assume that the producer only has access to a unique feature and considers a model with a single regressor. Again, we sample the forecast from a uniform distribution $x_t \sim U(10, 90)$ (MW) and the true wind generation series is built adding a normal noise $E_t = x_t + \epsilon_t$ with $\epsilon_t \sim \mathcal{N}(0, 6)$ (MW). Instead of the real DK1 data, we consider two possible scenarios with penalties $\psi_t^+ = 1, \psi_t^- = 3$

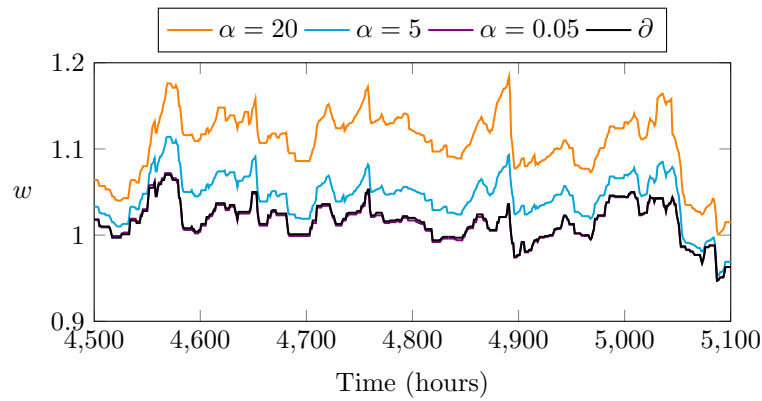


Figure 3.9: Example of the evolution of the coefficient w for different implementations of OLVN.

and $\psi_t^+ = 3, \psi_t^- = 1$, alternating every two months. This process generates 8 months of data (5760 hours) using the last 4 months (2880 hours) as the test set. The start of the test set is aligned with the beginning of a two-month scenario with $\psi_t^+ = 1$ and $\psi_t^- = 3$. The DR approach is implemented, solving the optimization problem (3.24) with a set of historical samples \mathcal{T} . Then, we leverage (3.31) to cast an offer based on the context $E_t^F = \pi(w_t^{\text{DR}}, x_t)$. The coefficient w_t^{DR} is refreshed every 24 hours solving problem (3.24) in a rolling window setting. The reason for a 24-hour update is twofold, namely it reproduces the algorithm in the previous application (see Section 3.1) and we empirically checked that there was little economical gain to be had with a lower update. The resolution time in the case of an hourly update, for example, took 24 times longer. Note that DR follows a rolling window approach that produce small changes in the training set, resulting in similar w_t^{DR} as we later discuss. We train four versions of the DR model with $|\mathcal{T}| = 720, 1440, 2160$ and 2880 (1, 2, 3, or 4 months), denoted as DR-1M to DR-4M, respectively. We use the first four months of the dataset to construct the initial training sets. Although the concept of training is substantially vaguer in the case of OLVN, the last month of the training set is used to update the value of w_t , originally initialized as $w_1 = 1$, to resemble a model that has been operating for some time.

Figure 3.10 depicts the evolution of the single regressor w_t in the test set, together with the optimal w^* to use in each penalty scenario. In the first two months, the higher value of ψ_t^- penalizes offers above the true production $E_t^F > E_t$, and consequently, the optimal strategy is to underestimate E_t^F with $w^* < 1$. In the final months, the opposite is the case. As expected, the evolution of the decision vector in the DR case is smoother, given that the optimization is performed on a data set of hundreds of hours. However, the OLVN method is substantially faster in tracking the optimal w^* . In fact, the trajectory of w_t produced by the models DR-1M to DR-4M is lagged with respect

	OLNV	DR-1M	DR-2M	DR-3M	DR-4M
AOL (%)	13	5	-5	-6	0

Table 3.5: Out-of-sample AOL (%) obtained in the test set of the illustrative example.

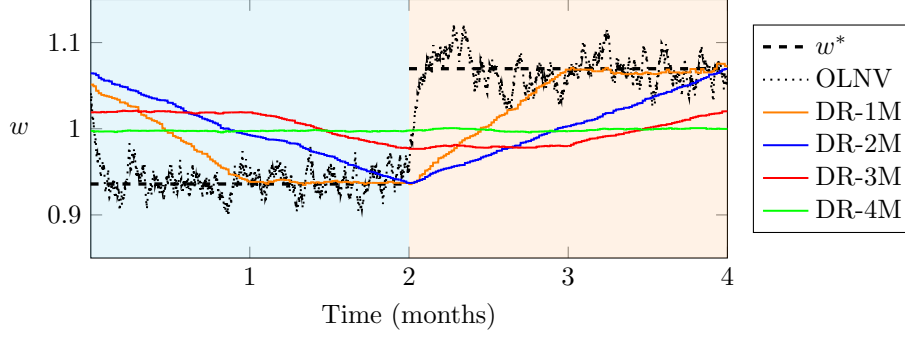


Figure 3.10: Evolution of w produced by five models over the test set. The blue and orange shaded periods correspond to the penalty scenarios $\psi_t^+ = 1, \psi_t^- = 3$ and $\psi_t^+ = 3, \psi_t^- = 1$, respectively. The entry w^* corresponds to the best single value for each penalty scenario.

to the change in the penalty scenario (emphasized by different background colors in Figure 3.10). This delay increases with the length of the training set to the point that DR-4M completely overlooks it. Note that the length of the training set in DR-4M and the period of the penalty scenarios are identical and therefore the number of samples that penalize under- or overproduction is equal and remains constant. As a result, DR-4M offers no incentive to overestimate or underestimate the forecast, yielding the same value as the one in the FO method (neglecting small deviations due to the finite sample and noise). Table 3.5 summarizes the out-of-sample AOL(%) obtained by each approach in the test set. In line with the previous analysis, DR-4M obtains the same performance as FO. The other three DR methods experience decreasing AOL(%) as the length of the training set and the lag of w_t increase. Finally, the superior adaptability of OLVN, underpinned by continuous point-wise updates based on the last information available, outperforms the DR approaches.

In this simplified example, we could have analyzed DR models with a shorter training set, probably resulting in reduced lag and better performances. However, in a realistic situation with a huge feature space and random penalties, months of data are typically required to capture the underlying relationships and generalize well in the out-of-sample set (see Section 3.1 or [101]). Therefore, the length of the training set of the DR models has to be selected as a trade-off; enough data is required to learn a policy that generalizes well, but shorter sets capture dynamics better. To the contrary, the OLVN approach completely avoids this dichotomy, providing a fast and effective method that adapts to seasonality and variations in the uncertain parameters.

year	DK1		DK2	
	Onshore	Offshore	Onshore	Offshore
2015	2966	843	608	428
2016	2966	843	608	428
2017	2966	843	608	428
2018	3664	1277	759	423
2019	3669	1277	757	423
2020	3645	1277	757	423
2021	3725	1277	756	423

Table 3.6: Installed capacity in MW by bidding zone and technology.

3.2.6 Case study

In this section, we consider the problem of a wind power producer participating in an online hour-ahead forward market with a dual-price settlement for imbalances as described in Section 3.2.1. The closure of the forward market happens just before the start of the next period. We assume that the marginal cost of the wind production is zero, and the wind power producer constantly participates in the market. Several benchmark methods are proposed to compare against OLNv. Finally, in the last part of this section, we analyze the numerical results obtained in the case study, including the regret, economical performance and computational cost of OLNv.

3.2.6.1 Data and experimental setup

This case study uses historical data compiled by the Danish TSO, Energinet.dk, since it includes market prices and several wind power forecasts that can be leveraged as quality features. We collect the true and day-ahead forecast issued by Energinet for the on- and offshore wind power production of both DK1 and DK2 Danish bidding zones together with the day-ahead and regulation prices of DK1 for the period 01/07/2015 to 06/04/2021 (mm/dd/yyyy). The day-ahead spot and regulation prices are mapped into hourly penalties through equations (3.3) and (3.4) and some small negative values, obtained due to rounding errors, are filtered out.

The raw wind power forecasts series are also processed to be used in our case study. Given that the installed capacity of the four wind categories shown in Table 3.6 evolves differently over the dataset, we independently normalize each series to lie between 0 and 100 MW, a figure that can easily represent the capacity of a standard power plant. Furthermore, according to the Danish TSO, the raw wind power forecasts are issued between 12 to 36 hours ahead, although the exact time is difficult to know because no timestamp is provided. To produce hour-ahead forecasts suitable for our case study, we feed these series into an ordinary least square linear regression model together with the last three lags of the true historical wind realization. We use the first 6 months of our

Model	DK1		DK2	
	Onshore	Offshore	Onshore	Offshore
original	6.19	9.55	6.77	10.68
persistent	3.36	6.39	3.90	7.49
improved	2.72	5.70	3.34	6.66

Table 3.7: Average RMSE (MWh) of the original forecast, the persistent (naive 1h lag) and improved 1h-ahead forecast computed on the out-of-sample period 07/01/2015 to 06/04/2021 with a normalized generation capacity of 100 MW.

dataset to independently train each of the four predictive models, one per column of Table 3.6.

Table 3.7 compares the root mean square error (RMSE) of the original and improved out-of-sample forecast against the naive benchmark provided by the first lag of each series (the wind power production of the previous hour), also known in the literature as persistent estimator. Results show that the improved hour-ahead series significantly outperforms the original and persistent estimator and therefore are suitable to be used in this case study. As a byproduct of this table, it is interesting to note that the wind forecasts issued by the Danish TSO have coherent RMSE being offshore harder to predict than onshore and DK2 harder than DK1 due to a reduced installed capacity and coverage area.

Once we have processed the wind power production series, we explain next how we use them in our case study. The stochastic generation of the wind power producer is simulated using the normalized onshore wind data series of the Danish DK1 bidding zone, which is consistent with the bidding zone of the imbalance penalties. The four hour-ahead forecasts of the wind power production of DK1 and DK2 are used as contextual information, resembling model FM3 described in Section 3.1.2.1. Although other wind forecasts could have been used as features, we restrict ourselves to these ones to avoid methodological inconsistencies between them that could cast doubt on the results obtained, as discussed in the previous application in this chapter.

Given that our goal is to reduce the imbalance cost incurred by a wind power producer, we also consider several price-related features to be used as contextual information. To this end, we include the first lag of the imbalance penalties ψ_{t-1}^+ and ψ_{t-1}^- in the vector of contextual information. As commented in Section 3.2.1, it is well known that the ratio between the penalties provides valuable information about the optimal decision of the newsvendor model and therefore we add the series $r_{t-1} = \psi_{t-1}^+ / (\psi_{t-1}^+ + \psi_{t-1}^- + v)$ where $v = 10^{-5}$ helps better condition the denominator. To complete our feature set, we add a column of ones that enable one of the regressors to become an intercept.

As a summary, let $E_t^{on1}, E_t^{of1}, E_t^{on2}, E_t^{of2}$ denote the hour-ahead wind power forecast of DK1 onshore, DK1 offshore, DK2 onshore and DK2 offshore, respectively. Then, at

the moment of delivering the offer, the producer has available a feature vector $\mathbf{x}_t = [1, E_t^{on1}, E_t^{of1}, E_t^{on2}, E_t^{of2}, \psi_{t-1}^+, \psi_{t-1}^-, r_{t-1}]^\top$ to infer the optimal offer E_t^F .

3.2.6.2 Benchmark methods and implementation details

In this section, we describe several benchmark methods against which we compare the performance of OLVN. The first opponent to beat is the normalized enhanced forecast of DK1 itself. Although a prediction that minimizes the RMSE may seem naive, one can expect that the deviation cost incurred by the producer vanishes as the RMSE approaches zero. Therefore, an hour-ahead forecast is expected to perform relatively well. We also use this hour-ahead forecast as the baseline to compute the metric AOL(%) for other approaches in the way described in Section 3.2.4.

The second method to be compared is the one proposed in the previous application discussed in Section 3.1.1.2 and published in [101]. Recall that this method uses a two-step approach leveraging two variants of model (3.24). In the first step, the first model only considers wind-related features plus the intercept $\mathbf{x}_t = [1, E_t^{on1}, E_t^{of1}, E_t^{on2}, E_t^{of2}]^\top$, and set $\psi_t^+ = \psi_t^- = 1, \forall t$. The result can be interpreted as an enhanced forecast of the wind energy production with a reduced mean absolute error. In a second step, this enhanced forecast is fed into model (3.24), considering this time the true historical penalties ψ_t^+, ψ_t^- but neglecting the capacity constraint (3.24b). The training set is updated following a rolling window, adding new samples and eliminating the same amount of the oldest. We replicate this method, called DR2 (decision rule 2-steps), in this application, considering the four hour-ahead enhanced wind forecasts of DK1 and DK2 as the input of the first problem. In line with the findings discussed in the previous application, we choose a training set of $T = |\mathcal{T}| = 4320$ (6 months) and a rolling window of 24 hours.

In addition, we analyze the direct application of the DR approach (see Section 2.2.2), also discussed in the illustrative example 3.2.5.2, that solves exactly (3.24) and (3.25) using the full contextual information vector. As in the case of DR2, we choose a training set length of 6 months and a rolling window step of 24 hours.

We discuss one last benchmark, not implementable in real applications, inspired by the static regret metric defined in (3.40). We assume perfect information of the whole dataset and leverage problem (3.24) once more to compute the best linear model in hindsight determined by the vector \mathbf{w}^H . Once this single vector is computed, the whole sequence of offers is determined analogously to (3.25). We name this benchmark FX (from fixed).

The OLVN algorithm does not need to solve an optimization model but requires initializing two parameters. To choose μ and η , we perform a grid search on the chunk of data spanning 07/01/2015 to 12/31/2015. After analyzing Table 3.8, we select the values $\mu = 0.7$ and $\eta = 0.001$ that obtain the best AOL(%). We assume a balanced

η	μ										
	0	0.1	0.2	0.3	0.4	0.5	0.6	0.7	0.8	0.9	1
1e-2	-13.8	19.2	33.7	19.2	27.7	8.4	39.7	29.2	32.3	32.3	42.0
1e-3	12.5	27.1	33.7	36.9	39.2	39.9	42.1	42.2	42.0	41.6	41.5
1e-4	-5.2	1.3	4.4	6.0	7.0	7.7	8.2	8.6	8.9	9.4	9.4

Table 3.8: Out-of-sample AOL (%) for different combinations of parameters μ and η_0 over the span 07/01/2015 to 12/31/2015. Highlighted in black are shown the best result and parameters selected.

penalty anchor $\bar{\psi}^+ = \bar{\psi}^- = 1$. Next, we initialize the OLVN regressor associated with the onshore DK1 forecast to 1 and the rest of the values to 0.01. In other words, we start the online offering with a strategy very close to FO, mainly relying on the forecast of the wind energy production. We use the next 6 months (01/01/2016 to 06/30/2016) to update (initialize) \mathbf{w}_t with the aim of having a fair comparison against DR and DR2.

The experiments carried out are conducted on the test set spanning from 07/01/2016 to 06/04/2021 (5 years with 43,200 samples). The optimization models DR, DR2, and FX are implemented with the python package Pyomo and solved through the optimization solver CPLEX⁹, whereas the implementation OLVN is developed by the authors based on standard python packages.

3.2.6.3 Numerical results

Next, we discuss the result obtained in this case study. We start examining the regret suffered by OLVN over the aforementioned dataset which has a length of $D = 43,200$ hours (60 months). Let $\tilde{T}_j = \cup_{i=1}^j \tilde{T}_i$ and recall $\mathbf{u}_t = \mathbf{w}_i^{\mathcal{H}} \forall t \in \tilde{T}_i$. We assess the average dynamic regret $R_{\tilde{T}}^d / \tilde{T}$ for each sequence $\tilde{T}_j, j = 1, \dots, D/l$ with partitions length $l = 2160, 4320, 8640$ hours (3, 6, 12 months). As an additional case, we compute the evolution of the static regret for a sequence $\tilde{T}_j, j = 1, \dots, 20$ with a step of $l = 2160$ hours (3 months). To this end, in each step we refresh the best single action in hindsight as $\mathbf{w}_j^{\mathcal{H}} = \arg \min_{\mathbf{w} \in W_j^{\mathcal{H}}} \sum_{t \in \tilde{T}_j} NV_t(\mathbf{w})$ and $\mathbf{u}_t = \mathbf{w}_j^{\mathcal{H}} \forall t$.

The four regret series are depicted in Figure 3.11. As expected, the average dynamic regret incurred by OLVN deteriorates quickly as l decreases and the dynamic regret approaches the worst-case regret definition (3.41). Nevertheless, Figure 3.11 clearly shows that OLVN achieves a sublinear static regret, i.e., $\lim_{T \rightarrow \infty} \sup \mathcal{R}_{\tilde{T}}^s / \tilde{T} \leq 0$. This is also the case for the dynamic regret with partitions of length $l \geq 6$ months, proving the ability of OLVN to track dynamic environments.

The economic gains are assessed through the average AOL(%) obtained in the test set, which is collated in Table 3.9. First, note that all methods outperform the naive

⁹IBM ILOG CPLEX Optimization Studio. See <https://www.ibm.com/analytics/cplex-optimizer>.

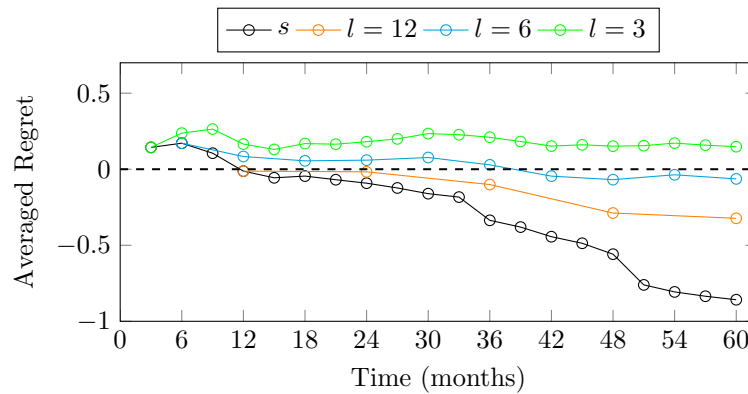


Figure 3.11: Average dynamic regret R_T^d/T for $l = 3, 6, 12$, months and static regret R_T^s/T updated every 3 months (denoted as s) of the OLVN method.

FO strategy of offering the DK1 forecast, obtaining positive values and demonstrating that this set of features contributes to reducing the deviation cost.

The DR2 method is developed in a context where recent lags in the penalties are not available. Indeed, the lack of penalty-related features translates into a modest score, showing the evident benefits of disclosing recent information in electricity markets, i.e., reducing the lead time. Even though FX determines the optimal $\mathbf{w}^{\mathcal{H}}$ in hindsight (i.e., under perfect information), its choice is limited to a single vector for the whole horizon. The fact that several approaches perform better than FX proves the dynamic behavior of the uncertain parameters and the need for updating the decision vector. Therefore, it does not come as a surprise that DR improves the first two approaches as it leverages the full vector of features and periodically updates \mathbf{w}_t^{DR} . However, the superior adaptability of OLVN allows it to obtain the best score, achieving an additional 7.6% compared to DR and a total 38.6% deviation cost reduction compared to FO. The latter figure translates into an extra 25,930.22 €/year on average for a wind power producer with a capacity of 100 MW.

	DR2	FX	DR	OLNV
AOL(%)	3.8	24.6	31.0	38.6
Time (s)	23366	53	16077	179

Table 3.9: Out-of-sample AOL (%) and execution time (s) over the span 07/01/2016 to 06/04/2021.

Finally, the last row of Table 3.9 summarizes the computational time corresponding to the four approaches. The FX method requires little time as it only solves a single optimization problem for the whole horizon. This contrasts with the significant amount of time required by the constant re-optimization of DR and DR2. It is noteworthy that even though OLVN produces 24 times more updates of the vector \mathbf{w}_t , the time invested is several orders of magnitude lower. In conclusion, OLVN is up to the challenge of

the electricity markets transformation achieving outstanding results with satisfactory computational performance.

3.3 Summary

This chapter addresses the problem of a wind power producer offering in two different wholesale market settings. Both markets penalizes the power imbalances asymmetrically.

The first application considers a day-ahead market where the available wind power production forecasts have limited accuracy, encouraging a two-step procedure which first improves the available forecasts and then produce an enhanced offer. Thus, the application of DR to this setting renders an interpretable and effective method that enhance both the tasks of renewable energy forecasting and trading using contextual information and historical market data. The effectiveness of this approach has been tested on a realistic case study where we aim, on the one hand, to improve the forecast issued by the Danish TSO for the onshore wind power production in the DK1 bidding zone of the pan-European electricity market, and, on the other, to formulate a competitive market bid for such a production. The numerical results highlight the benefits achieved by our approach, which amounts to a 8.53% of reduction in MAE and a 2.13% of improvement of AOL with respect to the benchmarks for the simulation period considered. These figures point out the intrinsic value of exploiting additional information such as spatially correlated forecasts. In this line, we have observed that the use (as features) of both on- and offshore wind power forecasts in areas geographically close to the zone to which the target wind power production belongs are valuable. This seems to be especially true if those areas pertain to the same country or domain of the same TSO.

The second application also addresses the wind power producer problem in a different market setting. In particular, this application considers a wind power producer offering in an hourly wholesale electricity market with minimum lead time. The continuous feedback in this setting allows us to implement the contextual online gradient descent algorithm in this problem, being the first time, to the best of our knowledge, that online gradient methods are applied in this setting. Several numerical examples are carried out to investigate the performance of this algorithm. In the first illustrative example, we compare the behavior of two alternative implementations, namely, a subgradient approach and a smooth approximation of the original newsvendor function, determining the superior economic performance of the former. The second example shows the faster adaptability of the online algorithm in dynamic environments, outperforming methods that use a training set of past information, such as DR. Furthermore, we analyze a case study based on data of the Danish TSO. The result shows a substantial reduction in the AOL and reduced computational cost with respect to several benchmark methods,

including an implementation of DR. The regret of this algorithm is also investigated under several alternative definitions, demonstrating sublinear performance empirically.

Chapter 4

Contextual optimization via prescriptive estimation

This chapter presents two applications in which we estimate the uncertain parameters taking into account the economic impact of the forecasting errors on the underlying optimization problem. To this end, we model prescriptive estimators as a function of the available contextual information in both applications.

The first application deals with the problem of a strategic power producer who manages a thermal unit (dispatchable power plant with marginal production cost greater than zero) and offers the generation in a forward electricity market with uncertain market conditions. In this context, we produce prescriptive estimators of the uncertain parameters that model the forward electricity market by means of the bilevel approach (BL) introduced in Section 2.2.4. Given the particular conditions fulfilled by the mathematical structure of this problem, the bilevel program—resulting from the application of BL to this problem—can be reformulated using the KKT optimality conditions as two variants (BL-R and BL-M) that can be efficiently solved using commercially available solvers.

In the second application in this chapter, we analyze the problem of a market operator in charge of clearing a two-stage electricity market consisting of a forward and a real-time settlement. The former pre-dispatches the power system following a least-cost merit order and facing an uncertain net demand, while the latter tackles the plausible deviations with respect to the forward schedule using power regulation during the actual operation of the system. Standard industry practice deals with the uncertain net demand in the forward stage by replacing it with a good estimate of its conditional expectation (usually referred to as a *point forecast*) so as to minimize the need for power regulation in the real-time market. However, it is well known that the cost structure of a power system is highly asymmetric and dependent on its operating point, with the result that minimizing the power imbalances is not necessarily aligned with minimizing operating costs. In this application, we propose a mixed-integer program which leverages the problem structure to construct, from the available contextual information and historical data, a *prescription* of the net demand, which does take into account the power system's cost asymmetry.

4.1 Contextual strategic bidding

Here we apply the bilevel decision-making framework introduced in Section 2.2.4 to the problem of a strategic producer partaking in a forward market [4]. This application appears in the published manuscript [102]. In this application, we consider a strategic firm aiming to determine the optimal offer in a market for a homogeneous product. This problem has a long tradition in the Economics and Management Science literature (see, for instance, [134, 142, 24]). More specifically, we use *electricity* for the product and thus, place ourselves in the context of electricity markets, where this problem has received a great deal of attention since the deregularization of the power sector [42, 117].

This problem is approached in the literature in countless ways depending on how the market and the competitors are modeled, making it practically impossible to address them all. For a general review of the topic, we refer the reader to the survey by [87]. The application in this chapter is closer to those approaches that first forecast the uncertain electricity market conditions, to then compute the decision that maximizes the producer's profit (as in the FO approach described in Section 2.2). In this vein, in [1] the authors review different strategies for forecasting the market-clearing price which can be used to determine the optimal offer in a price taker scenario, i.e., disregarding the influence of the producer's offer in the market-clearing price. Conversely, the reference [5] investigates how to predict an inverse residual demand function which can be used to determine the profit-maximizing bid of the strategic producer, accounting for her capacity to influence the market-clearing price.

In this application, we also consider a strategic producer interested in satisfying the residual demand of the forward electricity market, modeled through an inverse demand function. However, we use the contextual bilevel framework (BL), presented in Section 2.2.4, together with available contextual information, in order to produce prescriptive estimators of those uncertain parameters of the residual demand, taking into account the economic impact of an error in their estimation. The resulting bilevel program is reformulated into two alternative models. The first one is a regularized non-linear optimization program that is iteratively solved to find local optimal solutions quickly. The second model is a mixed-integer quadratic program with binary variables that can be solved to optimality with commercially available optimization solvers. The performance of these models is tested on a realistic case study that uses real data from the Iberian electricity market, showing their relevance to increasing market participation and the profitability of the portfolio.

4.1.1 Problem description

The decision task of a strategic player is to decide the produced quantity $q \in \mathbb{R}$ that maximizes her profits while facing some uncertainty pertaining to the conditions of the market where the product is sold. Let $c(q) : \mathbb{R} \rightarrow \mathbb{R}^+$ denote the generation cost function whose parameters are assumed to be known with certainty. Let $p(q; \mathbf{Y}) : \mathbb{R} \times \mathbb{R}^m \rightarrow \mathbb{R}$ represent the inverse demand function expressing the impact of the generation quantity q on the good's price. For some goods such as electricity, the inverse demand function varies depending on the season of the year, the day of the week, or the hour of the day. Besides, this function is also uncertain when producers must make their generation decisions q , since it may depend, for example, on weather conditions. If Q represents the known feasible region of variable q according to technical or economic constraints and $\mathbf{x} \in \mathbb{R}^p$ is a vector of contextual information available before deciding q , the strategic

producer must solve the following conditional stochastic optimization problem:

$$\min_{q \in Q} \mathbb{E}[c(q) - p(q; \mathbf{Y})q | \mathbf{X} = \mathbf{x}]. \quad (4.1)$$

As it is customary, we assume that the price and the demand are linearly related as $p(q; \alpha, \beta) = \alpha - \beta q$ where $\alpha \in \mathbb{R}$ and $\beta \in \mathbb{R}^+$ are unknown parameters that replace the generic uncertainty vector \mathbf{Y} in (4.1). Similarly, we assume that the production cost is computed through a quadratic cost function $c(q) = c_2 q^2 + c_1 q$ where $c_1, c_2 > 0$ are known parameters related, respectively, to proportional production costs (such as fuel cost) and the increase of marginal costs due to technological factors (such as efficiency loss) [48]. In order to ease the notation, we define $\alpha' = \alpha - c_1$ and $\beta' = \beta + c_2$. Finally, we consider that the production quantity q is bounded by known capacity limits, i.e., $\underline{q} \leq q \leq \bar{q}$ with $\underline{q}, \bar{q} \in \mathbb{R}^+$. Thus, problem (4.1) can be reformulated as

$$\min_{\underline{q} \leq q \leq \bar{q}} \mathbb{E}[\beta' q^2 - \alpha' q | \mathbf{X} = \mathbf{x}]. \quad (4.2)$$

Since the quantity decision q is independent of the outcome of the uncertainty (β', α') , the above can be further simplified to:

$$\min_{\underline{q} \leq q \leq \bar{q}} \mathbb{E}[\beta' | \mathbf{X} = \mathbf{x}] q^2 - \mathbb{E}[\alpha' | \mathbf{X} = \mathbf{x}] q. \quad (4.3)$$

Therefore, the optimal solution q^* is driven by the conditional expected values of α' and β' . To be more precise, since $\beta' > 0$, q^* could be equivalently computed as follows:

$$q^*(\mathbf{x}) \in \arg \min_{\underline{q} \leq q \leq \bar{q}} q^2 - \frac{\mathbb{E}[\alpha' | \mathbf{x}]}{\mathbb{E}[\beta' | \mathbf{x}]} q \implies q^*(\mathbf{x}) \in \left\{ \underline{q}, \frac{\mathbb{E}[\alpha' | \mathbf{x}]}{2\mathbb{E}[\beta' | \mathbf{x}]}, \bar{q} \right\}. \quad (4.4)$$

Unfortunately, $\mathbb{E}[\alpha' | \mathbf{x}]$ and $\mathbb{E}[\beta' | \mathbf{x}]$ are both unknown and therefore, they need to be estimated somehow. As explained further in Section 4.1.3.1, the producer has available a set of historical observations $S = \{(\alpha'_i, \beta'_i, \mathbf{x}_i), \forall i \in \mathcal{N}\}$ with $\alpha'_i \in \mathbb{R}$, $\beta'_i \in \mathbb{R}^+$ and $\mathbf{x}_i \in \mathbb{R}^p$ in order to accomplish such a task. At this point, it should be underlined that the strategic producer problem (4.1) *has no recourse* [125] and the uncertain parameters appear only in its objective function. If the reader is interested, the application of BL to conditional stochastic programs that include recourse variables is described in Appendix A together with two theoretical examples that address classical decision-making problems. Consequently, solving (4.1) is apparently as “simple” as estimating the two conditional expectations $\mathbb{E}[\alpha' | \mathbf{x}]$ and $\mathbb{E}[\beta' | \mathbf{x}]$. Our claim, however, is that the way the producer draws decisions from a *finite data sample* (all we usually have in practice) may have a significant impact on the actual expected performance of the producer’s strategy. Actually, the best estimates of $\mathbb{E}[\alpha' | \mathbf{x}]$ and $\mathbb{E}[\beta' | \mathbf{x}]$ from a *statistical*

sense do not necessarily result in the best offer q .

In Section 2.2, we introduced several strategies to approach this type of contextual decision-making problems under uncertainty, namely, the *predict-then-optimize* strategies FO, SP, and BL; method ML, which relies on a proxy of the true conditional distribution that is built using machine-learning techniques, and the decision-rule approach DR. Unfortunately, in the technical literature, methods SP and ML have only been applied to conditional stochastic optimization problems with a specific structure and they both lack a solution strategy for more general conditional stochastic programs. For this reason, in this application, we limit ourselves to comparing approaches FO, BL, and DR. Next, we particularize those methods to the strategic producer problem. According to the *predict-then-optimize* strategies, the surrogate model of this problem renders

$$\min_{\underline{q} \leq q \leq \bar{q}} \hat{\beta}' q^2 - \hat{\alpha}' q. \quad (4.5)$$

As explained in Section 2.2, the FO approach aims at learning the uncertain parameters α'_i, β'_i as a function of the available information \mathbf{x}_i . If we assume the family of linear functions, that is, $\hat{\alpha}'_i = \mathbf{w}_\alpha^\top \mathbf{x}_i$, $\hat{\beta}'_i = \mathbf{w}_\beta^\top \mathbf{x}_i$ with $\mathbf{w}_\alpha, \mathbf{w}_\beta \in \mathbb{R}^p$, and we choose the squared error as the loss function l^{FO} , then the standard implementation of (2.12) is

$$\mathbf{w}_\alpha^{\text{FO}} \in \arg \min_{\mathbf{w}_\alpha \in \mathbb{R}^p} \sum_{i \in \mathcal{N}} (\alpha'_i - \mathbf{w}_\alpha^\top \mathbf{x}_i)^2, \quad (4.6a)$$

$$\mathbf{w}_\beta^{\text{FO}} \in \arg \min_{\mathbf{w}_\beta \in \mathbb{R}^p} \sum_{i \in \mathcal{N}} (\beta'_i - \mathbf{w}_\beta^\top \mathbf{x}_i)^2. \quad (4.6b)$$

The optimal quantity under context $\mathbf{X} = \mathbf{x}$ is the solution to the following optimization problem:

$$q^{\text{FO}}(\mathbf{x}) \in \arg \min_{\underline{q} \leq q \leq \bar{q}} (\mathbf{w}_\beta^{\text{FO}})^\top \mathbf{x} q^2 - (\mathbf{w}_\alpha^{\text{FO}})^\top \mathbf{x} q \implies q^{\text{FO}}(\mathbf{x}) \in \left\{ \underline{q}, \frac{(\mathbf{w}_\alpha^{\text{FO}})^\top \mathbf{x}}{2(\mathbf{w}_\beta^{\text{FO}})^\top \mathbf{x}}, \bar{q} \right\}. \quad (4.7)$$

Alternatively, \mathbf{w}_α and \mathbf{w}_β can be determined following the BL approach by solving the following bilevel formulation:

$$\mathbf{w}_\alpha^{\text{BL}}, \mathbf{w}_\beta^{\text{BL}} \in \arg \min_{\mathbf{w}_\alpha, \mathbf{w}_\beta \in \mathbb{R}^p} \sum_{i \in \mathcal{N}} \beta'_i \hat{q}_i^2 - \alpha'_i \hat{q}_i \quad (4.8a)$$

$$\text{s.t. } \hat{q}_i \in \arg \min_{\underline{q} \leq q_i \leq \bar{q}} \mathbf{w}_\beta^\top \mathbf{x}_i q_i^2 - \mathbf{w}_\alpha^\top \mathbf{x}_i q_i, \quad \forall i \in \mathcal{N}. \quad (4.8b)$$

For this particular application, the bilevel optimization problem rendered by the proposed approach has a significant drawback, because the global optimal solution of (4.8) is $\mathbf{w}_\alpha = \mathbf{w}_\beta = \mathbf{0}$. Consequently, the lower-level problem (4.8b) can be replaced by the

feasibility condition $\underline{q} \leq \hat{q}_i \leq \bar{q}$, and the optimal values of \hat{q}_i are determined as if uncertain parameters α' and β' were known in advance, which violates non-anticipativity. While this solution does lead to the minimum value of objective function (4.8a), it is useless to determine the optimal decisions for any context $\mathbf{X} = \mathbf{x}$. This degenerate solution of the proposed approach occurs because all coefficients of the objective function (4.5) are uncertain. Interestingly, this shortcoming does not affect the newsvendor and product placement problems described in Appendix A, because the uncertainty only affects the feasible region in those applications.

In this application, we propose to ensure non-anticipativity by formulating a bilevel optimization problem that considers the modified surrogate model

$$\min_{\underline{q} \leq q \leq \bar{q}} q^2 - \gamma q, \quad (4.9)$$

where $\gamma = \frac{\alpha'}{\beta'}$. For known values of α' and β' , the optimal solution of (4.5) and (4.9) coincide. However, surrogate model (4.9) is simpler since it only includes one uncertain parameter instead of two. Assuming a linear relationship between the new uncertain parameter γ and the contextual information, the proposed methodology yields the following bilevel problem:

$$\mathbf{w}_\gamma^{\text{BL}} \in \arg \min_{\mathbf{w}_\gamma \in \mathbb{R}^p} \sum_{i \in \mathcal{N}} \beta'_i \hat{q}_i^2 - \alpha'_i \hat{q}_i \quad (4.10a)$$

$$\text{s.t. } \hat{q}_i \in \arg \min_{\underline{q} \leq q_i \leq \bar{q}} q_i^2 - \mathbf{w}_\gamma^\top \mathbf{x}_i q_i, \quad \forall i \in \mathcal{N}. \quad (4.10b)$$

Formulation (4.10) has the following advantages with respect to problem (4.8): i) it includes fewer parameters and therefore, it is less prone to overfitting, ii) it ensures non-anticipativity for any parameter vector \mathbf{w}_γ , and iii) under certain conditions, it is able to retrieve the true model that relates random variable γ and the context \mathbf{X} and the optimal solution to (4.2) as the sample size $|\mathcal{N}|$ grows to infinity, as shown in Proposition 1 in Appendix A. By replacing the lower-level problem with its KKT conditions, we obtain the following single-level problem:

$$\mathbf{w}_\gamma^{\text{BL}} \in \arg \min_{\mathbf{w}_\gamma \in \mathbb{R}^p} \sum_{i \in \mathcal{N}} \beta'_i \hat{q}_i^2 - \alpha'_i \hat{q}_i \quad (4.11a)$$

$$\text{s.t. } 2\hat{q}_i - \mathbf{w}_\gamma^\top \mathbf{x}_i - \underline{\lambda}_i + \bar{\lambda}_i = 0, \quad \forall i \in \mathcal{N} \quad (4.11b)$$

$$0 \leq (\hat{q}_i - \underline{q}) \perp \underline{\lambda}_i \geq 0, \quad \forall i \in \mathcal{N} \quad (4.11c)$$

$$0 \leq (\bar{q} - \hat{q}_i) \perp \bar{\lambda}_i \geq 0, \quad \forall i \in \mathcal{N}, \quad (4.11d)$$

where $\underline{\lambda}_i, \bar{\lambda}_i$ are the dual variables corresponding to the capacity limit constraints. Following the procedure described in Section 2.2.4, we can subsequently reformulate

program (4.11), replacing all complementarity constraints (4.11c) and (4.11d) by a single parametrized constraint. The resulting single-level non-linear programming (NLP) model is the following:

$$\mathbf{w}_\gamma^{\text{BL-R}} \in \arg \min_{\mathbf{w}, \hat{q}_i, \underline{\lambda}_i, \bar{\lambda}_i} \sum_{i \in \mathcal{N}} \beta'_i \hat{q}_i^2 - \alpha'_i \hat{q}_i \quad (4.12a)$$

$$\text{s.t. } 2\hat{q}_i - \mathbf{w}_\gamma^\top \mathbf{x}_i - \underline{\lambda}_i + \bar{\lambda}_i = 0, \quad \forall i \in \mathcal{N} \quad (4.12b)$$

$$\underline{q} \leq \hat{q}_i \leq \bar{q}, \quad \forall i \in \mathcal{N} \quad (4.12c)$$

$$\underline{\lambda}_i, \bar{\lambda}_i \geq 0, \quad \forall i \in \mathcal{N} \quad (4.12d)$$

$$\sum_{i \in \mathcal{N}} \underline{\lambda}_i (\hat{q}_i - \underline{q}) + \bar{\lambda}_i (\bar{q} - \hat{q}_i) \leq \epsilon, \quad (4.12e)$$

where $\epsilon \in \mathbb{R}^+$ is a small scalar. This model, which we called BL-R (bilevel regularized), can be directly solved with NLP solvers such as CONOPT¹. As explained in Section 2.2.4, the procedure to obtain a *local* optimal solution of (4.11) involves iteratively solving (4.12) for $\epsilon \rightarrow 0$ [122].

Alternatively, instead of regularizing the complementarity conditions, we can use the big-M approach as in [59], and thus, the reformulation of model (4.11) yields

$$\mathbf{w}_\gamma^{\text{BL-M}} \in \arg \min_{\mathbf{w}_\gamma, \hat{q}_i, \underline{u}_i, \bar{u}_i, \underline{\lambda}_i, \bar{\lambda}_i} \sum_{i \in \mathcal{N}} \beta'_i \hat{q}_i^2 - \alpha'_i \hat{q}_i \quad (4.13a)$$

$$\text{s.t. } (4.12b) - (4.12d) \quad (4.13b)$$

$$\underline{\lambda}_i \leq \underline{u}_i M^D, \quad \forall i \in \mathcal{N} \quad (4.13c)$$

$$\bar{\lambda}_i \leq \bar{u}_i M^D, \quad \forall i \in \mathcal{N} \quad (4.13d)$$

$$\hat{q}_i - \underline{q} \leq (1 - \underline{u}_i) M^P, \quad \forall i \in \mathcal{N} \quad (4.13e)$$

$$\bar{q} - \hat{q}_i \leq (1 - \bar{u}_i) M^P, \quad \forall i \in \mathcal{N} \quad (4.13f)$$

$$\underline{u}_i, \bar{u}_i \in \{0, 1\}, \quad \forall i \in \mathcal{N}. \quad (4.13g)$$

The resulting single-level BL-M (bilevel big-M) model (4.13) is a Mixed-Integer Quadratic Problem (MIQP) analogous to (2.29), that can be solved to global optimality using off-the-shelf optimization solvers such as CPLEX² or Gurobi³.

Finally, after obtaining a vector $\mathbf{w}_\gamma^{\text{BL}}$ either from (4.12) or (4.13), optimal decisions under context $\mathbf{X} = \mathbf{x}$ are made by solving:

$$q^{\text{BL}}(\mathbf{x}) \in \arg \min_{\underline{q} \leq q \leq \bar{q}} q^2 - (\mathbf{w}_\gamma^{\text{BL}})^\top \mathbf{x} q \implies q^{\text{BL}}(\mathbf{x}) \in \left\{ \underline{q}, \frac{(\mathbf{w}_\gamma^{\text{BL}})^\top \mathbf{x}}{2}, \bar{q} \right\}. \quad (4.14)$$

¹CONOPT. See <http://www.conopt.com/>.

²IBM ILOG CPLEX. See <https://www.ibm.com/analytics/cplex-optimizer>.

³Gurobi. See <https://www.gurobi.com/analytics/cplex-optimizer>.

The last approach we compare is the DR introduced in Section 2.2.2 and first proposed in [7]. This approach directly learns the optimal production as a function of the contextual information available. Assuming the linear mapping $\hat{q}_i = \mathbf{w}_q^\top \mathbf{x}_i$ with $\mathbf{w}_q \in \mathbb{R}^p$, problem (2.20) for this particular application is formulated as:

$$\mathbf{w}_q^{\text{DR}} \in \arg \min_{\mathbf{w}_q \in \mathbb{R}^p} \sum_{i \in \mathcal{N}} \beta'_i (\mathbf{w}_q^\top \mathbf{x}_i)^2 - \alpha'_i \mathbf{w}_q^\top \mathbf{x}_i \quad (4.15a)$$

$$\text{s.t. } \underline{q} \leq \mathbf{w}_q^\top \mathbf{x}_i \leq \bar{q}, \quad \forall i \in \mathcal{N}. \quad (4.15b)$$

Formulation (4.15) is a convex quadratic optimization problem and can also be solved using commercial software such as CPLEX or Gurobi. In line with (2.21), the optimal quantity under context $\mathbf{X} = \mathbf{x}$ is directly computed as:

$$q^{\text{DR}}(\mathbf{x}) = (\mathbf{w}_q^{\text{DR}})^\top \mathbf{x}. \quad (4.16)$$

Although not true in general, approaches (4.11) and (4.15) may lead to the same solution under specific conditions. For instance, if the produced quantity q is not limited by minimum/maximum bounds, then constraint (4.11b) boils down to $\hat{q}_i = \mathbf{w}_\gamma^\top \mathbf{x}_i/2$. Consequently, the solutions of (4.11) and (4.15) satisfy that $\mathbf{w}_q^{\text{DR}} = \mathbf{w}_\gamma^{\text{BL}}/2$ and therefore, $q^{\text{BL}}(\mathbf{x}) = q^{\text{DR}}(\mathbf{x})$ for any context $\mathbf{X} = \mathbf{x}$. As we show in the following sections, the decisions q^{BL} delivered by our approach are significantly more profitable than q^{DR} in the *constrained* case.

Next, we assess and compare the performance of the bilevel approach for the strategic producer problem using numerical simulations. In Section 4.1.2 we illustrate the advantages of BL with respect to FO and DR using a small example with a reduced data sample. Additionally, Section 4.1.3 presents the numerical results of a realistic case study that uses real data from the Iberian Electricity Market⁴ and the Spanish Transmission System Operator (TSO) uploaded to the ENTSO-e Transparency Platform⁵ (ETP).

4.1.2 Illustrative example

This section aims at gaining insight into the performance of the bilevel approach with a small example of the strategic producer problem. For the sake of simplicity, we only consider four realizations of the uncertain parameters α'_i, β'_i and a single feature $x_i \in [0, 10]$, whose values are shown in Table 4.1. Approach FO predicts the uncertain parameters using linear functions in the form $\hat{\alpha}_i = w_{\alpha,0}^{\text{FO}} + w_{\alpha,1}^{\text{FO}} x_i$ and $\hat{\beta}_i = w_{\beta,0}^{\text{FO}} + w_{\beta,1}^{\text{FO}} x_i$; approach BL assumes that $\hat{\gamma}_i = w_{\gamma,0}^{\text{BL}} + w_{\gamma,1}^{\text{BL}} x_i$; and approach DR considers $\hat{q}_i = w_{q0}^{\text{DR}} + w_{q1}^{\text{DR}} x_i$. These three approaches are compared with a benchmark method (BN) that assumes perfect knowledge of the uncertain parameters α', β' and, consequently,

⁴OMIE. See <https://www.omie.es/en/>.

⁵ENTSO-e Transparency Platform. See <https://transparency.entsoe.eu/>.

i	x_i	α'_i	β'_i	γ_i
1	2	2	10	0.20
2	4	17	10	1.70
3	8	8	3	2.67
4	9	16	6	2.67

Table 4.1: Data sample S for the illustrative example.

	q_1	q_2	q_3	q_4	I(€)	RI(%)
BN	0.10	0.85	1.33	1.33	23.33	100.0
FO	0.33	0.51	1.23	1.59	21.21	91.0
DR	0.27	0.61	1.29	1.46	22.36	95.9
BL	0.27	0.61	1.29	1.46	22.36	95.9

Table 4.2: Optimal offer and income for the unconstrained illustrative example (in-sample results). Parameter vectors w are: $w_{\alpha,0}^{\text{FO}} = 5.000$, $w_{\alpha,1}^{\text{FO}} = 1.000$, $w_{\beta,0}^{\text{FO}} = 12.298$, $w_{\beta,1}^{\text{FO}} = -0.878$, $w_{\gamma,0}^{\text{BL}} = -0.138$, $w_{\gamma,1}^{\text{BL}} = 0.341$, $w_{q_0}^{\text{DR}} = -0.069$, $w_{q_1}^{\text{DR}} = 0.170$.

yields the best possible offer for each time period. Obviously, this method cannot be implemented in practice and, accordingly, is just used here for comparison purposes. Given the reduced size of this example, the reformulations BL-R and BL-M provide the same results and are thus jointly referred to as BL.

First, we deal with the *unconstrained case*, that is, the case in which the capacity constraints are disregarded. Table 4.2 shows the in-sample results obtained from methods BN, FO, DR, and BL, namely, the optimal production quantity for each time period q_i , the absolute income (I), and the relative income with respect to the benchmark (RI). Notice that the income for each time period can be computed as $-\beta'_i q_i^2 + \alpha'_i q_i$. As discussed in Section 4.1.1, in connection with the unconstrained case, coefficients w^{DR} are equal to $w^{\text{BL}}/2$ and the decisions and incomes obtained by DR and BL are the same as a result. It is also interesting that the income of these two methods is 5% higher than that of FO. To explain this, we refer to Figure 4.1a, which depicts the optimal production quantities given by the different methods as a function of the context $x \in [0, 10]$, namely,

$$q^{\text{FO}}(x) = \frac{w_{\alpha,0}^{\text{FO}} + w_{\alpha,1}^{\text{FO}}x}{2(w_{\beta,0}^{\text{FO}} + w_{\beta,1}^{\text{FO}}x)} \quad q^{\text{BL}}(x) = \frac{w_{\gamma,0}^{\text{BL}} + w_{\gamma,1}^{\text{BL}}x}{2} \quad q^{\text{DR}}(x) = w_{q_0}^{\text{DR}} + w_{q_1}^{\text{DR}}x. \quad (4.17)$$

This figure shows that methods BL and DR can return decisions much closer to the benchmark ones than method FO for the four data points in the sample. Therefore, even for unconstrained optimization problems, the proposed methodology may outperform the classical “first-predict-then-optimize” approach, which is purely based on reducing the error of forecasting the uncertain parameters, simply because minimizing this error is not necessarily aligned with maximizing the decision value.

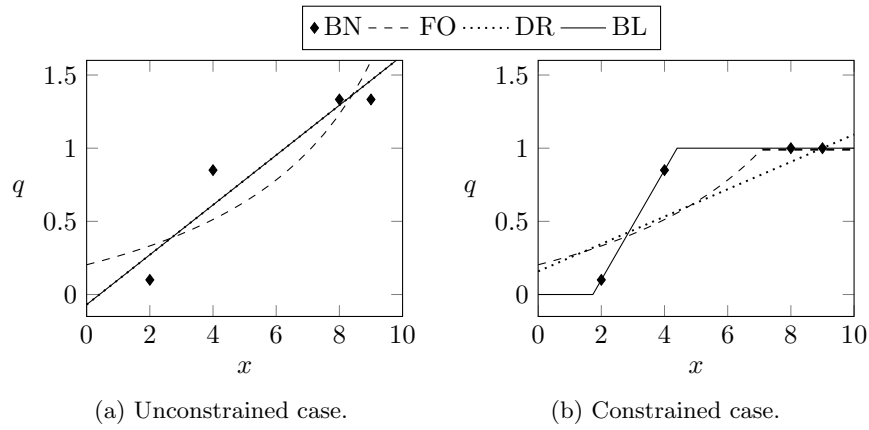


Figure 4.1: Decision quantity q versus feature x for the illustrative example.

Now we consider the *constrained case*, that is, we bring the capacity constraints back into this small example. In particular, the minimum and maximum outputs of the strategic producer are set to 0 and 1, respectively. Similarly to Table 4.2, the in-sample results obtained in the capacity-constrained case are collated in Table 4.3, where we can see that the optimal quantity q_i reaches its maximum value for some time periods and methods FO, DR and BL all provide different results. Methods FO and DR achieve an income 7.5% and 8.2% lower than the benchmark. This poor in-sample performance is better understood by means of Figure 4.1b, which similarly to Figure 4.1a, represents the optimal quantities as a function of the context for the constrained case according to (4.7), (4.14) and (4.16). First, since method FO is unaware of the feasibility region of the original conditional stochastic problem, it provides the same prediction of the uncertain parameters α, β in the unconstrained and constrained cases. However, using these forecasts in the surrogate model (4.5) enforces $q = 1$ for $x \geq 7.1$ in the constrained case. As observed, reducing the forecast error of α, β does not lead to the maximization of the decision value in the constrained case either. Second, method DR must ensure feasible solutions for all samples, a condition that also leads to quite poor approximations of the optimal quantities for most values of the context x . Furthermore, this approach would return infeasible solutions $q > 1$ for $x > 9$ as shown in Figure 4.1b. On the contrary, the proposed BL approach can find a linear relation between γ and x to be used in the surrogate model (4.9) that results in decisions q that perfectly match those provided by the benchmark for the four data points and therefore, this method achieves the highest possible income in sample.

In summary, this small example sheds light on the reasons why the BL methodology outperforms existing ones, specially, in constrained optimization problems under uncertainty: Our approach provides “forecasts”—more precisely, estimators—of the uncertain parameters based on contextual information that take into account the objective function and feasible region of the decision maker. Such prescriptive forecasts translate

	q_1	q_2	q_3	q_4	I(€)	RI(%)
BN	0.10	0.85	1.00	1.00	22.33	100.0
FO	0.33	0.51	1.00	1.00	20.65	92.5
DR	0.35	0.53	0.91	1.00	20.50	91.8
BL	0.10	0.85	1.00	1.00	22.33	100.0

Table 4.3: Optimal offer and income for the constrained illustrative example (in-sample results). Parameter vectors w are: $w_{\alpha,0}^{\text{FO}} = 5.000$, $w_{\alpha,1}^{\text{FO}} = 1.000$, $w_{\beta,0}^{\text{FO}} = 12.298$, $w_{\beta,1}^{\text{FO}} = -0.878$, $w_{\gamma,0}^{\text{BL}} = -1.300$, $w_{\gamma,1}^{\text{BL}} = 0.750$, $w_{q_0}^{\text{DR}} = 0.158$, $w_{q_1}^{\text{DR}} = 0.094$.

into decisions that are much closer to those obtained in the ideal perfect information instance.

4.1.3 Case study

In this section, we compare the proposed approach with existing ones using realistic data from the Iberian electricity market, as described in detail in Section 4.1.3.1. Sections 4.1.3.2, 4.1.3.3 and 4.1.3.4 investigate how the type of generation portfolio, the quadratic cost term c_2 , and the residual demand elasticity impact the performance of the proposed methodology, respectively. For the sake of conciseness, these three subsections only include the global optimal solutions given by BL-M. Finally, Section 4.1.3.5 provides computational solution times for all the approaches and discusses the differences between the BL-R and BL-M reformulations in that respect.

4.1.3.1 Experimental setup

In order to test our proposal, we consider a realistic case study based on actual data from the Iberian electricity market. We construct a data set of the form $\{(\mathbf{x}_i, \alpha_i, \beta_i), \forall i \in \mathcal{N}\}$ from which we derive the rest of the parameters required for our simulations as explained in Section 4.1.1. We gather raw market data from the forward market OMIE⁶ to compute parameters α_i, β_i of the inverse demand function. Furthermore, we collect wind and solar power forecasts of the aggregated production of Spain to be used as a vector of contextual information \mathbf{x}_i . The wind and solar forecasts, originally published by the Spanish TSO, are downloaded from the ETP⁷.

Historical raw hourly block-wise bids and offers submitted by buyers and sellers to the Iberian day-ahead energy market are processed to obtain parameters α_i, β_i as follows. For each hour of the year, we have access to the set of bids and offers defined as $\{(q_b, p_b), \forall b \in B\}$, $\{(q_o, p_o), \forall o \in O\}$, respectively, where $q_{b/o}$ is the amount of energy to buy/sell at price $p_{b/o}$. Thus, the residual demand r to be potentially covered by a new producer entering the market for each possible price p is defined as $r = \sum_{b \in B: p_b \geq p} q_b - \sum_{o \in O: p_o \leq p} q_o$, that is, the aggregated demand minus the aggregated

⁶OMIE. See <https://www.omie.es/en/>.

⁷ENTSO-e Transparency Platform. See <https://transparency.entsoe.eu/>.

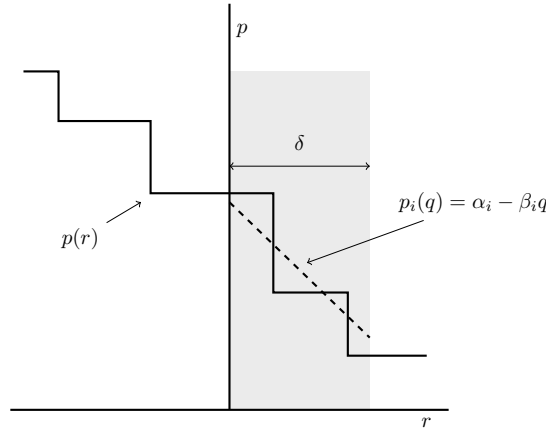


Figure 4.2: Inverse residual demand curve $p(r)$ (solid) and fitted inverse demand function $p_i(q)$ (dashed) in the interval $[0, \delta]$. The intercept and slope of the fitted line are α_i and $-\beta_i$, respectively.

production. The step-wise function relating the residual demand r and the electricity price p is plotted in Figure 4.2 for illustrative purposes.

Now consider that a new strategic producer enters the market with an offer to sell quantity q at offer price 0. If we assume that the remaining bids and offers stay unaltered, the market price would decrease following the right-hand part of the step-wise function depicted in Figure 4.2. Therefore, a strategic producer aiming at maximizing her profit is interested in modeling the dependence between her offered quantity q and the market price p in the shaded area, with parameter δ being a constant sufficiently larger than the producer's maximum generation capacity. In connection with Section 4.1.1, we approximate said dependency using a linear function such that $p_i(q) = \alpha_i - \beta_i q$ as illustrated in Figure 4.2 and therefore, the values of α_i, β_i for each hour are obtained by determining the linear function that best approximates the blocks shaded in gray.

We collect data from November 2018 to October 2019 in order to build a data set of 8600 hours (almost one year), which is divided into 43 bins of 200 consecutive samples. Each bin is randomly split into training and test sets with a ratio of 80%/20%, respectively. This process is repeated five times for each bin. Therefore, each approach is solved for 215 different training sets of 160 samples, and the obtained solutions are evaluated using the corresponding 215 test sets of 40 samples each. The out-of-sample results provided in Sections 4.1.3.2, 4.1.3.3, 4.1.3.4, and 4.1.3.5 are obtained by averaging the outcomes over these 215 test sets. We select a value of δ equal to 5 GW in order to encompass enough bids and offers to obtain accurate approximations of $p_i(q)$ throughout the whole data set. We determine the optimal parameters \mathbf{w} through problems (4.6), (4.11), and (4.15), which we denote FO, BL and DR, respectively.

Each bin is executed in parallel with the following resources: 1 CPUs Intel E5-2670

	c_1 (€/MWh)	c_2 (€/MWh ²)	\bar{q} (MW)	$\mathcal{N}_{q^{\text{BN}}=0}$ (%)	$\mathcal{N}_{0 < q^{\text{BN}} < \bar{q}}$ (%)	$\mathcal{N}_{q^{\text{BN}}=\bar{q}}$ (%)
Base	10	0.005	1000	8	16	76
Medium	35	0.005	500	32	29	39
Peak	50	0.005	250	79	12	9

Table 4.4: Generation technology data.

@ 2.6 GHz and 1 Gb of RAM. Each instance of model BL-M is solved using the MIQP solver CPLEX⁸ for a maximum time of 20 minutes or a relative gap of 10^{-8} . On the other hand, BL-R is executed using the NLP solver CONOPT without time limit. In order to speed up the solution of the BL-M method, we warm-start BL-M with the solution of BL-R, similarly to the process described in [109].

4.1.3.2 Impact of the generation portfolio

As previously stated, the main advantage of BL is that it produces estimates for the uncertain parameters that are tailored to the optimization problem by which the strategic power producer determines her optimal market sale. However, such an advantage may translate into higher or lower incomes depending on the firm's generation portfolio. In this section, therefore, we evaluate the performance of the various approaches for three generic power plants characterized by different linear costs (c_1) and capacities (\bar{q}).

Table 4.4 provides the values of c_1 , c_2 and \bar{q} for these three generic units. For simplicity, the minimum output \underline{q} of all units is assumed equal to 0 and the value of c_2 is set to 0.005 €/MWh² [48]. The base unit can represent a nuclear power station and is characterized by low fuel cost and high capacity. The medium unit can be, for example, a carbon-based power station with a lower capacity and higher fuel costs. Finally, peak units, such as combined cycle power plants, typically have the highest fuel cost and a smaller generation capacity. Table 4.4 also includes the percentage of time periods in which $q^{\text{BN}} = 0$, $0 < q^{\text{BN}} < \bar{q}$ and $q^{\text{BN}} = \bar{q}$ denoted as $\mathcal{N}_{q^{\text{BN}}=0}$, $\mathcal{N}_{0 < q^{\text{BN}} < \bar{q}}$, and $\mathcal{N}_{q^{\text{BN}}=\bar{q}}$, respectively, where q^{BN} represents the optimal quantity that the strategic firm would place into the market under the *true* inverse demand function (that is, the solution given by the benchmark approach). It is observed that the base unit generates at maximum capacity for most times periods and is only shut down in 8% of the cases. The medium generating unit is idle 32% of the time (if prices are too low) and is at maximum capacity during the 39% of the time periods. Finally, the peak unit is not dispatched most of the time since electricity prices are usually below its marginal production cost.

Table 4.5 provides the out-of-sample results computed by averaging over the 215 test sets of 40 samples each described in Section 4.1.3.1. These results include the absolute income for the benchmark approach (I^{BN}) for the considered time horizon, the relative

⁸IBM ILOG CPLEX. See <https://www.ibm.com/analytics/cplex-optimizer>.

	I^{BN} (M€)	RI^{FO} (%)	RI^{DR} (%)	RI^{BL-M} (%)	$INFES^{DR}$ (%)
Base	176.7	96.1	94.6	96.3	4.9
Medium	20.9	77.4	62.5	80.0	1.7
Peak	1.2	44.1	18.9	58.7	0.1

Table 4.5: Impact of generation technology.

income (RI) for methods FO, DR and BL-M, and the percentage of time periods for which method DR provides infeasible solutions ($INFES^{DR}$). A first obvious observation is that, as expected, the absolute income is higher for base units and lower for peak units. A second, probably more interesting remark relates to the impact of the uncertainty about the inverse demand function on the market revenues accrued by each generating technology. Since the base unit is at full capacity most of the time, the uncertainty pertaining to the residual demand does not affect revenues that much, and the three methods obtain relative incomes above 94%. On the contrary, the participation of the medium and peak units highly depends on market conditions and therefore, this very same uncertainty remarkably deteriorates market revenues, with the eventual result that the maximum relative incomes amount to 80% and 59%, respectively, for the method featuring the best performance (which is BL-M).

On a different front, the DR approach produces infeasible offers in a considerable number of time periods, whereas FO and BL-M are guaranteed to provide feasible production quantities in all cases. The percentage of periods for which method DR results in an infeasible q is higher for the base unit because the medium and peak units are idle more frequently. For this particular application, making DR decisions feasible can be easily achieved by computing $\min(\max(\hat{q}_i, \underline{q}), \bar{q})$. However, this post-processing step to guarantee feasibility can be much more challenging in applications with general convex feasible sets. It is also apparent that the DR approach provides the lowest RI for the three cases considered and therefore, this method is not even recommended for decision-making models where the decision vector is simply bounded component-wise.

Finally, we notice that, for the three generation technologies, the proposed method BL-M always provides higher incomes than the FO approach. However, relative income improvements vary widely for each case. For the base unit, the relative income of BL-M is only 0.2% higher than that of FO. This is understandable since this power plant is at full capacity most of the time and thus, the impact of the uncertainty is comparatively minor, as we mentioned before. For the peak unit, in contrast, the relative income of BL-M is 14.6% higher than that of FO. Note that, unlike for base units, making small errors in the forecasts of the market conditions can be catastrophic for peak units, because such deviations may mean the difference between producing nothing or producing at maximum capacity. The ability of BL-M to reduce the forecast error when consequences

	BN	FO	DR	BL-M
$\mathcal{N}_{I>0}(\%)$	20.6	9.0	6.6	10.1
$\mathcal{N}_{I<0}(\%)$	0.0	3.7	3.0	3.4
$\mathcal{N}_{I=0}(\%)$	79.4	87.3	90.4	86.4
$I^+(\text{M€})$	1.23	0.73	0.37	0.87
$I^-(\text{M€})$	0.00	-0.19	-0.14	-0.15

Table 4.6: Income distribution for the peak generating unit.

c_2 (€/MWh ²)	$\mathcal{N}_{q^{\text{BN}}=0}$ (%)	$\mathcal{N}_{0<q^{\text{BN}}<\bar{q}}$ (%)	$\mathcal{N}_{q^{\text{BN}}=\bar{q}}$ (%)
0.01	32	43	25
0.005	32	29	39
0.001	32	15	53

Table 4.7: Operating regime of a medium generating unit ($c_1 = 35\text{€/MWh}$, $\bar{q} = 500\text{MW}$).

are worse, together with the lower absolute incomes of peak units, explains this high difference in percentage. The gain of BL-M with respect to FO for the medium unit has an intermediate value of 2.6%.

To conclude this section, Table 4.6 includes, for the peak generating unit, the percentage of periods with a positive income, with a negative income and with an income equal to zero, denoted as $\mathcal{N}_{I>0}$, $\mathcal{N}_{I<0}$ and $\mathcal{N}_{I=0}$, in that order. The total sum of positive and negative incomes is also provided in the last two rows, represented by the symbols I^+ and I^- , respectively. Interestingly, BL-M achieves the highest percentage of periods with a positive income and succeeds in providing the highest value of I^+ .

4.1.3.3 Impact of parameter c_2

While parameter c_1 basically depends on the cost of the fuel used by each unit, the interpretation of c_2 is not as straightforward. Indeed, this parameter measures the decrease in the plant marginal cost as production increases and is connected to technological aspects of the plant's economy of scale, like the way the plant efficiency varies for different operating points. For this reason, in this section, we investigate the impact of c_2 on the performance of the proposed method. Notice that, if $\underline{q} = 0$ MW, then the unit marginal costs range from c_1 to $c_1 + c_2\bar{q}$. In a similar way, as Table 4.4 does, Table 4.7 shows the operating regime of a medium generating unit with $c_1 = 35\text{€/MWh}$, $\bar{q} = 500$ MW and different values of c_2 . As expected, a decrease in c_2 entails a reduction in the marginal production cost of the plant and, as a result, the amount of electricity the strategic firm places into the market increases.

Table 4.8 provides the same results as Table 4.5, but for different values of c_2 and the medium generating unit only. Naturally, reducing the plant marginal costs increases

c_2 (€/MWh ²)	I^{BN} (M€)	RI^{FO} (%)	RI^{DR} (%)	RI^{BL-M} (%)	$INFES^{DR}$ (%)
0.01	16.3	73.9	60.0	76.4	1.1
0.005	20.9	77.4	62.5	80.0	1.7
0.001	25.5	81.2	65.6	83.0	1.0

Table 4.8: Impact of parameter c_2 on a medium generating unit.

	I^{BN} (M€)	RI^{FO} (%)	RI^{DR} (%)	RI^{BL-M} (%)	$INFES^{DR}$ (%)
Normal	20.9	77.4	62.5	80.0	1.7
Low-elast	18.6	74.7	60.0	77.1	1.7

Table 4.9: Impact of residual demand elasticity .

both the absolute income for the benchmark approach and also the relative income achieved by all methods. Nevertheless, BL-M proves to be between 1.8% and 2.6% more profitable to the producer than the traditional FO approach for the values of c_2 considered.

4.1.3.4 Impact of the residual demand elasticity

So far we have centered our study on the cost structure of the generation portfolio owned by the strategic firm. Here, on the contrary, we focus on the elasticity of the market residual demand. Roughly speaking, this elasticity is inversely proportional to parameter β of the inverse demand function. Bearing this in mind, we compare the next two market situations, namely, the “Normal” and the “Low-elast” instances. The former corresponds to the values of β in the original data set, while the latter is obtained by multiplying these β -values by two.

Table 4.9 shows the incomes provided by each of the considered methods relative to those of the benchmark. The numbers correspond to the medium power plant of Table 4.4. The overall effect of increasing the residual demand elasticity (lower β -values) is analogous to that of decreasing parameter c_2 , i.e., the involvement of the strategic producer in the market augments, thus leading to higher revenues. Results in Table 4.9 show that the proposed BL approach outperforms FO and DR for different values of the residual demand elasticity, improving the competitive edge of the strategic producer in more than 2% with respect to FO in terms of relative income.

4.1.3.5 Computational results

In Sections 4.1.3.2, 4.1.3.3 and 4.1.3.4 we have only included results from BL-M, and not from BL-R, because the former variant of the bilevel framework we propose guarantees global optimality for the strategic producer problem for appropriate val-

	RI ^{BL-M}	RI ^{BL-R}
	(%)	(%)
Base	96.3	96.3
Medium	80.0	79.2
Peak	58.7	58.4

Table 4.10: Comparison of BL-M and BL-R.

ues of large constants M^P, M^D (Section 2.2.4). However, solving model BL-M can be computationally very expensive. Alternatively, local optimal solutions of the proposed bilevel model (4.10) can be efficiently found through BL-R by way of model (4.12).

Next, we compare the solutions given by methods BL-M and BL-R. In order to solve model BL-R, we iteratively shrink the regularization parameter ϵ taking values from the discrete set $\{10^6, 10^4, 10^2, 1, 10^{-1}, 10^{-2}, 0\}$. In each iteration, we initialize the model with the solution provided by the previous problem. It is also worth mentioning that method BL-M is warm-started with the solution delivered by BL-R.

Results in Table 4.10 are intended to compare the relative incomes of BL-M and BL-R for each generating unit whose data is collated in Table 4.4. Although method BL-R logically yields lower incomes, the differences with respect to BL-M are below 0.8%. This means that if model (4.8) does not satisfy the conditions to be reformulated as a MIQP or the computational resources are limited, then a good solution (i.e., a solution with a small loss of optimality) can be efficiently computed by solving the regularized NLP version of our approach.

	FO	DR	BL-R	BL-M
	(s)	(s)	(s)	(s)
Base	0.24	0.65	3.90	197.77
Medium	0.35	1.06	6.80	149.89
Peak	0.26	0.78	4.62	22.68

Table 4.11: Average computing time.

Finally, we compare the computational burden of methods FO, DR, BL-M, and BL-R. The average simulation time invested in solving problems (4.6), (4.11) and (4.15) for the three generation technologies are indicated in Table 4.11, where the maximum solution time has been limited to 20 minutes for all methods. These results highlight the higher computational burden required by BL-M to ensure global optimality. On the other hand, the computing times of BL-R are very affordable, especially considering the competitive edge that this method gives to the strategic firm.

4.2 Contextual economic dispatch

The application presented in this section analyzes a two-stage electricity market consisting of a forward and a real-time settlement. In such a setting, we propose a mixed-integer programming model to train an affine function that prescribes the value of the net demand, understood as (uncertain) demand minus (uncertain) stochastic generation of the system, to be cleared in a forward electricity market. The objective of this procedure is to replace the classical net demand estimator, obtained by minimizing the mean square error, to increase the efficiency of the market while maintaining standard industry practices. In the following paragraphs, we motivate the interest in this problem and review the relevant literature on it.

Since the liberalization of the sector in the 1990s, electricity markets worldwide include a forward market and a real-time market [66]. Traditionally, these two markets have been cleared sequentially as follows: the forward market is cleared sometime prior to the actual delivery of energy using demand forecasts, while the real-time market is cleared very close to the actual operation of the system to process the energy imbalances caused by forecast errors. Due to the integration of uncertain supply in electricity networks, in the late 2000s, some authors proposed energy-only stochastic market clearing procedures to determine the forward production schedule, taking into account the uncertainty pertaining to the energy supply from renewable sources [112, 96]. While these approaches maximize market efficiency, they also have significant drawbacks, preventing them from being adopted in actual electricity markets. For instance, energy-only stochastic markets violate the merit-order principle and, as a consequence, flexible thermal generating units must be willing to accept losses for some realizations of the uncertain parameters. In addition, stochastic market procedures lack transparency, as their outcome depends on the plausible scenario realizations considered. For these reasons, the scientific community is currently revisiting the sequential clearing of the forward and real-time markets because it is simpler and more transparent, and it guarantees revenue adequacy for all market players under any realization of the uncertainty.

It has also been shown that by prescriptively estimating the input parameters of current operational and market-clearing procedures, these can mimic the performance of their stochastic-programming-based counterparts to a large extent. For instance, in [98], the authors propose a bilevel programming model to compute the amount of (uncertain) renewable power generation that must be considered in a forward electricity market to maximize the short-run market efficiency. In the same vein, the authors in [54] show that, by properly setting the (uncertain) reserve requirements in a European-style two-stage electricity market, such a market can be almost as cost-efficient as the ideal two-stage electricity market given by a full stochastic programming approach. All told, these two references clearly show that the power sector can strongly benefit from

the aforementioned prescriptive estimation strategy. In fact, the authors of [50] apply precisely this strategy to power generation and grid-scale electricity battery operation. In [35], the authors instead focus on renewable energy producers, for which they propose different smart-predict strategies for energy trading. Lastly, the authors in [63] use a bilevel programming framework similar to that proposed in Section 4.1 whereby they train several autoregressive models to estimate the uncertain demand and the size of the energy reserves in a joint reserve allocation and energy dispatch problem. The last three references are also recent examples of the use of contextual information in electricity markets. Indeed, we have thoroughly discussed the benefits of prescriptively estimating the uncertain parameters considering the subsequent optimization problem in the context of a thermal power producer competing strategically in an electricity market in Section 4.1.

4.2.1 Problem description

As introduced in the section above, we consider a two-stage electricity market consisting of a forward and a real-time settlement that are *sequentially* organized. The forward market is cleared some time prior to the actual delivery of energy, for instance, from 12 hour to 36 hours in advance. The real-time market processes the energy imbalances with respect to the forward production schedule. Without loss of generality, to keep our model simple and computationally manageable, we make the following assumptions on our two-stage market setup:

- The inter-temporal constraints of power production portfolios, such as ramping limits and minimum up- and down-times, are not explicitly accounted for by the market-clearing algorithm.
- Network constraints are only taken care of in the real-time market using a pipeline representation of the transmission network.

With these two simplifying assumptions, our setup is closer to the European market, in line with the case study we present in Section 4.2.5. Nevertheless, any of the two assumptions above could be dropped at the expense of increasing the complexity of the resulting mathematical optimization model.

Very importantly, in today's electricity markets and, in particular, the European one, the forward (day-ahead) market is cleared with no or little account taken of its impact on the subsequent real-time operation of the power system. Our methodology is specifically tailored to this market setup, in the sense that it can be seamlessly integrated into this *modus operandi*. This is completely in contrast with those other approaches that make use of stochastic programming to *simultaneously* clear the forward and the real-time market stages, see, e.g., [2, 112, 146].

Therefore, in our framework, the forward market first determines the power dispatch that minimizes the anticipated electricity production costs as follows:

$$\min_{p_g, g \in G} \sum_{g \in G} C_g p_g \quad (4.18a)$$

$$\text{s.t.} \quad \sum_{g \in G} p_g = \hat{L} \quad (4.18b)$$

$$0 \leq p_g \leq \bar{P}_g, \quad \forall g \in G, \quad (4.18c)$$

where $p_g, \bar{P}_g, C_g \in \mathbb{R}^+$ and $G \subseteq \mathbb{N}$ is the set of generation blocks (can also represent generation units with a single block). Each block $g \in G$ has associated a production level p_g and a marginal cost C_g . Equation (4.18b) enforces the market equilibrium (i.e., production must equal consumption), with parameter $\hat{L} \in \mathbb{R}^+$ representing a point or single-value estimate of the total net demand $L \in \mathbb{R}^+$ in the system, which is unknown at the moment the forward market is cleared and thus, is to be treated as a random variable. We clarify that by total net demand, we refer, in this application, to the difference between the sum of the uncertain system demand minus the sum of the uncertain stochastic production generated in the system, assumed to be always greater or equal to zero. Finally, constraint (4.18c) sets the size of each production block.

The linear program (4.18) stands for an economic dispatch problem whereby production blocks are filled up following a *cost-merit order*, meaning that blocks g with a lower cost C_g are dispatched first. To ease the discussion that follows, hereinafter we consider that the blocks in the set G are ordered such that $g < g'$ if and only if $C_g < C_{g'}$. Imposing this assumption guarantees that problem (4.18) has a unique solution for any feasible value of the parameter \hat{L} and, moreover, this solution can be obtained through a closed-form expression once determined the marginal block. Let $g^m \in G$ be the index of the marginal block so that $\sum_{g=1}^{g^m-1} \bar{P}_g \leq \hat{L} \leq \sum_{g=1}^{g^m} \bar{P}_g$. Then, the optimal solution $\{p_g^*\}_{g \in G}$ to problem (4.18) is given by the following expression:

$$\{p_g^*\}_{g \in G} = \begin{cases} \bar{P}_g & \text{if } g < g^m, \\ \hat{L} - \sum_{j=1}^{g^m-1} \bar{P}_j & \text{if } g = g^m, \\ 0 & \text{if } g > g^m. \end{cases} \quad (4.19)$$

Since the system net demand is uncertain, the power dispatch that results from (4.19) is to be adjusted during the real-time operation of the power system to satisfy the *actual* net demand. This adjustment is conducted through the real-time market. Therefore, the aim of the real-time market is to correct the imbalance of the system in a cost-efficient manner. To this end, we consider a pipeline model where $G(b)$ and $D(b)$ represent the set of power blocks and loads that are connected to node b , in that order. With some

abuse of notation, let $(L_{di} \in \mathbb{R})_{d \in D(b)}$ be a certain realization $i \in \mathcal{N}$ of the net load $d \in D(b)$ connected to node b of the system. We also define $o(l)$ and $e(l)$ as the origin and ending nodes of line l , respectively. Thus, $\{l : o(l) = b\}$ and $\{l : e(l) = b\}$ represent the subset of lines that start or end at node b , in that order. Once introduced this notation, the real-time market under consideration renders

$$\min_{\Xi} \sum_{g=1}^G (C_g^u r_g^u - C_g^d r_g^d) \quad (4.20a)$$

$$\text{s.t. } 0 \leq p_g^* + r_g^u - r_g^d \leq \bar{P}_g, \quad \forall g \in G \quad (4.20b)$$

$$0 \leq r_g^u \leq R_g^u, \quad \forall g \in G \quad (4.20c)$$

$$0 \leq r_g^d \leq R_g^d, \quad \forall g \in G \quad (4.20d)$$

$$\sum_{g \in G(b)} (p_g^* + r_g^u - r_g^d) = \sum_{d \in D(b)} L_{di} + \sum_{l: o(l)=b} f_l - \sum_{l: e(l)=b} f_l, \quad \forall b \in B \quad (4.20e)$$

$$|f_l| \leq \bar{F}_l, \quad \forall l \in \Lambda, \quad (4.20f)$$

where $\Xi = \{r_g^u, r_g^d \in \mathbb{R}^+, g \in G, f_l \in \mathbb{R}, l \in \Lambda\}$ is the set of decision variables and $p_g^*, R_g^u, R_g^d, C_g^u, C_g^d, \bar{P}_g, \bar{F}_l \in \mathbb{R}^+$ and $L_{di} \in \mathbb{R}$ are known parameters.

The power output of each flexible block g may be increased by an amount r_g^u , based on the marginal cost for upward regulation C_g^u , or decreased by an amount r_g^d of downward regulation, which entails a marginal benefit (linked to fuel-cost savings) of C_g^d . These actions are driven by the nodal power balance equation (4.20e) and the minimization of the total regulation costs (4.20a). Naturally, the amount of regulation provided from each production block g , either upward or downward, plus the forward optimal schedule p_g^* of the block must be such that the eventual power output is positive and lower than the block size \bar{P}_g , as stated in (4.20b). Moreover, constraints (4.20c) and (4.20d) limit the amount of up- and down-regulation that can be deployed from each production block to R_g^u and R_g^d , which are indicative of how flexible the underlying generation asset actually is. Finally, line capacity limits are imposed by (4.20f), with f_l being the power flow through line l and \bar{F}_l the capacity of the line.

In [98] it is shown that the value \hat{L} of the system net demand that is used in (4.18) to clear the forward market (and thus determine the forward dispatch $\{p_g^*\}_{g \in G}$) may have a major impact on the subsequent regulation costs (4.20a) through constraint (4.20b), which conditions the ability of the generation fleet to deploy down- and upward regulation. Current practice, however, is content with a simple and direct solution, which is to take \hat{L} as a *point prediction* of L , that is, as an estimate of the expectation of L conditional on all the information at the forecaster's disposal. This information is usually referred to as *contextual information*. Yet, this expectation is oblivious to the minimization of the regulation costs that drives the clearing of the real-time market (4.20) and therefore, may turn out to be highly suboptimal.

Let L^F denote such a point prediction, obtained, for example, through the FO method introduced in Section 2.2. Instead of employing L^F as \hat{L} in (4.18), we propose a regression procedure that provides an *alternative value* for \hat{L} , also based on the context, that explicitly accounts for the potential impact of \hat{L} on the subsequent regulation costs. This alternative value is what is called a *prescription* and the procedure to obtain it is described in detail in the following section.

4.2.2 The contextual dispatch model

Suppose we have a sample of N data points expressed in the form $\{(L_i, \mathbf{x}_i)\}_{i \in \mathcal{N}} = \{(L_1, \mathbf{x}_1), \dots, (L_i, \mathbf{x}_i), \dots, (L_N, \mathbf{x}_N)\}$, where $\mathbf{x} \in \mathcal{X} \subseteq \mathbb{R}^p$ is a vector of *contextual information* and $L \in \mathbb{R}^+$ is the random net system demand.

Our objective is to utilize said sample to infer a functional relation $\hat{L} = g^P(\mathbf{x}; \mathbf{w})$ (P from prescriptive), with $g^P : \mathcal{X} \times \mathbb{R}^q \rightarrow \mathbb{R}^+$ such that, given the context \mathbf{x} , the provided prescription \hat{L} is trained to deliver the minimum total system costs in expectation when inserted into the power balance equation (4.18b).

In this application, we restrict g^P to the family of affine linear functions, i.e., $g^P(\mathbf{x}; \mathbf{w}) = \mathbf{w}^\top \mathbf{x}$, with $\mathbf{w} \in \mathbb{R}^p$ and with one of the features fixed to one. Although it may seem a restrictive selection, this model can learn non-linear relationships through the Taylor's approximation adding polynomial transformations of the features [7]. Furthermore, this model performs very satisfactorily in the numerical experiments in Section 4.2.5 while being easily interpretable.

In order to determine \mathbf{w} , we propose to combine problem (4.18) and (4.20) within a bilevel structure in the same spirit as [98], yielding

$$\min_{\mathbf{w}, \Upsilon} \frac{1}{N} \sum_{i \in \mathcal{N}} \sum_{g \in G} (C_g p_{gi} + C_g^u r_{gi}^u - C_g^d r_{gi}^d) \quad (4.21a)$$

$$\text{s.t. } 0 \leq p_{gi} + r_{gi}^u - r_{gi}^d \leq \bar{P}_{gi}, \quad \forall i \in \mathcal{N}, \quad \forall g \in G \quad (4.21b)$$

$$0 \leq r_{gi}^u \leq R_g^u, \quad \forall i \in \mathcal{N}, \quad \forall g \in G \quad (4.21c)$$

$$0 \leq r_{gi}^d \leq R_g^d, \quad \forall i \in \mathcal{N}, \quad \forall g \in G \quad (4.21d)$$

$$\sum_{g \in G(b)} (p_{gi} + r_{gi}^u - r_{gi}^d) = \sum_{d \in D(b)} L_{di} + \sum_{l: o(l)=b} f_{li} - \sum_{l: e(l)=b} f_{li}, \quad \forall i \in \mathcal{N}, \quad \forall b \in B \quad (4.21e)$$

$$|f_{li}| \leq \bar{F}_l, \quad \forall i \in \mathcal{N}, \quad \forall l \in \Lambda \quad (4.21f)$$

$$p_{gi} \in \{\arg \min_{p_g, g \in G} \sum_{g \in G} C_g p_g\} \quad (4.21g)$$

$$\text{s.t. } \sum_{g \in G} p_g = \hat{L}_i \quad (4.21h)$$

$$\hat{L}_i = \mathbf{w}^\top \mathbf{x}_i \quad (4.21i)$$

$$0 \leq p_g \leq \bar{P}_g, \quad \forall g \in G, \quad \forall i \in \mathcal{N}, \quad (4.21j)$$

where $\Upsilon = \{p_{gi}, r_{gi}^u, r_{gi}^d, f_{li}\}$. The bilevel estimation problem (4.21) first obtains an optimal power dispatch $\{p_{gi}\}_{g \in G}$ through the lower level (4.21g)–(4.21j) that is then evaluated in the upper level (4.21a)–(4.21f) using historical values of the demand L_{di} , replicating the sequential clearing of the forward and real-time markets (4.18) and (4.20), in that order. Note that the target coefficient vector $\mathbf{w} = [w_1, \dots, w_p]^\top$ is decided by the upper level problem and thus is treated as a constant in the lower level. Even though \mathbf{w} is a single coefficient vector, it can produce different estimators \hat{L}_i of the total net demand through (4.21i) and the contextual information vector \mathbf{x}_i , which results in a different lower level problem for each sample (L_i, \mathbf{x}_i) , $i \in \mathcal{N}$, with different optimal power dispatches $\{p_{gi}\}_{g \in G}$. This is why all the decision variables related to the power dispatch and the provision of regulating power, i.e., $p_{gi}, r_{gi}^u, r_{gi}^d$, appear augmented with the sample index i in (4.21). It is worth noting that the presence of multiple lower levels in the bilevel problem (4.21) contrasts with the single lower level considered in [98], given that the authors disregard contextual information and therefore, their approach only determines a single optimal dispatch.

As in the case of the bilevel approach discussed in the previous application, problem (4.21) can be solved by replacing the lower-level problem (4.21g)–(4.21j) with its KKT optimality conditions and subsequently reformulating the resulting model through a regularized complementarity condition [114] or big-M approach [59]. However, in this application, we can avoid such procedures since the optimal solution to the lower-level problem can be easily modeled by a set of constraints that can be directly embedded in commercial solvers. To this end, we define a new set of binary variables $u_{gi} \in \{0, 1\}$ that force block g in scenario i to be at full capacity \bar{P}_g when $u_{gi} = 1$. Then, we can leverage the merit order of the blocks imposing that each generation block can only be activated (i.e., $p_{gi} > 0$) if the preceding one is already at max capacity, mathematically $u_{gi} \leq u_{(g-1)i}, \forall g \in G : g > 1$. With these ingredients, we can formulate an equivalent version of problem (4.21) as follows:

$$\min_{\mathbf{w}, \Upsilon'} \frac{1}{N} \sum_{i \in \mathcal{N}} \sum_{g \in G} (C_g p_{gi} + C_g^u r_{gi}^u - C_g^d r_{gi}^d) \quad (4.22a)$$

$$\text{s.t. (4.21b) – (4.21f)} \quad (4.22b)$$

$$\sum_{g \in G} p_{gi} = \hat{L}_i, \quad \forall i \in \mathcal{N} \quad (4.22c)$$

$$\hat{L}_i = \mathbf{w}^\top \mathbf{x}_i, \quad \forall i \in \mathcal{N} \quad (4.22d)$$

$$u_{gi} \bar{P}_g \leq p_{gi} \leq u_{(g-1)i} \bar{P}_g, \quad \forall i \in \mathcal{N}, \quad \forall g \in G : g > 1 \quad (4.22e)$$

$$u_{gi} \bar{P}_g \leq p_{gi} \leq \bar{P}_g, \quad \forall i \in \mathcal{N}, \quad g = 1 \quad (4.22f)$$

$$u_{gi} \leq u_{(g-1)i}, \quad \forall i \in \mathcal{N}, \quad \forall g \in G : g > 1 \quad (4.22g)$$

$$u_{gi} \in \{0, 1\}, \quad \forall i \in \mathcal{N}, \quad \forall g \in G, \quad (4.22h)$$

where $\Upsilon' = \{p_{gi}, r_{gi}^u, r_{gi}^d, u_{gi}, f_{li}\}$. In this problem, the same constraints that model the real-time market are preserved unaltered in (4.22b). Conversely, a new set of constraints (4.22c)–(4.22h) replace the lower level (4.21g)–(4.21j). As in previous problems, equation (4.22c) enforces the power balance of the forward market. Equation (4.22d) expresses the prescription \hat{L}_i of the net system demand L under context \mathbf{x}_i as an affine function of the features, whose coefficients are to be computed by solving (4.22). Finally, the set of constraints (4.22e)–(4.22h) guarantee that the power dispatch $\{p_{gi}\}_{g \in G}$ coming from (4.22) for each sample i is optimal in the forward market (4.18). To this end, these constraints enforce an optimal dispatch analogous to (4.19).

Problem (4.22) is a mixed-integer linear program due to the binary character of variables u_{gi} , which are used to impose the cost-merit order. As such, this problem can be solved using commercially available solvers such as CPLEX⁹. Once we obtain the optimal coefficient vector \mathbf{w}^* , we can produce the net demand prescription $\hat{L} = (\mathbf{w}^*)^\top \mathbf{x}$, which is to be fed into (4.18b) under the vector of contextual information \mathbf{x} to readily obtain the day-ahead dispatch decisions.

As previously mentioned, the point prediction L^F , which has been and is typically used as \hat{L} to clear the forward market (4.18), is not consistent with the plausible asymmetry in the cost of dealing with the subsequent prediction errors through the real-time market (4.20). Indeed, it is most often the case that the cost of increasing the electricity production in real time is different from that of diminishing it. In this line, problem (4.22) offers a handy way to construct a new estimate \hat{L} that takes into account the referred cost asymmetry. In the next section, we illustrate the advantages of this approach using a small example. In particular, we show that, despite constraints (4.22e)–(4.22h) turn our training problem (4.22) into a mixed-integer program, enforcing the cost-merit order through these constraints is critical to train an affine model that renders economic benefits within the two-stage sequentially-cleared electricity market described in Section 4.2.1. Furthermore, even though the training problem (4.22) may require some computational effort to be solved, the affine model it delivers is intended to remain effective for a period of time (e.g., weeks or months), and hence, the task of solving the mixed-integer program (4.22) only has to be undertaken once in a while.

We finish this discussion with an important remark. In practice, the training problem (4.22) can be used to upgrade the point prediction L^F to a prescription for \hat{L} , which does account for the asymmetry of the power system's regulation costs. For this, it suffices to include L^F as one of the features that are part of the vector of contextual information \mathbf{x} . This is what we do in the following example and in the case study of Section 4.2.5.

⁹IBM ILOG CPLEX. See <https://www.ibm.com/analytics/cplex-optimizer>.

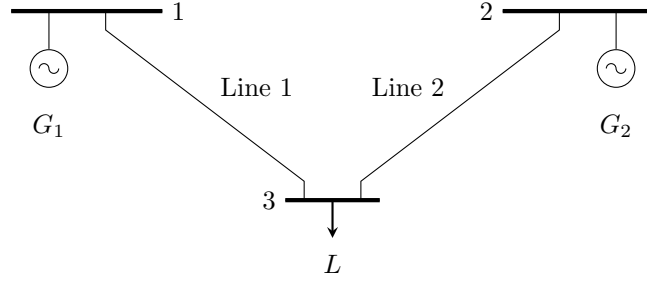


Figure 4.3: Three-bus power system with one random demand and two thermal generators.

4.2.3 Example

Consider the small three-bus system depicted in Figure 4.3, which is composed of one random demand L at node 3, two thermal generators, G_1 and G_2 , at buses 1 and 2, respectively; and two lines, Line 1 and Line 2, connecting nodes 1 and 3, and buses 2 and 3, in that order.

The offer of each unit is characterized by a single generation block with a fixed rate. The technical and economic details of generating units G_1 and G_2 are collated in Table 4.12. Note that, in comparison, unit G_1 is smaller and cheaper than G_2 . In contrast, the latter is significantly more flexible as it features re-dispatch costs, i.e., C_g^u and C_g^d , that are much more competitive. We remark that $C_1^d = -20 \text{ €/MWh}$ implies that this power unit must be paid 20 € for each MWh its production is decreased in the real-time market. Unless stated otherwise, line capacities are assumed infinite.

The only demand in the system, namely, L , is random. Suppose we have a sample $\{(L_i, \mathbf{x}_i)\}_{i=1}^N$, where the feature $\mathbf{x}_i = (1, L_i^F)^\top$ and each data point corresponds to the period of one hour. Again, L_i^F represents a classical point prediction of the demand L built out of whichever available information the forecaster had at her disposal to produce it by way of whatever machine learning or forecasting technique she could have developed to that end. We stress that this setup is very common in reality, where power system operators often count on specialized software to produce good point predictions L_i^F . Our objective is to use our methodology and training model (4.22) described in Section 4.2.2 to recycle this standard point prediction with the aim of fabricating a better value for \hat{L} in Equation (4.18b).

For this small example, we generate samples in the form $\{(L_i, \mathbf{x}_i)\}_{i=1}^N$ as follows. We consider that the per-unit (p.u.) point forecast of the net demand L follows a uniform distribution between a and b . Therefore, $L^F \sim \bar{L} \cdot U(a, b)$, where \bar{L} is a factor representing the maximum power load at bus 3. We further assume that the per-unit net demand itself follows a Beta distribution with mean equal to L^F/\bar{L} and standard deviation σ . Hence, $L \sim \bar{L} \cdot \text{Beta}(\alpha, \beta)$, where the scale and shape parameters are

	C_g (€/MWh)	C_g^u (€/MWh)	C_g^d (€/MWh)	\bar{P}_g (MW)	R_g^u (MW)	R_g^d (MW)
G_1	5	30	-20	60	60	60
G_2	15	20	10	150	150	150

Table 4.12: Illustrative example: Technical and economic specifications of power plants.

related to the mean L^F/\bar{L} and the standard deviation σ as follows:

$$\frac{L^F}{\bar{L}} = \frac{\alpha}{\alpha + \beta}, \quad (4.23a)$$

$$\sigma^2 = \frac{\alpha \cdot \beta}{(\alpha + \beta)^2(\alpha + \beta + 1)}. \quad (4.23b)$$

In this illustrative example we fix $\sigma = 0.075$ p.u. and generate 20 samples $\{(L_i, \mathbf{x}_i)\}_{i=1}^N$ with $N = 750$. Each L_i^F in \mathbf{x}_i is randomly drawn from $\bar{L} \cdot U(a, b)$. Given L_i^F/\bar{L} and σ , and provided that the system of non-linear equations (4.23) has a solution (notice that $\alpha, \beta > 0$), parameters α_i and β_i can be computed as

$$\alpha_i = -\frac{1}{\sigma^2} \left(\left(\frac{L_i^F}{\bar{L}} \right)^2 - \frac{L_i^F}{\bar{L}} + \sigma^2 \right) \frac{L_i^F}{\bar{L}}, \quad (4.24a)$$

$$\beta_i = \frac{1}{\sigma^2} \left(\left(\frac{L_i^F}{\bar{L}} \right)^2 - \frac{L_i^F}{\bar{L}} + \sigma^2 \right) \left(\frac{L_i^F}{\bar{L}} - 1 \right). \quad (4.24b)$$

Each L_i is then randomly taken from $\bar{L} \cdot \text{Beta}(\alpha_i, \beta_i)$. We take the first 500 data points of each sample as the training set and the last 250 as the test set.

We postulate the affine model $\hat{L} = w_0 + w_1 L^F$ and solve problem (4.22) on the training set to determine coefficients w_0 and w_1 . Finally, to evaluate the performance of the affine model, for each data point (L_i, \mathbf{x}_i) in the test set, we simulate the *sequential* clearing of the forward and real-time markets (4.18) and (4.20), with $\hat{L} = w_0 + w_1 L_i^F$ in (4.18b), and L_i in (4.20e). We then compute the sum of the forward and real-time production costs averaged over the 250 data points in the test set. This mean sum is further averaged over the 20 samples we generate. Our approach, which uses a *prescription* of the system net demand for market clearing, is referred to as P-MC (abbreviation of Prescriptive Market Clearing). We compare it with the customary practice of directly using the point *forecast* L_i^F as \hat{L} in (4.18b), which is referred to as F-MC (abbreviation of Forecasting Market Clearing). This procedure is exactly the FO approach described in Section 2.2. Furthermore, note that our approach boils down to the conventional one if $w_0 = 0$ and $w_1 = 1$. Finally, the relative cost difference between these approaches is denoted as Δcost .

In the results we discuss next, we set a base case with $a = 0.03$, $b = 0.97$, $\bar{L} = 100$ MW, and the technical and economic parameters of the three-bus system described above. We take $a = 0.03$ and $b = 0.97$ pu to ensure that (4.23) has a real solution. We then define variants of this case by changing one or some of those parameters.

4.2.3.1 Impact of power regulation costs

Table 4.13 provides the cost savings that our approach achieves with respect to the conventional one under different G_2 's power regulation costs. For completeness, this table also includes the average cost of these two approaches for the test set and the values of the intercept w_0 and the linear coefficient w_1 of the affine model for \hat{L} our approach utilizes. These values represent expectations over the test data points of the 20 samples generated as indicated above. Furthermore, the first row in the table corresponds to the base case.

Interestingly, our approach systematically corrects the point forecast of the net demand L *downwards*, with a linear coefficient w_1 which is, on average, lower than or equal to 1, and a negative intercept w_0 in expectation. This is so because it is economically advantageous for the system to cope with positive net demand errors (i.e., eventual demand increases) by deploying up-regulation from unit G_2 . Indeed, the alternative would be to deal with negative demand errors by down-regulating with unit G_1 , a recourse that is clearly much more expensive.

C_2 (€/MWh)	C_2^u (€/MWh)	C_2^d (€/MWh)	F-MC cost (€)	P-MC cost (€)	Δcost (%)	w_0	w_1
15	20	10	418.59	416.91	0.40	-0.277	0.982
15	15	10	404.40	391.88	3.10	-0.253	0.899
15	20	15	413.65	412.93	0.17	-0.285	1.009

Table 4.13: Cost savings in percentage under different values of G_2 's power regulation costs C_2^u and C_2^d .

C_2 (€/MWh)	C_2^u (€/MWh)	C_2^d (€/MWh)	F-MC cost (€)	L-MC cost (€)	Δcost (%)	w_0	w_1
15	20	10	418.59	444.05	-6.08	4.967	0.964
15	15	10	404.40	418.84	-3.57	5.490	0.883
15	20	15	413.65	680.92	-64.61	36.807	0.722

Table 4.14: Cost savings in percentage under different values of G_2 's power regulation costs C_2^u and C_2^d . Constraints (4.22e)–(4.22h) have been dropped from the training model (4.22).

To further elaborate on this phenomenon, the second row in Table 4.13 provides

results for a variant of the base case in which C_2^u has been decreased from 20 to 15 €/MWh. Now that up-regulating through unit G_2 is even cheaper, the downward correction of our approach to the net demand point forecast is more pronounced and the associated cost savings due to said phenomenon become larger. On the contrary, if it is the provision of downward regulation by G_2 what becomes 5 €/MWh cheaper and, hence, free (see third row of Table 4.13), the net demand point forecast is barely corrected and the costs savings brought by our approach (with regard to F-MC) become smaller as a result. Note that correcting the point forecast *upwards* in this case (in an attempt to profit from the free downward regulation provided by G_2) would be counterproductive in reality, as the system may risk having to resort to the high-cost down-regulation of unit G_1 in those likely scenarios in which the net demand ends up being lower than the capacity of this unit.

At this point, it may be instructive to see what happens when we drop constraints (4.22e)–(4.22h) from the mixed-integer program through which we train the affine model $\hat{L} = w_0 + w_1 L^F$. This is indeed very tempting, because, if these constraints are removed, the training model (4.22) becomes a very pleasant linear program, similar to the stochastic-programming-based market-clearing formulation advocated, for instance, in [112] (with the data points in (4.22) playing the role of the “scenarios” in [112]). However, these constraints ensure the optimality of the lower-level problem (4.21g)–(4.21j) and guarantee that the above affine model is learned by taking into account that the forward market (4.18) is cleared following a cost-merit-order principle. Therefore, if these constraints are dropped from (4.22), the affine model $\hat{L} = w_0 + w_1 L^F$ is not trained for the target task. This is exactly what Table 4.14 shows. This table is analogous to Table 4.13, but for a linear training model made up of constraints (4.22a)–(4.22d) only. We denote this approach as L-MC from “Linear”). The training model L-MC ignores the merit order and hence, takes for granted that the system can benefit from the cheap downward regulation of unit G_2 by allocating a non-zero production to this unit in the forward market regardless of whether unit G_1 has been fully dispatched or not. This is, however, an strategy forbidden by the market, which explains the poor actual performance of L-MC. This phenomenon is especially notorious for the case $C_2^d = 15$ €/MWh, in which the demand is heavily overestimated (the mean of the estimated demand is increased by 45%) and only the free downward regulation from unit G_2 is used.

Therefore, due to the catastrophic impact that removing the merit-order constraints (4.22e)–(4.22h) from the training model (4.22) may have on the actual performance of the obtained affine model, the strategy L-MC is no longer considered in the rest of our analysis.

\bar{F}_1 (MW)	F-MC cost (€)	P-MC cost (€)	Δ cost (%)	w_0	w_1
∞	418.59	416.91	0.40	-0.277	0.982
30	1034.70	724.46	29.98	15.725	0.175

Table 4.15: Impact of grid congestion on cost savings.

4.2.3.2 Impact of grid congestion

Here we introduce a variant of the base case in which the capacity of Line 1 has been set to 30 MW. Recall that the capacity of this line in the base case is unlimited, which we denote by symbol “ ∞ ” in Table 4.15. The results collated in this new table are analogous to those in Table 4.13.

Recall that the estimation problem (4.22), whereby we determine the affine function $\hat{L} = w_0 + w_1 L^F$, explicitly accounts for network constraints. In contrast, the computation of the net-demand point forecast L^F is typically based on statistical criteria alone and, consequently, ignores any possible limiting effect of the grid.

When the capacity of Line 1 is limited to 30 MW, our approach strongly corrects the point prediction L^F downwards, so that \hat{L} is kept in between 16 and 32 MW approximately. Thus, unit G_1 is dispatched well below the expected demand. This is clever because, in doing so, no (expensive) downward regulation from this unit has to be deployed in real time to comply with the limiting capacity of Line 1. In this way, the eventual realized demand at bus 3 can be satisfied, instead, with cheaper up-regulation from unit G_2 through Line 2. The ultimate result is that using \hat{L} , given by our approach, to clear the forward market is way more profitable than using the raw point forecast L^F .

4.2.3.3 Impact of the peak demand

Now we change the peak demand and consider two variants of the base case in which we take $\bar{L} = 50$ MW and $\bar{L} = 150$ MW (in the base case, $\bar{L} = 100$ MW). The results of this new analysis are compiled in Table 4.16.

Again, as in the analysis of the impact of G_2 's power regulation costs in Section 4.2.3.1, our approach systematically corrects the net-demand point forecast downwards to reduce the usage of down-regulation from G_1 in favor of the up-regulation from G_2 . However, the cost savings achieved by our approach get diluted as the peak demand is augmented. The reason for this is twofold. First, the probability of events where the net demand takes on a value below the capacity of unit G_1 diminishes with growing \bar{L} . For instance, when $\bar{L} = 50$ MW, the probability that the net demand is smaller than the capacity of G_1 is equal to one, which explains why our method delivers the highest

\bar{L} (MW)	F-MC cost (€)	P-MC cost (€)	Δcost (%)	w_0	w_1
50	182.92	181.55	0.75	-0.138	0.982
100	418.59	416.91	0.40	-0.277	0.982
150	751.73	750.54	0.16	-0.421	0.997

Table 4.16: Impact of peak demand.

cost savings in this variant (from among the three cases considered in this analysis). In contrast, as \bar{L} grows, that probability diminishes and the cheaper down-regulation from G_2 becomes more available. Second, the regulation costs account for a lower percentage of the total costs as the peak demand \bar{L} increases.

4.2.3.4 Impact of the net demand regime

We conclude this small example by studying how the net demand regime affects the prescriptive power of the affine function $\hat{L} = w_0 + w_1 L^F$ that we determine by way of problem (4.22). To this end, we modify the support of the uniform distribution from which the per-unit net-demand point prediction is randomly drawn. Thus, we distinguish a *low-demand* regime, with $L^F \sim \bar{L} \cdot U(0.03, 0.5)$, and a *high-demand* regime, with $L^F \sim \bar{L} \cdot U(0.5, 0.97)$. We also consider the base case, where $L^F \sim \bar{L} \cdot U(0.03, 0.97)$ and therefore, no demand regime is differentiated. The corresponding results are provided in Table 4.17.

In line with the observations in the previous analysis of the impact of the peak demand, under a low-demand regime, the expensive, but flexible unit G_2 is not dispatched in the forward market. The downward correction to the net-demand point forecast our approach prescribes is then intended to benefit from the up-regulation provided by G_2 , which is clearly more competitive than the down-regulation offered by G_1 . The system features, therefore, a distinct cost asymmetry given by the expensive down-regulation of G_1 versus the cheap up-regulation of G_2 . Our approach sees this asymmetry and corrects the net-demand point forecast downwards accordingly. In addition, since the beta distribution modeling the point forecast error is right-skewed for low levels of demand, said correction leads to substantial cost savings. In contrast, under a high-demand regime, G_2 is very likely to participate in the forward dispatch, whereas there is a lower probability that G_1 be needed to down-regulate, since the distribution of the point forecast error is left-skewed. Consequently, the cost structure of the system looks very different under a high-demand regime, which prompts a quite different affine function and reduces the cost savings obtained from our method.

Most importantly, in the base case, when no net-demand regime is distinguished, most of the benefits our approach can potentially bring for low values of net demand

U(a, b)	F-MC cost (€)	P-MC cost (€)	Δcost (%)	w_0	w_1
U(0.03, 0.97)	418.59	416.91	0.40	-0.277	0.982
U(0.03, 0.50)	239.60	234.54	2.11	-0.102	0.917
U(0.50, 0.97)	587.82	586.42	0.24	-6.646	1.088

Table 4.17: Impact of the net-demand regime.

are lost. This motivates us to cluster net-demand observations into different regimes and use optimization problem (4.22) to compute a possibly different affine model in the form $\hat{L} = w_0 + w_1 L^F$ for each demand regime, similarly to segmented regression in classical statistics. This is formalized in the next section.

4.2.4 Data clustering and partitioning

Take $\mathcal{N} = \{1, \dots, i, \dots, N\}$, that is, the index set of the data sample $\{(L_i, \mathbf{x}_i)\}_{i=1}^N$ with $\mathbf{x}_i \in \mathbb{R}^p$ and $L_i \in \mathbb{R}^+$, $\forall i \in \mathcal{N}$. We partition \mathcal{N} into a collection $\{\mathcal{N}_k\}_{k=1}^K$ of K subsets that are pairwise disjoint and whose union is equal to \mathcal{N} . Consider the one-to-one mapping $\phi : \mathcal{N} \rightarrow \{1, 2, \dots, K\}$, such that $\phi(i) = k$ if data point $(L_i, \mathbf{x}_i) \in \mathcal{N}_k$. Therefore, $\mathcal{N}_k = \{i \in \mathcal{N} : \phi(i) = k\}$.

We compute K affine models of the form $\hat{L} = \mathbf{w}_k^\top \mathbf{x}$, $k \leq K$, by solving the estimation problem (4.22) for each subset sample \mathcal{N}_k . In practice, this means replacing N and \mathcal{N} in (4.22) with $|\mathcal{N}_k|$ and \mathcal{N}_k , respectively.

To construct a meaningful mapping ϕ , we employ the K -means algorithm that is implemented in the Python package *scikit-learn* [108], using the Euclidean distance. We note that, to construct ϕ , this algorithm receives the feature sample $\{\mathbf{x}\}_{i \in \mathcal{N}}$ as input. In addition, the algorithm allows extrapolating the mapping ϕ to new outcomes of the feature vector \mathbf{x} . That is, given a new observation of \mathbf{x} , say \mathbf{x}_{N+1} , $\phi(\mathbf{x}_{N+1}) = k$ means that \mathbf{x}_{N+1} is predicted to belong to partition \mathcal{N}_k , and therefore, $\hat{L} = \mathbf{w}_k^\top \mathbf{x}_{N+1}$ is to be used in the clearing of the forward market (4.18).

On a different issue, the estimation problem (4.22) is a MIP program and, as such, computationally expensive in general. Actually, the size of (4.22) grows linearly with the sample size. To keep the time to solve (4.22) reasonably low, we reduce the cardinality of subsets $\{\mathcal{N}_k\}_{k=1}^K$ by means of the PAM K-medoids algorithm [78] through the Python package implementation *scikit-learn-extra*. This algorithm selects the most representative data points within each subset \mathcal{N}_k , the so-called *medoids*, by minimizing the sum of distances between each point in \mathcal{N}_k and said medoids. We remark that this reduction process results in data points (the medoids) with *unequal* probability masses, so extra care should be taken when formulating objective function (4.22a) for each subset \mathcal{N}_k considering the medoids only. More specifically, the uniform weight $\frac{1}{N}$ appearing in the objective function (4.22a) should be replaced with a medoid-dependent weight

Country	AT	BE	BG	CH	CZ	DE	DK	EE	ES	FI	FR	GB	GR	HR
base	0.4	6.1	6.7	3.4	14.4	46	2.4	2.0	16.3	6.5	68.3	20.6	3.9	1.3
peak	5.9	6.8	1.0	0.6	1.3	27.9	1.7	0.2	29.6	3.6	11.9	31.2	4.9	0.7
Country	HU	IE	IT	LT	LU	LV	NL	NO	PL	PT	RO	SE	SI	SK
base	3.3	1.8	8.7	0.0	0.0	0.0	4.5	0.0	27.8	1.8	5.4	11.1	1.8	2.7
peak	4.1	4.2	46.2	1.8	0.1	1.2	19.3	0.0	3.5	4.6	2.9	1.1	0.7	1.5

Table 4.18: Base and peak generation capacity (GW) installed per node of the European network.

representing the probability mass assigned to each medoid as a result of the reduction process.

4.2.5 Case Study

In this section, we assess the performance of our approach in a realistic case study that is based on the stylized model for the European power system that is described in [103]. Accordingly, we consider a pipeline network model with 28 nodes, each representing an European country. The capacities of the lines are also obtained from [103], in particular, we take the values from “Table 14. Transmission capacities between model regions (GW)” that correspond to the year 2020. We assume that each node in the network (i.e., each European country) includes two types of power plants technologies, which we denote as *base* and *peak*, respectively. Again, the available capacity of both technologies has been assigned based on the data in [103] corresponding to 2020 for each country. More specifically, the base power-plant capacities have been obtained by adding up the installed capacities of the technologies “Nuclear”, “Hard coal”, “Oil” and “Lignite” and the peak power-plant capacities from the technologies “Natural Gas”, “Waste” and “Other gases”. The nodes of the system and the resulting generation capacities of each type are listed in Table 4.18.

To build a data sample of the form $\{(L_i, \mathbf{x}_i)\}_{i \in \mathcal{N}}$, we have collected the actual aggregate hourly demand, wind, solar and hydro energy production for each country (node of the system) in 2020 from the ENTSO-e Transparency Platform¹⁰ (ETP). We have also retrieved the day-ahead forecast of the hourly demand and the produced wind and solar energy from this platform. To get series of net demand values (both forecast and actual), we have subtracted the respective wind, solar and hydro power data series from the aggregate day-ahead forecast/actual demand series. We clarify that no day-ahead forecast for the hydro power production is available in ETP, so the series of real hydro power production has been used (instead of the missing day-ahead hydro forecast) for the computation of day-ahead forecasts of the nodal net demands. Some minor gaps in the data extracted from ETP have been filled through linear interpolation.

The marginal costs of energy generation and up- and down-regulation of each unit are randomly sampled from the uniform distributions specified in Table 4.19. The

¹⁰ENTSO-e Transparency Platform. See <https://transparency.entsoe.eu/>.

	C	C^u	C^d
base	U(8, 12)	U(60, 70)	U(-40, -50)
peak	U(36, 44)	U(45, 50)	U(30, 35)

Table 4.19: Uniform distributions from which the marginal production, up- and down-regulation costs of the units in the European system have been sampled.

so-obtained values for these costs have remained fixed throughout the experiments performed in this section. We point out that in the uniform distributions of Table 4.19, we have considered that base power units are cheap but inflexible, and thus, with costly regulation. In contrast, peak power plants are expensive, but flexible, and hence, with more competitive regulation costs.

We conduct a rolling window simulation (see Section 2.3 for more details on the rolling window setting) on the data of 2020, in which we gradually select non-overlapping windows of 150 points each. From each window, we randomly sub-sample (without replacement) the indexes corresponding to the training and test sets, which are eventually made up of 100 and 50 samples, respectively. We take ten windows over which we average the results that follow.

As in the example of Section 4.2.3, we consider a feature vector \mathbf{x} made up of the day-ahead forecast of the system net demand, L^F , (measured in MWh), enlarged with an additional feature fixed to one to accommodate the intercept of the affine models $\hat{L} = \mathbf{w}_k^\top \mathbf{x} = w_{0k} + w_{1k}L^F$, $k \leq K$.

In the analysis we conduct next, we consider various values for K (number of partitions and hence of affine models) and several percentage reductions of the number of data in each partition $\mathcal{N}_k, k \leq K$. The results of this analysis are summarized in Table 4.20, where “ $r\%$ ” in the first column means that only that percentage of medoids in the partition \mathcal{N}_k (more precisely $\lceil \frac{r}{100} |\mathcal{N}_k| \rceil$, where $\lceil \cdot \rceil$ denotes the ceiling operator) have been used to estimate the affine function $\hat{L} = \mathbf{w}_k^\top \mathbf{x}$ through (4.22). This table shows, on the one hand, the cost savings achieved by our approach in percentage with respect to the cost of the conventional one and, on the other, the average time the solution to the K estimation problems (4.22) takes. The reported cost savings have been computed out of sample, that is, on the test sets. Beyond the fact that these savings are significant in general, it is clear that our prescriptive approach benefits from exploiting different affine models under different net-demand regimes, which confirms the preliminary conclusion we draw in this regard through the small example of Section 4.2.3. Nevertheless, it is also true that the added benefit rapidly plateaus as K grows. Actually, the bulk of the economic gains we get through the partitioning of the data sample is already reaped with $K = 2$. On the other hand, increasing K has a positive side effect: It remarkably reduces the time to solve the MIP problem (4.22). In addition, this time can be shortened even further, with a tolerable reduction in cost savings, by using only the medoids

	K=1	K=2	K=5	K=7
100%	2.83	4.29	4.74	4.75
r 50%	2.67	4.23	4.39	4.06
20%	2.38	4.12	4.12	3.97

(a) Cost savings in percentage (%).

	K=1	K=2	K=5	K=7
100%	2127.7	283.7	75.9	28.0
r 50%	180.0	27.2	7.4	5.5
20%	8.3	3.2	1.1	1.4

(b) Computational time (s).

Table 4.20: Average cost savings in percentage (%) and average time (s) to solve the estimation problem (4.22) for a number K of partitions and various levels r of reduction in the size of the original training sets (out-of-sample results).

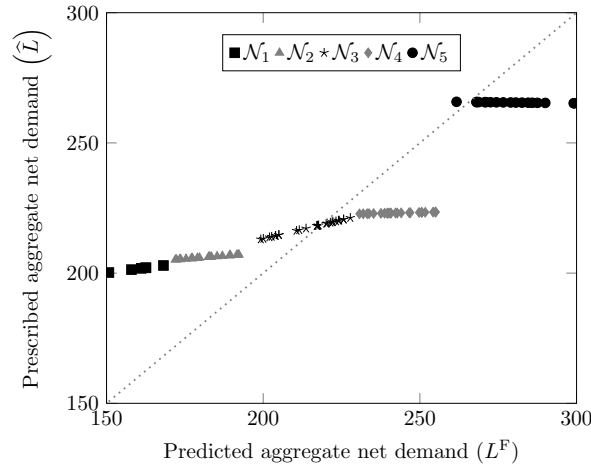


Figure 4.4: Prescribed affine transformation of the day-ahead net-demand forecast (aggregated system-wise). Demand is given in GW.

of the partitions $\mathcal{N}_k, k \leq K$, when estimating the affine models through (4.22).

To comprehend where those cost savings our approach yields come from, in Figure 4.4 we plot the predicted aggregate net demand L^F against the one prescribed by our method, i.e., \hat{L} . The plot corresponds to one window of 150 data points taken at random out of the ten we have considered in the rolling-window simulation. Furthermore, the figure depicts results from the case with five partitions ($K = 5$). It can be seen that, when the system net demand is predicted low, our method prescribes to overestimate it. This prescription is motivated by two facts. On the one hand, the overestimation of the net demand in the forward market is covered by cheap power plants, whereas it reduces the need for upward regulation. On the other, even though it slightly increases the demand for downward regulation, the group of units that down-regulate remains the same in any case, i.e., with and without the overestimation, due to the limitations of the network. As a result, the cost savings linked to the reduction in up-regulation outweigh the extra costs incurred by the increase in down-regulation. It is interesting to note that system operators, based on their accumulated experience, often introduce an upward bias into the net demand forecast [34].

As the level of net demand grows, the overestimation of the system net load that our method prescribes diminishes to a point where the prescribed amount flattens (see partitions \mathcal{N}_4 and \mathcal{N}_5). Again, this phenomenon is caused by the network and the limitations it imposes. Indeed, our method avoids dispatching power plants in the forward market which, despite being their turn in the cost-merit order, would have been irretrievably down-regulated in real time because of network bottlenecks. For instance, in partition \mathcal{N}_4 , F-MC consistently dispatches the DE base generator, with its massive 46 GW, to maximum capacity. However, due to grid constraints, this unit is subsequently down-regulated to around 30 GW. On the contrary, P-MC takes into consideration that this power plant is one of the latest to be scheduled in this partition and foresees the grid limitation on the power flow, thus constraining the aggregated energy production and systematically dispatching such a unit to the previously mentioned 30 GW.

4.3 Summary

One of the classical approaches to dealing with problems with uncertain parameters is to produce statistically accurate forecasts of their expected values. Given the simplicity and natural intuitiveness of this strategy, this approach is still widely used in many industrial applications despite its suboptimal performance. In the applications presented in this chapter, we demonstrate the benefits of smartly estimating the uncertain parameters using contextual information and taking into account the target optimization problem. This strategy shows substantial economic gains in the decision-making tasks while requiring minimal changes in current business procedures.

Along these lines, in the first application, the bilevel framework developed in Section 2.2.4 is applied to the problem of a strategic producer, competing in a market for a homogeneous product, in this case, electricity. The result is two alternative models with complementary features that can be directly solved by off-the-shelf optimization solvers. This application evaluates the performance of both models in a realistic case study of a strategic producer participating in the Iberian electricity market. The illustrative example compares the bilevel framework against the alternative strategies discussed in this thesis, emphasizing the advantages of BL: it guarantees feasibility and obtains economic improvements in constrained decision-making problems. Numerical results show that BL, not only significantly increases the revenue streams of the firm in general, but also proves to be critical to generation portfolios principally comprising peak power units. Indeed, the market revenues of a strategic peak generation portfolio are especially sensitive to the uncertainty in the inverse demand function. Therefore, in this case, the strategic firm may put at risk the bulk of its market incomes by being left out of the market or trading in deficit. Our approach, however, is, by construction, aware of that sensitivity and thus, is able to retain most of the profit the firm would make under a perfectly predictable inverse demand function.

In the second application in this chapter, we propose a data-driven method to prescribe the value of net demand that the forward settlement (in a two-stage electricity market) should clear in order to minimize the expected total cost of operating the underlying power system. Leveraging the problem structure, we formulate a mixed-integer linear program that trains an affine function to map the *predicted* net demand into the *prescribed* one. This is done taking into account the cost asymmetry and network constraints of the underlying power system and ensuring the merit order dispatch of the generators. Numerical experiments conducted out of sample on a stylized model of the European electricity market reveal that the cost savings implied by the estimated affine mappings are substantial. Furthermore, on the grounds that the cost structure of a power system is highly dependent on its operating point, and hence, on the level of net demand, we have devised a K -means-based partition strategy of the data sample to train different affine mappings for different net-demand regimes. The use of this strategy is shown to have a positive twofold effect in the form of substantially increased cost savings and a remarkable drop in the computational burden of the proposed MIP training model. Finally, we have added further to the partitioning of the data sample with a medoid-based reduction in the size of the partitions, achieving additional speedups in solution times. Taken together, this opens up the possibility of leveraging our prescriptive approach in larger instances.

Chapter 5

Closure

This chapter summarizes the main aspects of this thesis and discusses some avenues for future work.

5.1 Summary and conclusions

The development of information technologies has created a new resource for decision makers: *data*. The subset of data that is generated within the context of the decision task and which can help obtain better decisions is called *contextual information*. This thesis is part of a new gold rush to exploit the potential of data and, in particular, of contextual information in decision making. To this end, in this thesis, we have developed efficient data-driven mathematical frameworks and optimization models that leverage contextual information to improve decision making in problems characterized by the presence of uncertain parameters.

Electricity markets are a clear example of a sector in which decision making plays a crucial role in both the long-term and daily activity. Decision making in electricity markets became more challenging with the development of renewable energy, because, among other reasons, it dramatically increased uncertainty, affecting most of the tasks faced by the agents operating in said markets. Many of these tasks involve operational decisions characterized by being low risk and due periodically. We refer to those tasks within this thesis as *iterative decision-making tasks*. This thesis applies current and new innovations in contextual decision making, to the iterative decision-making tasks that agents face in electricity markets.

In **Chapter 1**, we provide a brief historical evolution of decision making in electricity markets, highlighting the golden opportunity for agents operating in them to improve their operations through contextual information.

Chapter 2 picks up the baton, formally discussing the aforementioned classical decision making paradigms and observing the general presentation that the widespread use of these techniques in other fields deserves. Chapter 2 continues with a discussion on the potential of contextual information and how to incorporate this valuable resource in decision making. Starting from the canonical contextual stochastic problem, we have confronted the advantages and disadvantages of different state-of-the-art frameworks designed to address this problem type. Our contribution to this scientific effort is a bilevel framework with notable features and general scope. The last part of the chapter addresses the particularities of iterative decision-making tasks and deals with two main, related topics: the rolling window setting and the online learning paradigm. Concerning the first topic, we emphasize the benefits of the rolling window setting, which combined with the frameworks previously described in the chapter, allows for addressing iterative tasks in practice. As for the second, we review the connections of online learning with the rolling window and the other decision frameworks and propose a new online gradient descent algorithm tailored to iterative decision making tasks with contextual

information.

Chapter 3 is the first of the two chapters dedicated to presenting various applications of the previously introduced contextual decision frameworks in electricity markets. This chapter discusses the problem of a wind power producer offering her production in a wholesale electricity market with a dual-price settlement for imbalances. Two market variants are analyzed, and in each case an approach designed to better suit the characteristics of the market. The resulting approaches have in common that the decision variable (the offer to the market) is encoded through a linear decision rule of the features.

The first application presented in Chapter 3 proposes an interpretable and effective method to enhance both the tasks of renewable energy forecasting and trading. Our method is based on a data-driven newsvendor-type optimization model which leverages extra available information to produce an improved renewable energy forecast or a renewable energy offer that can be directly placed in the day-ahead electricity market. The effectiveness of our approach has been tested on a realistic case study with the aim, on the one hand, to improve the wind power production forecast issued by the Danish transmission system operator and, on the other, to formulate a competitive market offer for a producer managing such a production. To this end, we have built a rolling-window simulation setup that mimics the actual processes of forecasting and bidding, thereby exploiting the information available when the forecast is issued or the offer must be placed. The numerical results highlight the benefits achieved by this approach, which amounts to a 8.53% of reduction in mean absolute error and a 2.13% of improvement in the economic metric with respect to the benchmark—the standard “predict, then optimize” approach—for the simulation period considered. These figures highlight the intrinsic value of exploiting contextual information such as spatially correlated forecasts. In the same vein, we have observed that the use (as contextual information) of both on- and offshore wind power forecasts in areas geographically close to the zone to which the target wind power production belongs are valuable. This seems to be especially true if those areas pertain to the same country or domain of the same transmission system operator.

The second application envisions an hourly wholesale electricity market with a minimum time between the offer and the delivery of energy. In this application, we implement the contextual online gradient descent algorithm, proposed in Section 2.3.3, given the continuous feedback the producer receives in this market setting. To the best of our knowledge, this is the first time online gradient algorithms have been applied to this problem. The contextual online gradient descent algorithm is used to improve the profits obtained by a wind power producer equipped with geographically close wind forecasts who offers her production to the market. Several numerical experiments were carried out to assess the properties of the proposed online algorithm. The result ob-

tained in the case study, built upon realistic data of the Danish transmission system operator Energinet.dk, shows that the online algorithm achieves a 38.6% imbalance cost reduction against using a standard point forecast through the “predict, then optimize” approach and 7.6% imbalance cost reduction compared to a state-of-the-art decision rule approach. These substantial improvements are, in part, justified due to the fast-tracking ability, which allows it to follow patterns obviated by other methods based on a training set of samples, and the design of the market, which enables the algorithm to exhibit its best performance. Interestingly, these economic gains are accompanied by a drastic reduction in computational cost, allowing the application of the online algorithm even in the most challenging markets. Furthermore, we have empirically analyzed several dynamic definitions of the online regret metric, showing the pursued sublinear convergence.

Chapter 4 discusses two applications that smartly estimate the uncertain parameters, considering the underlying optimization problem. These estimators are constructed through two approaches that take historical data and contextual information as input.

In the first application, we apply the contextual bilevel approach, presented in Section 2.2.4, to the problem of a strategic power producer who manages a portfolio of thermal units. The producer offers the portfolio generation in a wholesale electricity market modeled through an uncertain inverse residual demand function. The idea is to produce prescriptive estimators of the uncertain parameters that shape the inverse residual demand function, taking into account the objective function and feasibility region of the underlying problem in their estimation. Under convexity assumptions, the resulting bilevel optimization program can be reformulated as a non-linear regularized program and a mixed-integer quadratic program. The former optimization problem is iteratively solved for decreasing values of a regularization parameter, achieving local optimal solutions in minimum time. The mixed-integer program is computationally more expensive but, given the properties of the problem, can be solved to optimality.

We have evaluated the performance of our approach and its practical relevance through a realistic case study of a strategic producer, participating in the Iberian electricity market. Specifically, the numerical results show that our framework, not only significantly increases the revenue streams of the producer in general, but also proves to be critical to those generation portfolios which mainly comprise peak power units. Indeed, the market revenues of a strategic peak generation portfolio are especially sensitive to the uncertainty in the inverse demand function. Therefore, in this case, the strategic producer may put the bulk of the market incomes at risk by being left out of the market or trading in deficit. Our approach, however, is, by construction, aware of that sensitivity and thus, is able to retain most of the profit the producer would make under a perfectly predictable inverse demand function, increasing the benefits obtained with respect to the “predict, then optimize” strategy by 14.6% in the case of peak units.

The second application described in this chapter analyzes the problem of a market operator in charge of clearing a two-stage electricity market consisting of a forward and a real-time settlement. In this context, we propose a data-driven optimization program to prescribe the value of net demand that the forward settlement should clear in order to minimize the expected total cost of operating the underlying power system. The proposed mixed-integer linear program trains an affine mapping, considering the technical and economic characteristics of the power plant reserves and grid constraints. This mapping modifies the available net demand forecast to produce an estimator with better economic performance. The final procedure respects the merit order dispatch of the units and requires minimal changes in current business practices to be implemented.

This approach has been investigated in a case study that resembles the European electricity market. Given that the operating point of the system is highly variable, we use several clustering techniques to partition the data sample and produce different affine mappings for different net-demand regimes. The utilization of these clustering techniques is shown to have a positive twofold effect in the form of substantially increased cost savings and a remarkable drop in the computational burden of training the proposed mixed-integer program. Numerical experiments reveal that the cost savings implied by the proposed strategy are substantial, well above 2%.

5.2 Future work

This section discusses some directions for future work related to the main contributions and applications addressed in this thesis.

Contextual online gradient descent

Our plans for future work include delving into the theoretical guarantees that this framework offers in terms of average long-term regret in a similar fashion to other online algorithms. Faster convergence rates or improved performance may be obtained with another procedure to compute the learning rate. On a different front, non-linear mappings, i.e., kernels or generalized additive models, can extend the regression capabilities of the algorithm.

Contextual bilevel framework

Potential extensions of this work could include the use of more advanced techniques in the resolution of our bilevel framework, such as those employed in more general MPCC problems. Another interesting aspect would be to explore alternative formulations aimed at the pessimistic solution of the bilevel program, which could prevent the known issues of this framework when the lower level has multiple solutions. Likewise, the generalization of our approach to multi-stage decision-making problems under

uncertainty requires further analysis.

Wind power producer

Another possible path to take could be to focus on the development of robust counterparts of the proposed models with the aim of reducing the volatility of the improvements achieved. Variable selection methodologies may also be implemented to determine the best subset of regressors to feed into the models and to enhance model interpretability. Likewise, non-linear mappings between contextual information and the response variable (wind forecast or offer) could be captured within our approach by performing non-linear transformations on the features or by way of kernels. Finally, while the data-driven model for renewable energy trading that we have developed is tailored to electricity markets with a dual-price settlement for imbalances, such as Nordpool-DK1 or MIBEL (Spain), it could also be adapted to any market where deviations with respect to a predefined forward schedule entail an opportunity cost.

Online wind power producer

Although the focus of this research is on wind energy producers, the online algorithm is readily applicable to managing a portfolio of variable renewable energies with zero marginal cost, including wind, solar and other technologies. Similar algorithms could therefore be developed when the producer's portfolio includes other assets such as loads, thermal power plants, or energy storage facilities, replacing the aggregated source of uncertainty, i.e., the variable net production of energy by a lineal decision rule. In this case, the projection step on the feasible region would likely involve solving a quadratic optimization program that can still be efficiently solved with modern solvers, provided that the feasible region is convex.

Strategic thermal producer

As a starting point, we suggest the study of more complex functions to model the cost structure of the producer and the shape of the residual demand. Additionally, the inter-temporal constraints of the portfolio can be accounted for to prevent technical issues in the implementation of the strategy. On a different front, analyzing the price-maker counterpart of this problem could have potential applications in markets where a reduced number of firms control large portfolios of generating units.

Contextual economic dispatch

Future work may investigate how to optimize the partitioning of the data sample by embedding it inside the proposed mixed-integer training model. From a market

clearing perspective, extending this model to those markets that consider more detailed representations of the network in the forward and real-time stages is also relevant. Likewise, including inter-temporal constraints, such as ramping limits and minimum up-/down-times of the units taking part in the market, can produce more precise solutions.

Appendix A

Contextual optimization via bilevel programming: Auxiliary material

This appendix includes complementary material related to the bilevel programming approach (BL) proposed in Section 2.2.4 for contextual decision making under uncertainty. Section A.1 describes how to apply the bilevel approach when the original stochastic problem includes recourse variables. Section A.2 discusses two theoretical applications of BL to classical problems in Operations Research, comparing the cases with and without full recourse. Finally, Section A.3 proves the asymptotic consistency of the model resulting from applying BL to the strategic producer problem addressed in Section 4.1.

A.1 Solving the bilevel approach with recourse variables

In this section, we elaborate on how to solve the general-purpose bilevel program (2.23) when the contextual stochastic program includes recourse variables. For an introduction on two-stage stochastic problems with recourse variables, we refer the reader to [125]. We start the derivation particularizing the generic formulation (2.10) as follows:

$$\min_{\mathbf{z}, s(\mathbf{Y})} \mathbb{E}[f(\mathbf{z}, s(\mathbf{Y}); \mathbf{Y}) | \mathbf{X} = \mathbf{x}] \quad (\text{A.1a})$$

$$\text{s.t. } h_k^{in}(\mathbf{z}, s(\mathbf{Y}); \mathbf{Y}) \leq 0, \quad \forall k \quad (\text{A.1b})$$

$$h_l^{eq}(\mathbf{z}, s(\mathbf{Y}); \mathbf{Y}) = 0, \quad \forall l, \quad (\text{A.1c})$$

where \mathbf{z} constitutes the vector of *here-and-now* variables independent of the uncertainty, $s(\mathbf{Y})$ represents the *wait-and-see* decisions, and constraints (A.1b), (A.1c) must be satisfied for almost all \mathbf{y} given the context \mathbf{x} (i.e., with probability one). We also assume that f, h_k^{in} are convex functions with respect to all variables, h_l^{eq} are affine functions, and function g^{BL} , already introduced in Section 2.2.4, is continuous in the parameter vector \mathbf{w} .

Our method solves the following bilevel optimization problem:

$$\mathbf{w}^{\text{BL}} \in \arg \min_{\mathbf{w} \in \mathbb{R}^q; \hat{\mathbf{z}}_i, \hat{\mathbf{s}}_i} \sum_{i \in \mathcal{N}} f(\hat{\mathbf{z}}_i, \hat{\mathbf{s}}_i; \mathbf{y}_i) \quad (\text{A.2a})$$

$$\text{s.t. } h_k^{in}(\hat{\mathbf{z}}_i, \hat{\mathbf{s}}_i; \mathbf{y}_i) \leq 0, \quad \forall k, \forall i \in \mathcal{N} \quad (\text{A.2b})$$

$$h_l^{eq}(\hat{\mathbf{z}}_i, \hat{\mathbf{s}}_i; \mathbf{y}_i) = 0, \quad \forall l, \forall i \in \mathcal{N} \quad (\text{A.2c})$$

$$\hat{\mathbf{z}}_i \in \{\arg \min_{\mathbf{z}, \mathbf{s}} f(\mathbf{z}, \mathbf{s}; g^{\text{BL}}(\mathbf{x}_i; \mathbf{w}))\} \quad (\text{A.2d})$$

$$\text{s.t. } h_k^{in}(\mathbf{z}, \mathbf{s}; g^{\text{BL}}(\mathbf{x}_i; \mathbf{w})) \leq 0, \quad \forall k \quad (\text{A.2e})$$

$$h_l^{eq}(\mathbf{z}, \mathbf{s}; g^{\text{BL}}(\mathbf{x}_i; \mathbf{w})) = 0, \quad \forall l, \forall i \in \mathcal{N}. \quad (\text{A.2f})$$

On the assumption that the lower-level minimization problems (A.2d)–(A.2f) satisfy some constraint qualification, the classical strategy to solve (A.2) is to replace each lower level (A.2d)–(A.2f) with its equivalent Karush-Kuhn-Tucker (KKT) conditions

[28], that is,

$$\mathbf{w}^{\text{BL}} \in \arg \min_{\mathbf{w} \in \mathbb{R}^q; \hat{\mathbf{z}}_i, \hat{\mathbf{s}}_i, \lambda_{ki}, v_{li}} \sum_{i \in \mathcal{N}} f(\hat{\mathbf{z}}_i, \hat{\mathbf{s}}_i; \mathbf{y}_i) \quad (\text{A.3a})$$

$$\text{s.t. } h_k^{\text{in}}(\hat{\mathbf{z}}_i, \hat{\mathbf{s}}_i; \mathbf{y}_i) \leq 0, \quad \forall k, \forall i \in \mathcal{N} \quad (\text{A.3b})$$

$$h_l^{\text{eq}}(\hat{\mathbf{z}}_i, \hat{\mathbf{s}}_i; \mathbf{y}_i) = 0, \quad \forall l, \forall i \in \mathcal{N} \quad (\text{A.3c})$$

$$\begin{aligned} \nabla f(\hat{\mathbf{z}}_i, \hat{\mathbf{s}}_i; g^{\text{BL}}(\mathbf{x}_i; \mathbf{w})) + \sum_{k=1}^K \lambda_{ki} \nabla h_k^{\text{in}}(\hat{\mathbf{z}}_i, \hat{\mathbf{s}}_i; g^{\text{BL}}(\mathbf{x}_i; \mathbf{w})) + \\ + \sum_{l=1}^L v_{li} \nabla h_l^{\text{eq}}(\hat{\mathbf{z}}_i, \hat{\mathbf{s}}_i; g^{\text{BL}}(\mathbf{x}_i; \mathbf{w})) = 0, \quad \forall i \in \mathcal{N} \end{aligned} \quad (\text{A.3d})$$

$$h_k^{\text{in}}(\hat{\mathbf{z}}_i, \hat{\mathbf{s}}_i; g^{\text{BL}}(\mathbf{x}_i; \mathbf{w})) \leq 0, \quad \forall k, \forall i \in \mathcal{N} \quad (\text{A.3e})$$

$$h_l^{\text{eq}}(\hat{\mathbf{z}}_i, \hat{\mathbf{s}}_i; g^{\text{BL}}(\mathbf{x}_i; \mathbf{w})) = 0, \quad \forall l, \forall i \in \mathcal{N} \quad (\text{A.3f})$$

$$\lambda_{ki} \geq 0, \quad \forall k, \forall i \in \mathcal{N} \quad (\text{A.3g})$$

$$\lambda_{ki} h_k^{\text{in}}(\hat{\mathbf{z}}_i, \hat{\mathbf{s}}_i; g^{\text{BL}}(\mathbf{x}_i; \mathbf{w})) = 0, \quad \forall k, \forall i \in \mathcal{N}, \quad (\text{A.3h})$$

where $\lambda_{ki}, v_{li} \in \mathbb{R}$ are, respectively, the Lagrange multipliers related to constraints (A.2e) and (A.2f) for each lower-level problem; (A.3a) and (A.3b)-(A.3c) are, in that order, the objective function and constraints of the upper-level problem, and constraints (A.3d), (A.3e)-(A.3f), (A.3g), (A.3h), are, respectively, the stationarity, primal feasibility, dual feasibility and slackness conditions of the lower-level problems. As we already mentioned in Section 2.2.4, problem (A.3) violates the Mangasarian-Fromovitz constraint qualification at every feasible point [121] and therefore, interior-point methods fails to find even a local optimal solution to this problem. To overcome this issue, a regularization approach was first introduced in [122] and further investigated in [114]. This method replaces all complementarity constraints (A.3h) with inequality (A.4c) below:

$$\mathbf{w}^{\text{BL}} \in \arg \min_{\mathbf{w} \in \mathbb{R}^q; \hat{\mathbf{z}}_i, \hat{\mathbf{s}}_i, \lambda_{ki}, v_{li}} \sum_{i \in \mathcal{N}} f(\hat{\mathbf{z}}_i, \hat{\mathbf{s}}_i; \mathbf{y}_i) \quad (\text{A.4a})$$

$$\text{s.t. } (\text{A.3b}) - (\text{A.3g}) \quad (\text{A.4b})$$

$$- \sum_{k=1}^K \lambda_{ki} h_k^{\text{in}}(\hat{\mathbf{z}}_i, \hat{\mathbf{s}}_i; g^{\text{BL}}(\mathbf{x}_i; \mathbf{w})) \leq \epsilon, \quad \forall i \in \mathcal{N}, \quad (\text{A.4c})$$

where ϵ is a small non-negative scalar that allows to reformulate (A.3) as the parametrized non-linear optimization problem (A.4), which typically satisfies a constraint qualification and can be then efficiently solved by standard non-linear optimization solvers. Authors of [122] prove that, as ϵ tends to 0, the solution of (A.4) tends to a *local* optimal solution of (A.3). In this manuscript, we have referred to this approach as BL-R.

Alternatively, following the same procedure already introduced in Section 2.2.4, the complementarity slackness conditions can be linearized according to [59] as follows:

$$\mathbf{w}^{\text{BL}} \in \arg \min_{\mathbf{w} \in \mathbb{R}^q; \hat{\mathbf{z}}_i, \hat{\mathbf{s}}_i, \lambda_{ki}, u_{li}, u_{ki}} \sum_{i \in \mathcal{N}} f(\hat{\mathbf{z}}_i, \hat{\mathbf{s}}_i; \mathbf{y}_i) \quad (\text{A.5a})$$

$$\text{s.t. (A.3b) -- (A.3g)} \quad (\text{A.5b})$$

$$\lambda_{ki} \leq u_{ki} M^{\text{D}}, \quad \forall k, \quad \forall i \in \mathcal{N} \quad (\text{A.5c})$$

$$h_k^{\text{in}}(\hat{\mathbf{z}}_i, \hat{\mathbf{s}}_i; g^{\text{BL}}(\mathbf{x}_i; \mathbf{w})) \geq (u_{ki} - 1) M^{\text{P}}, \quad \forall k, \quad \forall i \in \mathcal{N} \quad (\text{A.5d})$$

$$u_{ki} \in \{0, 1\}, \quad \forall k, \quad \forall i \in \mathcal{N}, \quad (\text{A.5e})$$

where u_{ki} are binary variables, and $M^{\text{P}}, M^{\text{D}} \in \mathbb{R}^+$ are large enough constants whose values can be determined as proposed in [109]. The resulting model (A.5) is a single-level mixed-integer non-linear problem. We have denoted this method as BL-M.

Solving the bilevel problem (A.2) using either BL-R or BL-M is valid for a conditional stochastic problem that satisfies the conditions described in this section. Nonetheless, the complexity of solving the regularized non-linear problem (A.4) or the mixed-integer non-linear program (A.5) highly depends on functions $f, h_k^{\text{in}}, h_l^{\text{eq}}, g^{\text{BL}}$. In some cases (see, for instance, the particular applications discussed in Chapter 4), problem (A.5) can be reformulated as a mixed-integer linear/quadratic optimization problem that can be solved to global optimality using standard optimization solvers. In the general case, problems (A.4) and (A.5) can also be solved using off-the-shelf optimization solvers, but global optimality may not be guaranteed. Notwithstanding this, local optimal solutions of the proposed bilevel formulation (A.2) may still lead to decisions that are significantly better than those computed by the traditional “predict, then optimize” approach FO discussed in Section 2.2.

A.2 Applications of BL with and without full recourse

This section shows the application of BL in problems with and without full recourse using the newsvendor problem—a well-known stochastic programming problem with simple recourse (Section A.2.1)—and the product placement problem (Section A.2.2), which is a two-stage stochastic programming problem with full recourse.

A.2.1 Newsvendor problem

We start with the popular newsvendor problem in the spirit of [7], a work that elicited renewed interest [100, 20] in the solution to the conditional stochastic program (2.10) presented in Chapter 2. In the newsvendor problem, the goal of the decision maker is to find the optimal ordering quantity for a product with unknown random demand ($y \in \mathbb{R}^+$) $\sim Y$. In turn, this (positive) demand may be influenced by a random vector of features ($\mathbf{x} \in \mathbb{R}^p$) $\sim \mathbf{X}$ representing, for instance, product information, weather conditions, customer profiles, etc. The decision maker has, therefore, a collection of

observations $\{(y_i, \mathbf{x}_i), \forall i \in \mathcal{N}\}$, which s/he would like to exploit to make an informed ordering quantity $z \in \mathbb{R}^+$ under the context $\mathbf{X} = \mathbf{x}$. Let d and r , with $r > d > 0$, be the cost and revenue of manufacturing and selling one product unit, respectively. This problem can be formulated as the following conditional stochastic program:

$$\min_{z \in \mathbb{R}^+} \mathbb{E}[dz - r \min(z, Y) | \mathbf{X} = \mathbf{x}]. \quad (\text{A.6})$$

Approaches FO and BL both follow a “predict-then-optimize” strategy, whereby the ordering quantity is obtained as the solution to the following surrogate decision-making model:

$$\min_{z \in \mathbb{R}^+} dz - r \min(z, \hat{y}). \quad (\text{A.7})$$

We can use an auxiliary variable s to get rid of the inner minimization and write instead

$$\min_{z, s} dz - rs \quad (\text{A.8a})$$

$$\text{s.t. } s \leq z \quad (\text{A.8b})$$

$$s \leq \hat{y}, \quad (\text{A.8c})$$

whose solution is $z^* = s^* = \hat{y}$.

FO and BL differ in the particular single value or scenario \hat{y} that each of them uses. In the case of FO, \hat{y} is an estimate of $\mathbb{E}[Y | \mathbf{X} = \mathbf{x}]$. Consequently, it becomes apparent that, for the newsvendor problem, approach FO is fundamentally inconsistent, because it is well-known that the solution to (A.6) corresponds to the quantile $\frac{r-d}{r}$ of the demand distribution Y conditional on $\mathbf{X} = \mathbf{x}$. Naturally, this quantile is generally different from $\mathbb{E}[Y | \mathbf{X} = \mathbf{x}]$.

Now, if we take $\hat{y} = g^{\text{BL}}(\mathbf{x}; \mathbf{w}) = \mathbf{w}^\top \mathbf{x}$ in our approach, the optimal vector of linear coefficients \mathbf{w}^{BL} is computed as follows:

$$\mathbf{w}^{\text{BL}} \in \arg \min_{\mathbf{w} \in \mathbb{R}^p; \hat{z}_i} \sum_{i \in \mathcal{N}} d\hat{z}_i - r \min(\hat{z}_i, y_i) \quad (\text{A.9a})$$

$$\text{s.t. } \hat{z}_i \in \left\{ \arg \min_{z_i, s_i} dz_i - rs_i \right. \quad (\text{A.9b})$$

$$\text{s.t. } s_i \leq z_i \quad (\text{A.9c})$$

$$s_i \leq \mathbf{w}^\top \mathbf{x}_i, \forall i \in \mathcal{N}, \quad (\text{A.9d})$$

which, based on our previous argument, boils down to

$$\mathbf{w}^{\text{BL}} \in \arg \min_{\mathbf{w} \in \mathbb{R}^p; \hat{z}_i} \sum_{i \in \mathcal{N}} d\hat{z}_i - r \min(\hat{z}_i, y_i) \quad (\text{A.10a})$$

$$\text{s.t. } \hat{z}_i = \mathbf{w}^\top \mathbf{x}_i, \quad \forall i \in \mathcal{N}. \quad (\text{A.10b})$$

Therefore, our approach coincides exactly with that proposed in [7], which, in turn, is given by problem (2.20) in Chapter 2 when $g^{\text{DR}}(\mathbf{x}; \mathbf{w}) = \mathbf{w}^\top \mathbf{x}$. This equivalence is far from being general though, as we have seen in the strategic producer application presented in Section 4.1.

A.2.2 Product placement problem

Given a graph $\mathcal{G} = (\mathcal{B}, \mathcal{A})$ with node-arc matrix \mathbf{A} , in the product placement problem, the goal is to decide the amount $z_b \in \mathbb{R}^+$ of a certain product to be placed in each node $b \in \mathcal{B}$ of the grid [17]. After this decision is made, the demand for the product at each node y_b is realized, and the inventories of product throughout the network are shipped across the arcs \mathcal{A} so as to satisfy the actually observed nodal demands. As in the newsvendor problem, these demands may be affected by some exogenous factors \mathbf{X} that may be also random, but that are disclosed before the product placement decision is to be made. Let $\mathbf{h} \in \mathbb{R}^{|\mathcal{B}|}$ and $\mathbf{g} \in \mathbb{R}^{|\mathcal{A}|}$ be the cost of initially placing products in the nodes of the network and the cost of shipping products through the edges of the graph, respectively. The product placement problem under uncertain demand, but with contextual information, can be formulated as follows:

$$\min_{\mathbf{z} \geq 0} \mathbb{E}[c(\mathbf{z}; \mathbf{Y}) | \mathbf{X} = \mathbf{x}], \quad (\text{A.11})$$

where

$$c(\mathbf{z}; \mathbf{y}) = \mathbf{h}^\top \mathbf{z} + \min_{\mathbf{f} \geq 0, \mathbf{p} \geq 0} \mathbf{g}^\top \mathbf{f} + \mathbf{r}^\top \mathbf{p} \quad (\text{A.12a})$$

$$\text{s.t. } \mathbf{A}\mathbf{f} \leq \mathbf{z} - \mathbf{y} + \mathbf{p}. \quad (\text{A.12b})$$

In problem (A.12), we have included a variable vector $\mathbf{p} \in \mathbb{R}_{\geq 0}^{|\mathcal{B}|}$ to allow for unsatisfied demand, with the associated penalty cost $\mathbf{r} \in \mathbb{R}^{|\mathcal{B}|}$. Furthermore, the decision vector $\mathbf{f} \in \mathbb{R}^{|\mathcal{A}|}$ represents the amount of product shipped across the arcs of the network. The cost function (A.12a) takes the form of a two-stage linear cost, with the integration of a recourse problem. More importantly, unlike in the newsvendor problem, the recourse is given by a full-fledged (linear) minimization problem. The surrogate decision-making model associated with the *predict-then-optimize* strategies FO and BL is as follows:

$$\min_{\mathbf{z} \geq 0, \mathbf{f} \geq 0, \mathbf{p} \geq 0} \mathbf{h}^\top \mathbf{z} + \mathbf{g}^\top \mathbf{f} + \mathbf{r}^\top \mathbf{p} \quad (\text{A.13a})$$

$$\text{s.t. } \mathbf{A}\mathbf{f} \leq \mathbf{z} - \hat{\mathbf{y}} + \mathbf{p}. \quad (\text{A.13b})$$

To ease the exposition and the notation that follows, we make the additional assumption that $\mathbf{r} > \mathbf{h} > 0$, where the inequality holds component-wise. In this case, variable vector \mathbf{p} in (A.13) is zero at the optimum and the surrogate model can be simplified to

$$\min_{\mathbf{z} \geq 0, \mathbf{f} \geq 0} \mathbf{h}^\top \mathbf{z} + \mathbf{g}^\top \mathbf{f} \quad (\text{A.14a})$$

$$\text{s.t. } \mathbf{A}\mathbf{f} \leq \mathbf{z} - \hat{\mathbf{y}}. \quad (\text{A.14b})$$

As previously discussed, problem (A.14) is a deterministic mathematical program whereby the decision \mathbf{z} is solely optimized for the point prediction of demand $\hat{\mathbf{y}}$. While the traditional FO approach sets such a prediction to $\mathbb{E}[\mathbf{Y}|\mathbf{X} = \mathbf{x}]$, the rationale behind the approach BL is to compute a W -parameterized function such that the surrogate problem (A.14) delivers the decision \mathbf{z} that minimizes the in-sample cost, that is:

$$\mathbf{W}^{\text{BL}} \in \arg \min_{\mathbf{W} \in \mathbb{R}^{|\mathcal{B}| \times p}, \Upsilon} \sum_{i \in \mathcal{N}} \mathbf{h}^\top \hat{\mathbf{z}}_i + \mathbf{g}^\top \hat{\mathbf{f}}_i + \mathbf{r}^\top \hat{\mathbf{p}}_i \quad (\text{A.15a})$$

$$\text{s.t. } \mathbf{A}\hat{\mathbf{f}}_i \leq \hat{\mathbf{z}}_i - \mathbf{y}_i + \hat{\mathbf{p}}_i, \quad \forall i \in \mathcal{N} \quad (\text{A.15b})$$

$$\hat{\mathbf{f}}_i, \hat{\mathbf{p}}_i \geq 0, \quad \forall i \in \mathcal{N} \quad (\text{A.15c})$$

$$\hat{\mathbf{z}}_i \in \left\{ \arg \min_{\mathbf{z}_i \geq 0, \mathbf{f}_i \geq 0} \mathbf{h}^\top \mathbf{z}_i + \mathbf{g}^\top \mathbf{f}_i \right. \quad (\text{A.15d})$$

$$\left. \text{s.t. } \mathbf{A}\mathbf{f}_i \leq \mathbf{z}_i - \mathbf{W}\mathbf{x}_i \right\}, \quad \forall i \in \mathcal{N}, \quad (\text{A.15e})$$

where $\Upsilon = \{\hat{\mathbf{z}}_i, \hat{\mathbf{f}}_i, \hat{\mathbf{p}}_i\}$ and we have taken $\hat{\mathbf{y}} = g^{\text{BL}}(\mathbf{x}; \mathbf{W}) = \mathbf{W}\mathbf{x}$ with $\mathbf{W} \in \mathbb{R}^{|\mathcal{B}| \times p}$. As discussed in Section 2.2.4, the lower-level problem (A.15d)–(A.15e) must have a unique solution. This can be guaranteed if, for example, all the shipping routes that can be taken to satisfy each demand in the graph entail a different cost. If this condition is not satisfied, the degeneracy of the lower-level problem can be eliminated by using classical results from the linear programming literature as described in [63]. As stated in Section 2.2.4, the solution to (A.15) can be addressed by replacing the lower-level linear program (A.15d)–(A.15e) with its KKT optimality conditions, yielding

$$\mathbf{W}^{\text{BL}} \in \arg \min_{\mathbf{W} \in \mathbb{R}^{|\mathcal{B}| \times p}, \Upsilon'} \sum_{i \in \mathcal{N}} \mathbf{h}^\top \hat{\mathbf{z}}_i + \mathbf{g}^\top \hat{\mathbf{f}}_i + \mathbf{r}^\top \hat{\mathbf{p}}_i \quad (\text{A.16a})$$

$$\text{s.t. } \mathbf{A}\hat{\mathbf{f}}_i \leq \hat{\mathbf{z}}_i - \mathbf{y}_i + \hat{\mathbf{p}}_i, \quad \forall i \in \mathcal{N} \quad (\text{A.16b})$$

$$\hat{\mathbf{f}}_i, \hat{\mathbf{p}}_i \geq 0, \quad \forall i \in \mathcal{N} \quad (\text{A.16c})$$

$$0 \leq (\mathbf{h} - \boldsymbol{\alpha}_i) \perp \hat{\mathbf{z}}_i \geq 0, \quad \forall i \in \mathcal{N} \quad (\text{A.16d})$$

$$0 \leq (\mathbf{g} + \mathbf{A}^\top \boldsymbol{\alpha}_i) \perp \hat{\mathbf{f}}_i \geq 0, \quad \forall i \in \mathcal{N} \quad (\text{A.16e})$$

$$0 \leq (\hat{\mathbf{z}}_i - \mathbf{A}\hat{\mathbf{f}}_i - \mathbf{W}\mathbf{x}_i) \perp \boldsymbol{\alpha}_i \geq 0, \quad \forall i \in \mathcal{N}, \quad (\text{A.16f})$$

where $\Upsilon' = \{\hat{\mathbf{z}}_i, \hat{\mathbf{f}}_i, \hat{\mathbf{p}}_i, \boldsymbol{\alpha}_i\}$ and $\boldsymbol{\alpha}_i \in \mathbb{R}^{|\mathcal{B}|}$ is the vector of Lagrange multipliers associated with constraint (A.15e). Thus, problem (A.16) can be solved by regularizing the complementary slackness conditions or by using their Fortuny-Amat big-M reformulation. In the latter case, we arrive to a MIP problem that can be solved using commercial optimization software such as CPLEX or GUROBI.

Finally, if we also take a linear decision mapping $z(\mathbf{x}) = g^{\text{DR}}(\mathbf{x}; \mathbf{W}) = \mathbf{W}\mathbf{x}$ where $\mathbf{W} \in \mathbb{R}^{|\mathcal{B}| \times p}$, the DR approach solves the following minimization problem to compute the optimal matrix of linear coefficients \mathbf{W}^{DR} :

$$\mathbf{W}^{\text{DR}} \in \arg \min_{\mathbf{W} \in \mathbb{R}^{|\mathcal{B}| \times p}, \Upsilon} \sum_{i \in \mathcal{N}} \mathbf{h}^\top \hat{\mathbf{z}}_i + \mathbf{g}^\top \hat{\mathbf{f}}_i + \mathbf{r}^\top \hat{\mathbf{p}}_i \quad (\text{A.17a})$$

$$\text{s.t. } \mathbf{A}\hat{\mathbf{f}}_i \leq \hat{\mathbf{z}}_i - \mathbf{y}_i + \hat{\mathbf{p}}_i, \quad \forall i \in \mathcal{N} \quad (\text{A.17b})$$

$$\hat{\mathbf{f}}_i, \hat{\mathbf{p}}_i \geq 0, \quad \forall i \in \mathcal{N} \quad (\text{A.17c})$$

$$\hat{\mathbf{z}}_i \geq 0, \quad \forall i \in \mathcal{N} \quad (\text{A.17d})$$

$$\hat{\mathbf{z}}_i = \mathbf{W}\mathbf{x}_i, \quad \forall i \in \mathcal{N}, \quad (\text{A.17e})$$

where $\Upsilon = \{\hat{\mathbf{z}}_i, \hat{\mathbf{f}}_i, \hat{\mathbf{p}}_i\}$. It is apparent that the estimation problems (A.16) and (A.17), which BL and DR solve, respectively, are structurally different and so are \mathbf{W}^{BL} and \mathbf{W}^{DR} in general. For instance, think of a graph for which $\min\{g_\ell\}_{\ell \in \mathcal{A}} > \max\{h_b\}_{b \in \mathcal{B}}$. This represents a network where it is always cheaper to satisfy the nodal demand y_b , $b \in \mathcal{B}$, through the amount z_b of product that is initially placed at the demand location, that is, a graph where product shipping would be uneconomical if the nodal demands were certainly known in advance. Indeed, take the ℓ -th row of $\mathbf{g} + \mathbf{A}^\top \boldsymbol{\alpha}_i$ in equation (A.16e) for any $i \in \mathcal{N}$, that is, $g_\ell + \alpha_{o(\ell),i} - \alpha_{e(\ell),i}$, where $o(\ell)$ and $e(\ell)$ denote the origin and end nodes of arc ℓ , respectively. We have that $\inf\{g_\ell + \alpha_{o(\ell),i} - \alpha_{e(\ell),i} : \alpha_{o(\ell),i} \in [0, h_{o(\ell)}], \alpha_{e(\ell),i} \in [0, h_{e(\ell)}]\} = g_\ell - h_{e(\ell)} > 0$. Hence, $f_\ell = 0, \forall \ell \in \mathcal{A}$ and the system of inequalities (A.16d)-(A.16f) boils down to

$$0 \leq (\mathbf{h} - \boldsymbol{\alpha}_i) \perp \hat{\mathbf{z}}_i \geq 0, \quad \forall i \in \mathcal{N} \quad (\text{A.18a})$$

$$0 \leq (\hat{\mathbf{z}}_i - \mathbf{W}\mathbf{x}_i) \perp \boldsymbol{\alpha}_i \geq 0, \quad \forall i \in \mathcal{N}, \quad (\text{A.18b})$$

which, unlike (A.17d)-(A.17e), allows for feasible solutions in the form $\hat{z}_{b,i} = 0$ with $\mathbf{w}_b^\top \mathbf{x}_i < 0$ (and $\alpha_{b,i} = 0$), where \mathbf{w}_b is the b -th row of matrix \mathbf{W} . Furthermore, recasting (A.17e) as $\hat{\mathbf{z}}_i - \mathbf{W}\mathbf{x}_i = 0$ and setting $\boldsymbol{\alpha}_i = \mathbf{h}$, $\forall i \in \mathcal{N}$, it is straightforward to see that any feasible point of DR is also feasible for BL. Since the feasible region of (A.17) is contained in the feasible region of (A.16), but the opposite is not true, the optimum of (A.16) is in general lower than that of (A.17).

A.3 Asymptotic consistency of the bilevel approach applied to the strategic producer problem

This section provides a mathematical proof of the asymptotic consistency of the data-driven bilevel problem (4.8) to the optimal solution under the assumption of a fix joint distribution that generates the sample $S = \{(\alpha'_i, \beta'_i, \mathbf{x}_i), \forall i \in \mathcal{N}\}$.

Proposition 1. *1 Let $S = \{(\alpha'_i, \beta'_i, \mathbf{x}_i), \forall i \in \mathcal{N}\}$ be an i.i.d sample of size N and suppose that there exists a linear relationship between α' and $\beta' > 0$ given by $\frac{\alpha'}{\beta'} = \mathbf{a}^\top \mathbf{x} + \xi$, with ξ being a zero-mean noise independent of \mathbf{x} , α' and β' , and that the expectations $\mathbb{E}[\alpha']$, $\mathbb{E}[\beta']$ and $\mathbb{E}[\alpha' \mathbf{x}]$ are all finite. Then, it almost surely holds in the limit $N \rightarrow \infty$ that the optimizer of the problem*

$$\min_{\mathbf{w}_\gamma \in \mathcal{W}; \hat{q}_i} \frac{1}{N} \sum_{i \in \mathcal{N}} \beta'_i \hat{q}_i^2 - \alpha'_i \hat{q}_i \quad (\text{A.19a})$$

$$\text{s.t. } \hat{q}_i \in \arg \min_{q \leq q_i \leq \bar{q}} q_i^2 - \mathbf{w}_\gamma^\top \mathbf{x}_i q_i, \quad \forall i \in \mathcal{N}, \quad (\text{A.19b})$$

with $\mathcal{W} \subset \mathbb{R}^p$ being a compact set containing \mathbf{a} , is attained at $\mathbf{w}_\gamma = \mathbf{a}$.

Proof. First, notice that $\frac{\alpha'}{\beta'} = \mathbf{a}^\top \mathbf{x} + \xi$ implies that $\frac{\mathbb{E}[\alpha' | \mathbf{x}]}{\mathbb{E}[\beta' | \mathbf{x}]} = \mathbf{a}^\top \mathbf{x}$, since $\alpha' = \beta' \mathbf{a}^\top \mathbf{x} + \beta' \xi$, and thus, $\mathbb{E}[\alpha' | \mathbf{x}] = \mathbf{a}^\top \mathbf{x} \mathbb{E}[\beta' | \mathbf{x}]$ given the independent nature of the noise ξ .

The *true* expectation problem associated with the sample average approximation (A.19) is given by

$$\min_{\mathbf{w}_\gamma \in \mathcal{W}; \hat{q}(\mathbf{x})} \int_{\mathcal{X} \times \mathbb{R}^+ \times \mathbb{R}} (\beta' \hat{q}^2(\mathbf{x}) - \alpha' \hat{q}(\mathbf{x})) Q(d\mathbf{x}, d\beta', d\alpha') \quad (\text{A.20a})$$

$$\text{s.t. } \hat{q}(\mathbf{x}) \in \arg \min_{q \leq q \leq \bar{q}} q^2 - \mathbf{w}_\gamma^\top \mathbf{x} q, \quad \forall \mathbf{x} \in \mathcal{X}, \quad (\text{A.20b})$$

where Q is the joint probability law governing the random parameters β' and α' and the feature vector X .

We first show that \mathbf{a} is the unique solution to problem (A.20). To this end, we note that the lower-level problem (A.20b) renders the following decision mapping for almost all $\mathbf{x} \in \mathcal{X}$: $\hat{q}(\mathbf{x}) = \max\left(\underline{q}, \min\left(\frac{\mathbf{w}_\gamma^\top \mathbf{x}}{2}, \bar{q}\right)\right)$, which is a continuous function in \mathbf{w}_γ .

Now let Q_X be the probability measure of X . Consider the following optimization problem, which is a relaxation of (A.20):

$$\begin{aligned} & \min_{q(\mathbf{x}) \in [\underline{q}, \bar{q}], \forall \mathbf{x} \in \mathcal{X}} \int_{\mathcal{X} \times \mathbb{R}^+ \times \mathbb{R}} (\beta' q^2(\mathbf{x}) - \alpha' q(\mathbf{x})) Q(d\mathbf{x}, d\beta', d\alpha') = \\ & \min_{q(\mathbf{x}) \in [\underline{q}, \bar{q}], \forall \mathbf{x} \in \mathcal{X}} \int_{\mathcal{X}} (q^2(\mathbf{x}) \mathbb{E}[\beta' | \mathbf{x}] - q(\mathbf{x}) \mathbb{E}[\alpha' | \mathbf{x}]) Q_X(d\mathbf{x}) = \\ & \int_{\mathcal{X}} \left(\min_{q(\mathbf{x}) \in [\underline{q}, \bar{q}]} q^2(\mathbf{x}) \mathbb{E}[\beta' | \mathbf{x}] - q(\mathbf{x}) \mathbb{E}[\alpha' | \mathbf{x}] \right) Q_X(d\mathbf{x}). \end{aligned}$$

The inner pointwise minimum results in the following optimal decision rule: $q(\mathbf{x}) = \max\left(\underline{q}, \min\left(\frac{\mathbb{E}[\alpha'|\mathbf{x}]}{2\mathbb{E}[\beta'|\mathbf{x}]}, \bar{q}\right)\right) = \max\left(\underline{q}, \min\left(\frac{\mathbf{a}^\top \mathbf{x}}{2}, \bar{q}\right)\right)$ for almost all $\mathbf{x} \in \mathcal{X}$.

Therefore, since $\mathbf{w}_\gamma = a$ is feasible in the true expectation problem (A.20), then it is also an optimal solution to this problem. Furthermore, this solution is unique, if there exists a subset of \mathcal{X} with measure greater than zero such that $\underline{q} < \frac{\mathbb{E}[\alpha'|\mathbf{x}]}{2\mathbb{E}[\beta'|\mathbf{x}]} < \bar{q}$.

In addition, note that all the samples in S are i.i.d. and that $\beta'q^2(\mathbf{x}) - \alpha'q(\mathbf{x})$ is dominated by the function $\max\left(\beta'\bar{q}^2 - \alpha'\bar{q}, \beta'\underline{q}^2 - \alpha'\underline{q}, \frac{\alpha'^2}{4\beta'}\right)$, which is integrable because the expectations $\mathbb{E}[\alpha']$, $\mathbb{E}[\beta']$ and $\mathbb{E}[\alpha'\mathbf{x}]$ are all finite. Indeed, since $\frac{\alpha'}{\beta'} = \mathbf{a}^\top \mathbf{x} + \xi$ by assumption, we have that $\mathbb{E}[\frac{\alpha'^2}{4\beta'}] = \frac{1}{4}\mathbb{E}[\alpha'\frac{\alpha'}{\beta'}] = \frac{1}{4}\mathbb{E}[\alpha'(\mathbf{a}^\top \mathbf{x} + \xi)] = \frac{\mathbf{a}^\top}{4}\mathbb{E}[\alpha'\mathbf{x}]$.

Therefore, by invoking Theorems 5.3 and 7.48 in [125], we have that the minimizer of the sample average approximation problem (A.19) converges to \mathbf{a} almost surely as the sample size N grows to infinity.

□

References

- [1] S. K. Aggarwal, L. M. Saini, and A. Kumar. Electricity price forecasting in deregulated markets: A review and evaluation. *International Journal of Electrical Power & Energy Systems*, 31(1):13–22, 2009.
- [2] J. Aghaei, H. Shayanfar, and N. Amjady. Joint market clearing in a stochastic framework considering power system security. *Applied Energy*, 86(9):1675–1682, 2009.
- [3] J. Aitchison. Goodness of prediction fit. *Biometrika*, 62(3):547–554, 1975.
- [4] B. Allaz and J.-L. Vila. Cournot competition, forward markets and efficiency. *Journal of Economic Theory*, 59(1):1 – 16, 1993.
- [5] G. Aneiros, J. M. Vilar, R. Cao, and A. M. San Roque. Functional prediction for the residual demand in electricity spot markets. *IEEE Transactions on Power Systems*, 28(4):4201–4208, 2013.
- [6] M. Badii, N. Li, and A. Wierman. Online convex optimization with ramp constraints. In *2015 54th IEEE Conference on Decision and Control (CDC)*, pages 6730–6736. IEEE, 2015.
- [7] G.-Y. Ban and C. Rudin. The big data newsvendor: Practical insights from machine learning. *Operations Research*, 67(1):90–108, 2019.
- [8] Z. Bar-Yossef, Y. Birk, T. Jayram, and T. Kol. Index coding with side information. *IEEE Transactions on Information Theory*, 57(3):1479–1494, 2011.
- [9] L. A. Barroso and A. J. Conejo. Decision making under uncertainty in electricity markets. In *2006 IEEE Power Engineering Society General Meeting*, pages 3–5. IEEE, 2006.
- [10] R. Barth, H. Brand, P. Meibom, and C. Weber. A stochastic unit-commitment model for the evaluation of the impacts of integration of large amounts of intermittent wind power. In *2006 international conference on probabilistic methods applied to power systems*, pages 1–8. IEEE, 2006.

- [11] A. A. Bashir and M. Lehtonen. Day-ahead rolling window optimization of islanded microgrid with uncertainty. In *2018 IEEE PES Innovative Smart Grid Technologies Conference Europe (ISGT-Europe)*, pages 1–6. IEEE, 2018.
- [12] G. N. Bathurst, J. Weatherill, and G. Strbac. Trading wind generation in short term energy markets. *IEEE Transactions on Power Systems*, 17(3):782–789, August 2002.
- [13] A. Ben-Tal, L. El Ghaoui, and A. Nemirovski. *Robust optimization*. Princeton University Press, 2009.
- [14] F. E. Benth, J. S. Benth, and S. Koekebakker. *Stochastic modelling of electricity and related markets*, volume 11. World Scientific, 2008.
- [15] D. Bertsimas and D. B. Brown. Constructing uncertainty sets for robust linear optimization. *Operations research*, 57(6):1483–1495, 2009.
- [16] D. Bertsimas and D. den Hertog. Robust and adaptive optimization. *Dynamic Ideas LLC*, 958, 2020.
- [17] D. Bertsimas and N. Kallus. From predictive to prescriptive analytics. *Management Science*, 66(3):1025–1044, 2020.
- [18] D. Bertsimas and A. Thiele. Robust and data-driven optimization: modern decision making under uncertainty. In *Models, methods, and applications for innovative decision making*, pages 95–122. INFORMS, 2006.
- [19] D. Bertsimas and B. Van Parys. Bootstrap robust prescriptive analytics. *Mathematical Programming*, pages 1–40, 2021.
- [20] D. Bertsimas, V. Gupta, and N. Kallus. Robust sample average approximation. *Mathematical Programming*, 171(1):217–282, 2018.
- [21] D. Bertsimas, C. McCord, and B. Sturt. Dynamic optimization with side information. *European Journal of Operational Research*, 2022.
- [22] O. Besbes, Y. Gur, and A. Zeevi. Non-stationary stochastic optimization. *Operations Research*, 63(5):1227–1244, 2015.
- [23] H.-G. Beyer and B. Sendhoff. Robust optimization—a comprehensive survey. *Computer methods in applied mechanics and engineering*, 196(33-34):3190–3218, 2007.
- [24] K. Bimpikis, S. Ehsani, and R. Ilkılıç. Cournot competition in networked markets. *Management Science*, 65(6):2467–2481, 2019.

- [25] J. R. Birge and F. Louveaux. *Introduction to stochastic programming*. Springer Science & Business Media, 2011.
- [26] E. Y. Bitar, R. Rajagopal, P. P. Khargonekar, K. Poolla, and P. Varaiya. Bringing wind energy to market. *IEEE Transactions on Power Systems*, 27(3):1225–1235, August 2012.
- [27] A. L. Blum and P. Langley. Selection of relevant features and examples in machine learning. *Artificial intelligence*, 97(1-2):245–271, 1997.
- [28] S. Boyd, S. P. Boyd, and L. Vandenberghe. *Convex optimization*. Cambridge university press, 2004.
- [29] P. Brézillon. *Modeling and using context: Past, present and future*. PhD thesis, LIP6, 2002.
- [30] P. Brézillon and J.-C. Pomerol. Using contextual information in decision making. In *Context Sensitive Decision Support Systems*, pages 158–173. Springer, 1998.
- [31] E. Brynjolfsson, L. M. Hitt, and H. H. Kim. Strength in numbers: How does data-driven decisionmaking affect firm performance? *Available at SSRN 1819486*, 2011.
- [32] D. W. Bunn and N. Karakatsani. Forecasting electricity prices. *London Business School*, 1, 2003.
- [33] D. W. Bunn and S. N. Paschentis. Development of a stochastic model for the economic dispatch of electric power. *European Journal of Operational Research*, 27(2):179–191, 1986.
- [34] California Independent System Operator. 2019 Annual Report on Market Issues and Performance. Technical report, Department of Market Monitoring, June 2020. Available (online): <http://www.caiso.com/Documents/2019AnnualReportonMarketIssuesandPerformance.pdf>.
- [35] T. Carriere and G. Kariniotakis. An integrated approach for value-oriented energy forecasting and data-driven decision-making. application to renewable energy trading. *IEEE Transactions on Smart Grid*, 10(6):6933–6944, November 2019.
- [36] C. Casorrán, B. Fortz, M. Labbé, and F. Ordóñez. A study of general and security Stackelberg game formulations. *European Journal of Operational Research*, 278(3):855–868, 2019.
- [37] N. Cesa-Bianchi and G. Lugosi. *Prediction, learning, and games*. Cambridge university press, 2006.

- [38] J. Cludius, H. Hermann, F. C. Matthes, and V. Graichen. The merit order effect of wind and photovoltaic electricity generation in germany 2008–2016: Estimation and distributional implications. *Energy economics*, 44:302–313, 2014.
- [39] M. Colombino, E. Dall’Anese, and A. Bernstein. Online optimization as a feedback controller: Stability and tracking. *IEEE Transactions on Control of Network Systems*, 7(1):422–432, 2019.
- [40] A. J. Conejo and X. Wu. Robust optimization in power systems: a tutorial overview. *Optimization and Engineering*, pages 1–23, 2021.
- [41] A. J. Conejo, M. Carrión, and J. M. Morales. *Decision Making Under Uncertainty in Electricity Markets*, volume 153. Springer New York, 2010.
- [42] A. K. David and F. Wen. Strategic bidding in competitive electricity markets: a literature survey. In *2000 Power Engineering Society Summer Meeting (Cat. No. 00CH37134)*, volume 4, pages 2168–2173. IEEE, 2000.
- [43] S. Dempe. Directional differentiability of optimal solutions under slater’s condition. *Mathematical Programming*, 59(1):49–69, 1993.
- [44] S. Dempe. *Bilevel Optimization: Reformulation and First Optimality Conditions*, pages 1–20. Springer Singapore, Singapore, 2017.
- [45] S. Dempe, J. Dutta, and B. Mordukhovich. New necessary optimality conditions in optimistic bilevel programming. *Optimization*, 56(5-6):577–604, 2007.
- [46] C. J. Dent, J. W. Bialek, and B. F. Hobbs. Opportunity cost bidding by wind generators in forward markets: Analytical results. *IEEE Transactions on Power Systems*, 26(3):1600–1608, August 2011.
- [47] S. Diao and S. Sen. Distribution-free algorithms for learning enabled optimization with non-parametric estimation. *Management Science*, 66(3):1025–1044, 2020.
- [48] M. Ž. Djurović, A. Milačić, and M. Kršulja. A simplified model of quadratic cost function for thermal generators. *Proceedings of the 23rd International DAAAM Symposium*, 23(1):25–28, 2012.
- [49] R. Doherty, H. Outhred, and M. O’Malley. Establishing the role that wind generation may have in future generation portfolios. *IEEE Transactions on Power Systems*, 21(3):1415–1422, 2006.
- [50] P. Donti, B. Amos, and J. Z. Kolter. Task-based end-to-end model learning in stochastic optimization. *Advances in Neural Information Processing Systems*, pages 5484–5494, 2017.

- [51] E. Du, N. Zhang, C. Kang, B. Kroposki, H. Huang, M. Miao, and Q. Xia. Managing wind power uncertainty through strategic reserve purchasing. *IEEE Transactions on Power Systems*, 32(4):2547–2559, July 2017.
- [52] N. J. Dudley and O. R. Burt. Stochastic reservoir management and system design for irrigation. *Water Resources Research*, 9(3):507–522, 1973.
- [53] J. Dupačová. Applications of stochastic programming: Achievements and questions. *European Journal of Operational Research*, 140(2):281–290, 2002.
- [54] V. Dvorkin, S. Delikaraoglou, and J. M. Morales. Setting reserve requirements to approximate the efficiency of the stochastic dispatch. *IEEE Transactions on Power Systems*, 34(2):1524–1536, 2018.
- [55] E. Ela, M. Milligan, A. Bloom, A. Botterud, A. Townsend, and T. Levin. Evolution of wholesale electricity market design with increasing levels of renewable generation, 2014.
- [56] A. N. Elmachtoub and P. Grigas. Smart “Predict, then Optimize”. *Management Science*, 68(1):9–26, 2022.
- [57] P. M. Esfahani and D. Kuhn. Data-driven distributionally robust optimization using the wasserstein metric: Performance guarantees and tractable reformulations. *Mathematical Programming*, 171(1-2):115–166, 2018.
- [58] A. Esteban-Pérez and J. M. Morales. Distributionally robust stochastic programs with side information based on trimmings. *Mathematical Programming*, pages 1–37, 2021.
- [59] J. Fortuny-Amat and B. McCarl. A representation and economic interpretation of a two-level programming problem. *Journal of the operational Research Society*, 32(9):783–792, 1981.
- [60] V. Gabrel, C. Murat, and A. Thiele. Recent advances in robust optimization: An overview. *European journal of operational research*, 235(3):471–483, 2014.
- [61] L. Gan and S. H. Low. An online gradient algorithm for optimal power flow on radial networks. *IEEE Journal on Selected Areas in Communications*, 34(3):625–638, 2016.
- [62] A. Garcés. *Mathematical Programming for Power Systems Operation: From Theory to Applications in Python*. John Wiley & Sons, 2021.
- [63] J. D. Garcia, A. Street, T. H. de Mello, and F. D. Muñoz. Application-driven learning via joint prediction and optimization of demand and reserves requirement. *arXiv 2102.13273*, 2021.

- [64] J. Goh and M. Sim. Distributionally robust optimization and its tractable approximations. *Operations research*, 58(4-part-1):902–917, 2010.
- [65] E. Gonzalez-Romera, M. A. Jaramillo-Moran, and D. Carmona-Fernandez. Monthly electric energy demand forecasting based on trend extraction. *IEEE Transactions on power systems*, 21(4):1946–1953, 2006.
- [66] R. J. Green and D. M. Newbery. Competition in the british electricity spot market. *Journal of political economy*, 100(5):929–953, 1992.
- [67] Z. Guo, P. Pinson, S. Chen, Q. Yang, and Z. Yang. Online optimization for real-time peer-to-peer electricity market mechanisms. *IEEE Transactions on Smart Grid*, 12(5):4151–4163, 2021.
- [68] G. A. Hanasusanto, D. Kuhn, and W. Wiesemann. A comment on “computational complexity of stochastic programming problems”. *Mathematical Programming*, 159(1):557–569, 2016.
- [69] A. Hauswirth, S. Bolognani, G. Hug, and F. Dörfler. Projected gradient descent on riemannian manifolds with applications to online power system optimization. In *2016 54th Annual Allerton Conference on Communication, Control, and Computing (Allerton)*, pages 225–232. IEEE, 2016.
- [70] A. Hauswirth, A. Zanardi, S. Bolognani, F. Dörfler, and G. Hug. Online optimization in closed loop on the power flow manifold. In *2017 IEEE Manchester PowerTech*, pages 1–6. IEEE, 2017.
- [71] E. Hazan, A. Rakhlin, and P. Bartlett. Adaptive online gradient descent. *Advances in Neural Information Processing Systems*, 20, 2007.
- [72] E. Hazan et al. Introduction to online convex optimization. *Foundations and Trends® in Optimization*, 2(3-4):157–325, 2016.
- [73] H. Heitsch and W. Römisch. Scenario reduction algorithms in stochastic programming. *Computational optimization and applications*, 24(2):187–206, 2003.
- [74] J. Huber, S. Müller, M. Fleischmann, and H. Stuckenschmidt. A data-driven newsvendor problem: From data to decision. *European Journal of Operational Research*, 278(3):904–915, 2019.
- [75] P. L. Joskow. Lessons learned from electricity market liberalization. *The Energy Journal*, 29(Special Issue# 2), 2008.
- [76] Y.-H. Kao, B. V. Roy, and X. Yan. Directed regression. *Advances in Neural Information Processing Systems 22*, pages 889–897, 2009.

- [77] G. Kariniotakis. *Renewable Energy Forecasting: From Models to Applications*. Woodhead Publishing Series in Energy. Elsevier - Woodhead Publishing, 2017.
- [78] L. Kaufman and P. J. Rousseeuw. *Finding Groups in Data: An Introduction to Cluster Analysis*, volume 344. John Wiley & Sons, 2009.
- [79] R. Kerr, J. Scheidt, A. Fontanna, and J. Wiley. Unit commitment. *IEEE Transactions on Power Apparatus and Systems*, pages 417–421, 1966.
- [80] S. Kim, R. Pasupathy, and S. G. Henderson. A guide to sample average approximation. *Handbook of simulation optimization*, pages 207–243, 2015.
- [81] D. P. Kingma and J. Ba. Adam: A method for stochastic optimization. In *ICLR (Poster)*, 2015.
- [82] A. J. Kleywegt, A. Shapiro, and T. Homem-de Mello. The sample average approximation method for stochastic discrete optimization. *SIAM Journal on Optimization*, 12(2):479–502, 2002.
- [83] D. Kuhn, P. M. Esfahani, V. A. Nguyen, and S. Shafieezadeh-Abadeh. Wasserstein distributionally robust optimization: Theory and applications in machine learning. In *Operations research & management science in the age of analytics*, pages 130–166. Informs, 2019.
- [84] A. Lesage-Landry and D. S. Callaway. Dynamic and distributed online convex optimization for demand response of commercial buildings. *IEEE Control Systems Letters*, 4(3):632–637, 2020.
- [85] A. Lesage-Landry, H. Wang, I. Shames, P. Mancarella, and J. A. Taylor. On-line convex optimization of multi-energy building-to-grid ancillary services. *IEEE Transactions on Control Systems Technology*, 28(6):2416–2431, 2019.
- [86] A. Lesage-Landry, I. Shames, and J. A. Taylor. Predictive online convex optimization. *Automatica*, 113:108771, 2020.
- [87] G. Li, J. Shi, and X. Qu. Modeling methods for genco bidding strategy optimization in the liberalized electricity spot market—a state-of-the-art review. *Energy*, 36(8):4686–4700, 2011.
- [88] J. Li, C. Wan, and Z. Xu. Robust offering strategy for a wind power producer under uncertainties. In *2016 IEEE International Conference on Smart Grid Communications (SmartGridComm)*, pages 752–757. IEEE, 2016.
- [89] S. A. Malcolm and S. A. Zenios. Robust optimization for power systems capacity expansion under uncertainty. *Journal of the operational research society*, 45(9):1040–1049, 1994.

- [90] J. Mandi, P. J. Stuckey, T. Guns, et al. Smart predict-and-optimize for hard combinatorial optimization problems. In *Proceedings of the AAAI Conference on Artificial Intelligence*, volume 34, pages 1603–1610, 2020.
- [91] J. Matevosyan and L. Soder. Minimization of imbalance cost trading wind power on the short-term power market. *IEEE Transactions on Power Systems*, 21(3): 1396–1404, August 2006.
- [92] N. Mazzi and P. Pinson. Purely data-driven approaches to trading of renewable energy generation. In *13th International Conference on the European Energy Market (EEM)*, pages 1–5, June 2016.
- [93] P. Mohajerin Esfahani and D. Kuhn. Data-driven distributionally robust optimization using the wasserstein metric: Performance guarantees and tractable reformulations. *Mathematical Programming*, 171(1):115–166, 2018.
- [94] J. M. Morales, A. J. Conejo, and J. Pérez-Ruiz. Short-term trading for a wind power producer. *IEEE Transactions on Power Systems*, 25(1):554–564, February 2010.
- [95] J. M. Morales, R. Mínguez, and A. J. Conejo. A methodology to generate statistically dependent wind speed scenarios. *Applied Energy*, 87(3):843–855, 2010.
- [96] J. M. Morales, A. J. Conejo, K. Liu, and J. Zhong. Pricing electricity in pools with wind producers. *IEEE Transactions on Power Systems*, 27(3):1366–1376, 2012.
- [97] J. M. Morales, A. J. Conejo, H. Madsen, P. Pinson, and M. Zugno. *Integrating Renewables in Electricity Markets: Operational Problems*, volume 205. Springer Science & Business Media, 2014.
- [98] J. M. Morales, M. Zugno, S. Pineda, and P. Pinson. Electricity market clearing with improved scheduling of stochastic production. *European Journal of Operational Research*, 235(3):765–774, 2014.
- [99] A. Mosavi, M. Salimi, S. Faizollahzadeh Ardabili, T. Rabczuk, S. Shamshirband, and A. R. Varkonyi-Koczy. State of the art of machine learning models in energy systems, a systematic review. *Energies*, 12(7):1301, 2019.
- [100] N. Mundru. *Predictive and prescriptive methods in operations research and machine learning: an optimization approach*. PhD thesis, Massachusetts Institute of Technology, 2019.

- [101] M. A. Muñoz, J. M. Morales, and S. Pineda. Feature-driven improvement of renewable energy forecasting and trading. *IEEE Transactions on Power Systems*, 35(5):3753–3763, 2020.
- [102] M. A. Muñoz, S. Pineda, and J. M. Morales. A bilevel framework for decision-making under uncertainty with contextual information. *Omega*, 108:102575, 2022.
- [103] P. Nahmmacher, E. Schmid, and B. Knopf. Documentation of LIMES-EU – A long-term electricity system model for Europe, 2014.
- [104] B. Narayanaswamy, V. K. Garg, and T. Jayram. Online optimization for the smart (micro) grid. In *Proceedings of the 3rd International Conference on Future Energy Systems*, pages 1–10, 2012.
- [105] H. A. Nielsen, T. S. Nielsen, H. Madsen, M. J. S. I. Pindado, and I. Marti. Optimal combination of wind power forecasts. *Wind Energy*, 10(5):471–482, 2007.
- [106] M. Nonhoff and M. A. Müller. Online gradient descent for linear dynamical systems. *IFAC-PapersOnLine*, 53(2):945–952, 2020.
- [107] F. Orabona. A modern introduction to online learning. *arXiv preprint arXiv:1912.13213*, 2022.
- [108] F. Pedregosa, G. Varoquaux, A. Gramfort, V. Michel, B. Thirion, O. Grisel, M. Blondel, P. Prettenhofer, R. Weiss, V. Dubourg, J. Vanderplas, A. Passos, D. Cournapeau, M. Brucher, M. Perrot, and E. Duchesnay. Scikit-learn: Machine learning in Python. *Journal of Machine Learning Research*, 12:2825–2830, 2011.
- [109] S. Pineda, H. Bylling, and J. Morales. Efficiently solving linear bilevel programming problems using off-the-shelf optimization software. *Optimization and Engineering*, 19(1):187–211, 2018.
- [110] P. Pinson, C. Chevallier, and G. N. Kariniotakis. Trading wind generation from short-term probabilistic forecasts of wind power. *IEEE Transactions on Power Systems*, 22(3):1148–1156, August 2007.
- [111] D. J. Power. Understanding data-driven decision support systems. *Information Systems Management*, 25(2):149–154, 2008.
- [112] G. Pritchard, G. Zakeri, and A. Philpott. A single-settlement, energy-only electric power market for unpredictable and intermittent participants. *Operations research*, 58(4-part-2):1210–1219, 2010.
- [113] Y. Qin, R. Wang, A. J. Vakharia, Y. Chen, and M. M. Seref. The newsvendor problem: Review and directions for future research. *European Journal of Operational Research*, 213(2):361–374, 2011.

- [114] D. Ralph and S. J. Wright. Some properties of regularization and penalization schemes for mpecs. *Optimization Methods and Software*, 19(5):527–556, 2004.
- [115] P. Robison, M. Sengupta, and D. Rauch. Intelligent energy industrial systems 4.0. *It Professional*, 17(3):17–24, 2015.
- [116] R. T. Rockafellar, S. Uryasev, et al. Optimization of conditional value-at-risk. *Journal of risk*, 2:21–42, 2000.
- [117] C. Ruiz, A. Conejo, and R. García-Bertrand. Some analytical results pertaining to Cournot models for short-term electricity markets. *Electric Power Systems Research*, 78(10):1672 – 1678, 2008.
- [118] A. Ruszczyński and A. Shapiro. *Stochastic programming (handbooks in operations research and management science)*. Elsevier, 2003.
- [119] I. Sánchez. Short-term prediction of wind energy production. *International Journal of Forecasting*, 22(1):43 – 56, 2006.
- [120] I. Sánchez. Adaptive combination of forecasts with application to wind energy. *International Journal of Forecasting*, 24(4):679–693, 2008. ISSN 0169-2070.
- [121] H. Scheel and S. Scholtes. Mathematical programs with complementarity constraints: Stationarity, optimality, and sensitivity. *Mathematics of Operations Research*, 25(1):1–22, 2000.
- [122] S. Scholtes. Convergence properties of a regularization scheme for mathematical programs with complementarity constraints. *SIAM Journal on Optimization*, 11(4):918–936, 2001.
- [123] S. Sen and J. L. Higle. An introductory tutorial on stochastic linear programming models. *Interfaces*, 29(2):33–61, 1999.
- [124] S. Shalev-Shwartz. Online learning and online convex optimization. *Foundations and Trends in Machine Learning*, 4(2):107–194, 2011.
- [125] A. Shapiro, D. Dentcheva, and A. Ruszczyński. *Lectures on stochastic programming: modeling and theory*. SIAM, 2021.
- [126] A. Skajaa, K. Edlund, and J. M. Morales. Intraday trading of wind energy. *IEEE Transactions on Power Systems*, 30(6):3181–3189, November 2015.
- [127] S. Soares, C. Lyra, and H. Tavares. Optimal generation scheduling of hydrothermal power systems. *IEEE Transactions on Power Apparatus and Systems*, pages 1107–1118, 1980.

- [128] T. H. Soukissian and A. Papadopoulos. Effects of different wind data sources in offshore wind power assessment. *Renewable Energy*, 77:101–114, 2015.
- [129] P. R. Srivastava, Y. Wang, G. A. Hanasusanto, and C. P. Ho. On data-driven prescriptive analytics with side information: A regularized nadaraya-watson approach. *arXiv preprint arXiv:2110.04855*, 2021.
- [130] X. A. Sun, A. J. Conejo, et al. *Robust Optimization in Electric Energy Systems*. Springer, 2021.
- [131] A. A. Sánchez de la Nieta, J. Contreras, and J. I. Muñoz. Optimal coordinated wind-hydro bidding strategies in day-ahead markets. *IEEE Transactions on Power Systems*, 28(2):798–809, May 2013.
- [132] J. Tastu, P. Pinson, E. Kotwa, H. Madsen, and H. A. Nielsen. Spatio-temporal analysis and modeling of short-term wind power forecast errors. *Wind Energy*, 14(1):43–60, 2011.
- [133] C. Uçkun, A. Botterud, and J. R. Birge. An improved stochastic unit commitment formulation to accommodate wind uncertainty. *IEEE Transactions on Power Systems*, 31(4):2507–2517, 2015.
- [134] X. Vives. Duopoly information equilibrium: Cournot and Bertrand. *Journal of Economic Theory*, 34(1):71 – 94, 1984.
- [135] H. Vu, P. Pruvot, C. Launay, and Y. Harmand. An improved voltage control on large-scale power system. *IEEE transactions on power systems*, 11(3):1295–1303, 1996.
- [136] O. Wagner, T. Adisorn, L. Tholen, and D. Kiyar. Surviving the energy transition: development of a proposal for evaluating sustainable business models for incumbents in germany’s electricity market. *Energies*, 13(3):730, 2020.
- [137] S. W. Wallace and S.-E. Fleten. Stochastic programming models in energy. *Handbooks in operations research and management science*, 10:637–677, 2003.
- [138] Q. Wang, C. Zhang, Y. Ding, G. Xydis, J. Wang, and J. Østergaard. Review of real-time electricity markets for integrating distributed energy resources and demand response. *Applied Energy*, 138:695–706, 2015.
- [139] W. Wiesemann, D. Kuhn, and M. Sim. Distributionally robust convex optimization. *Operations Research*, 62(6):1358–1376, 2014.
- [140] B. Wilder, B. Dilkina, and M. Tambe. Melding the data-decisions pipeline: Decision-focused learning for combinatorial optimization. *Proceedings of the AAAI Conference on Artificial Intelligence*, 33:1658–1665, 2019.

- [141] K. Wood, G. Bianchin, and E. Dall’Anese. Online projected gradient descent for stochastic optimization with decision-dependent distributions. *IEEE Control Systems Letters*, 6:1646–1651, 2021.
- [142] J. Wu, X. Zhai, and Z. Huang. Incentives for information sharing in duopoly with capacity constraints. *Omega*, 36(6):963–975, 2008.
- [143] L. Xie, Y. Gu, X. Zhu, and M. G. Genton. Short-term spatio-temporal wind power forecast in robust look-ahead power system dispatch. *IEEE Transactions on Smart Grid*, 5(1):511–520, January 2014.
- [144] P. Xiong, P. Jirutitijaroen, and C. Singh. A distributionally robust optimization model for unit commitment considering uncertain wind power generation. *IEEE Transactions on Power Systems*, 32(1):39–49, 2016.
- [145] X. Xu, W. Hu, D. Cao, Q. Huang, Z. Liu, W. Liu, Z. Chen, and F. Blaabjerg. Scheduling of wind-battery hybrid system in the electricity market using distributionally robust optimization. *Renewable Energy*, 156:47–56, 2020.
- [146] V. M. Zavala, K. Kim, M. Anitescu, and J. Birge. A stochastic electricity market clearing formulation with consistent pricing properties. *Operations Research*, 65(3):557–576, 2017.
- [147] M. D. Zeiler. Adadelta: an adaptive learning rate method. *arXiv preprint arXiv:1212.5701*, 2012.
- [148] Y. Zhang, Z. Dai, and B. K. H. Low. Bayesian optimization with binary auxiliary information. In *Uncertainty in Artificial Intelligence*, pages 1222–1232. PMLR, 2020.
- [149] Y. Zhao, L. Ye, P. Pinson, Y. Tang, and P. Lu. Correlation-constrained and sparsity-controlled vector autoregressive model for spatio-temporal wind power forecasting. *IEEE Transactions on Power Systems*, 33(5):5029–5040, September 2018.
- [150] S. Zheng. Gradient descent algorithms for quantile regression with smooth approximation. *International Journal of Machine Learning and Cybernetics*, 2(3):191–207, 2011.
- [151] X. Y. Zhou and D. Li. Continuous-time mean-variance portfolio selection: A stochastic lq framework. *Applied Mathematics and Optimization*, 42(1):19–33, 2000.

- [152] M. Zinkevich. Online convex programming and generalized infinitesimal gradient ascent. In *Proceedings of the 20th International Conference on Machine Learning (ICML-03)*, pages 928–936, 2003.
- [153] M. Zugno, T. Jónsson, and P. Pinson. Trading wind energy on the basis of probabilistic forecasts both of wind generation and of market quantities. *Wind Energy*, 16(6):909–926, 2013.